Graz University of Technology
Institute of Hydraulic Engineering and Water Resources Management

Numerical studies on the influence of seismic retrofit on the non-linear response of Koyna Dam

Master thesis
submitted by
Patricia Walch, BSc

Provided to obtain the
academic degree of a Master
of Civil Engineering

Graz, September 2020

Supervisor of the master thesis:
Univ.-Prof. Dipl.-Ing. Dr.techn. Gerald Zenz

.....

Co-Supervisor:
Dipl.-Ing. Edwin Josef Staudacher BSc

.....

Declaration of authorship

I declare that I have authored this thesis independently, that I have not used other than the declared sources/resources, and that I have explicitly indicated all material which has been quoted either literally or by content from the sources used. The text document uploaded to TUGRAZonline is identical to the present master's thesis.

This thesis was not previously presented to another examination board and has not been published.

Graz, September 2020 .....

Eidesstattliche Erklärung

Ich erkläre an Eides statt, dass ich die vorliegende Arbeit selbstständig verfasst, andere als die angegebenen Quellen/Hilfsmittel nicht benutzt, und die in den benutzten Quellen wörtlich und inhaltlich entnommenen Stellen als solche kenntlich gemacht habe. Das im TUGRAZonline hochgeladene Textdokument ist mit der vorliegenden Masterarbeit identisch.

Ich versichere, dass ich dieses Masterarbeitsthema bisher weder im In- noch im Ausland (einer Beurteilerin oder einem Beurteiler) in irgendeiner Form als Prüfungsarbeit vorgelegt habe.

Graz, im September 2020 .....

Acknowledgement

At this point I would like to thank all people who have taken this long path of studying with me, who have supported me over the years and those who have motivated me all the time. First of all my thanks go to Univ.-Prof. Gerald Zenz, who has supervised this master thesis and who inspired me in his lectures on hydraulic engineering.

A very special thanks goes to Dipl.-Ing. Edwin Staudacher, who was there to help me with any problems and open questions. He was always willing to help me in an uncomplicated way, without his assistance I would not have completed this master thesis in the same period.

Also special thanks goes to Shervin Shahriari, M.Sc., who provided the base for the APDL script and the corresponding tutorial for the finite element analysis software, without it the numerical modelling would not be possible to carry out.

As well I want to thank my family, including my parents, my brother and my cats, who supported me throughout my studies and motivated me all the time.

Many thanks go to my boyfriend, who went through this study with me and supported me in all ups and downs of the past years.

Also I want to thank my friends and colleagues for the unforgettable memories and the wonderful time we spent together during the past years.

Finally many thanks to the colleagues from the FvBau, thank you for the great time of working together and the enjoyable seminars and weekend trips.

Abstract

The Koyna Dam in India, which was subjected to seismic loading by an earthquake of Richter magnitude 6.5 on December 11, 1967, is the main topic of this master thesis. This construction has already been examined intensively. In this thesis the goal is pursued that the cross-section with the largest building height of the dam is modeled and discretized in a finite element software as intact and subsequently as a cracked cross-section. There a horizontal crack is assumed, that is based on the observed crack on Koyna Dam caused by the earthquake, which stretches through the entire cross-section from the upstream side to the downstream side. The crest part is thus separated from the bottom part of the dam. Through discretization of the crack the dam consists of two bodies which are in contact in the crack area. First the system is calculated with the crack closed, in the next step with the open crack, where the stability against displacements of the upper part is based on friction only. The ground motion is applied on the model in horizontal and vertical direction and the calculations are carried out with a partially filled as well as an empty reservoir. The water level in the reservoir corresponds to that one on the day of the earthquake. Also a foundation is taken into account, on which the dam is founded, which is assumed to be massless. In further investigations, the influence on the behavior of the system is examined if the structure was reinforced with anchors. First one anchor is used, which is implemented in the middle of the crest part, then a system with two anchors is modeled, whereby the geometry and the prestressing force were taken from Koyna Dam, which was reinforced with anchors after the 1967 earthquake. The deformations (displacements) of the part separated from the lower part of the dam in different models are compared at selected points. The anchor force is shown over time and the distribution of the contact stresses along the assumed crack is determined. Finally, the Newmark rigid-block method is presented as an alternative calculation method to calculate the permanent displacements of the crest part. So it is possible to provide the required verification of stability for this extreme event.

Kurzfassung

Die Koyna Staumauer in Indien, welche am 11. Dezember 1967 von einem Erdbeben der Richtermagnitude 6.5 erschüttert wurde, ist das Hauptthema dieser Masterarbeit. Dieses Bauwerk wurde bereits intensiv untersucht. In dieser Arbeit wird das Ziel verfolgt, den Querschnitt mit größter Bauwerkshöhe der Mauer in einer Finite Elemente Software als intakt und in weiterer Folge als gerissener Querschnitt zu modellieren und diskretisieren. Dabei wird ein horizontaler Riss angenommen, welcher auf dem beobachteten, durch das Erdbeben entstandenen Riss der Koyna Mauer basiert, der sich durch den gesamten Querschnitt von der Oberwasserseite zur Unterwasserseite zieht. Somit ist die Mauerkrone vom unteren Teil der Mauer getrennt. Durch die Diskretisierung des Risses besteht die Mauer aus zwei Körpern, die in der Rissebene in Kontakt stehen. Zuerst wird das System mit geschlossenem Riss berechnet, im nächsten Schritt mit geöffnetem Riss, wobei die Stabilität gegen die Verschiebung des oberen Teils nur noch auf Reibung basiert. Die Bodenbeschleunigung wird in horizontaler und vertikaler Richtung auf das Modell aufgebracht und die Berechnungen werden mit einem teilweise gefüllten sowie leeren Reservoir durchgeführt. Der Wasserstand im Reservoir entspricht jenem am Tag des Erdbebens. Ebenso wird ein Felsuntergrund modelliert, auf dem die Staumauer gegründet ist, welcher als masselos angenommen werden kann. In weiteren Untersuchungen wird der Einfluss auf das Systemverhalten untersucht, wenn das Bauwerk durch Ankern verstärkt wäre. Zuerst wird ein Anker verwendet, welcher in der Mitte der Krone implementiert wird, dann wird ein System mit zwei Ankern modelliert, wobei die Geometrie und die Vorspannung von der Koyna Staumauer übernommen werden, die nach dem Erdbeben von 1967 mit Anker verstärkt wurde. Die Verformungen (Verschiebungen) von dem unteren Teil der Talsperre getrennten Bauteils werden unter den verschiedenen Modellen an ausgewählten Punkten verglichen. Die Ankerkraft wird über die Zeit und zusätzlich wird der Verlauf der Kontaktspannungen entlang des angenommenen Risses dargestellt. Abschließend werden noch mit der Blockgleitmethode nach Newmark als alternative Berechnungsmethode die permanenten Verformungen der Mauerkrone berechnet. Damit gelingt es den geforderten Standsicherheitsnachweis für dieses Extremereignis zu führen.

List of contents

1. Introduction

The structural assessment of dams on earthquake safety especially with numerical methods is common practice nowadays. Beside static load cases, earthquake loading is one of the most important components to evaluate the structures response. In this master thesis Koyna Dam in India is used and represented in a two- and a three-dimensional numerical model that consists of three parts, which are dam, foundation block and reservoir. The reservoir is filled up to a certain level, which coincide to the observed water level when the Koyna earthquake on December 11, 1967 struck the dam, where the height of the reservoir was almost the maximum water height. Koyna Dam and its surrounding environment were subjected to an earthquake of Richter magnitude of 6.5 on that day. Actually Koyna Dam is used for many numerical calculations due to its special design of the cross-section and the occurrence of a strong earthquake in a usually non-seismic region.

Therefore, the centerpiece of this work is the modelling of Koyna Dam in a Finite Element program and implementing a fictional horizontal aligned crack, that extends through the dam body from the upstream to the downstream face based on given information from the reports of Koyna Dam. First it is modelled as two-dimensional system without a crack und subjected to the dynamic loading that consists of the acceleration in horizontal and vertical direction of the Koyna earthquake. In the next step the assumed crack is activated as acting with frictional resistance and the seismic response is calculated with a full and an empty reservoir. The fluid-structure interaction is considered by coupling of the structure elements with so-called acoustic elements that represent the fluid body of the reservoir. The composition of the contacts in the crack and between foundation and structure is an important part of the model. In addition to the aforementioned models, the system is modeled as three-dimensional section with 1 m thickness and is reinforced with passive and posttensioned anchors, first with only one anchor located in the middle of the crest and then two anchors, where the design is taken from the original Koyna Dam, which was reinforced after the 6.5 magnitude earthquake.

Additionally the basics of structural dynamics and the Finite Element Method are briefly summarized to achieve a fundamental understanding of these topics. Furthermore, the utilization and failure causes of passive and prestressed anchors in dams are described and the design of a strand anchor is shown as this type is used in the Koyna models. Prestressed anchors are often used in already constructed dams to improve the structural safety against dynamic loading.

Koyna Dam models are compared with each other in terms of deformations at the crest and the crack at the upstream side, the anchor forces developing with time during the earthquake and the contact pressure in the crack area. Finally a rigid-block analysis based on Newmark is conducted to obtain the permanent displacements for comparison with the numerical analysis.

2. Fundamentals

In this chapter the necessary fundamentals of the Finite-Element-Method (FEM) and structural dynamics are briefly explained as these are essential for a numerical analysis of a structure.

2.1 Finite Element Method [1, 2]

Since the FEM is a very far-reaching topic, this section will briefly summarize the basics of this kind of analysis.

2.1.1 Basic concept

When mathematical calculations are not enough to find a proper solution, the Finite Element Method (FEM) can create an approximated solution for a particular problem with an adequate amount of time.

The body or surface used is split up in connected parts that are known as elements, which are connected by joints that are called nodes located on the edges of the elements. For each single element an approximated solution has to be defined.

The idea of the FEM was invented long time ago, but the name itself was mentioned first by Clough in 1960. It was considered similar to the Rayleigh-Ritz method from the 1960s. After the invention of digital computers and their commercial availability, the development of the finite element method increased rapidly. For example, Zienkiewicz et al. [2] introduced its efficiency and it has been used widely in structural mechanics.

2.1.2 General description

The following steps generally describe the procedure how a finite element problem is solved (Rao et al. [1]):

1. The surface or body is split into smaller parts, the elements, which is called discretization or meshing.

2. A suitable interpolation function is defined, which is used to approximate the variables of an element. Usually the interpolation function is a polynomial.

3. The load vectors and element stiffness matrices can be determined by approximating the stiffness matrix $[k]$ and the load vector $\{p\}$ should be determined.

4. To get the equilibrium equations, the element stiffness matrices and load vectors have to be put together, which is given as

$$[k]\{u\} = \{p\} \tag{1}$$

with $[k]$ as the stiffness matrix, $\{u\}$ is the displacement vector and $\{p\}$ is the force vector.

5. For calculation of the displacements, boundary conditions have to be integrated, so the nodal values are known. Then the required results can be computed.

2.1.3 FEM for a two-dimensional problem

For explaining the basics of the FEM, the calculation steps for a 2D problem are demonstrated. With Hooke's Law the elasticity for 2D is considered here, so the displacement vector is given within the x and y coordinates:

$$\{u\} = \begin{Bmatrix} u(x,y) \\ v(x,y) \end{Bmatrix} \tag{2}$$

Stress and strain vectors are given as following:

$$\{\sigma\} = \begin{Bmatrix} \sigma_x \\ \sigma_y \\ \tau_{xy} \end{Bmatrix} \; and \; \{\varepsilon\} = \begin{Bmatrix} \varepsilon_x \\ \varepsilon_y \\ \gamma_{xy} \end{Bmatrix} \tag{3}$$

The D-Matrix, which is called the elasticity matrix of moduli, includes stresses and strains:

$$[D] = \frac{E}{1-\nu^2}\begin{bmatrix} 1 & \nu & 0 \\ \nu & 1 & 0 \\ 0 & 0 & \frac{1-\nu}{2} \end{bmatrix} \quad for\ plane\ stress \tag{4}$$

$$[D] = \frac{E}{(1+\nu)(1-2\nu)}\begin{bmatrix} 1-\nu & \nu & 0 \\ \nu & 1-\nu & 0 \\ 0 & 0 & \frac{1-2\nu}{2} \end{bmatrix} \quad for\ plane\ strain \tag{5}$$

The stress vector can be obtained with this relationship:

$$\{\sigma\} = [D]\{\varepsilon\} \tag{6}$$

For the strains there are following equations:

$$\varepsilon_x = \frac{\partial u}{\partial x} \qquad \varepsilon_y = \frac{\partial v}{\partial y} \qquad \gamma_{xy} = \frac{\partial u}{\partial y} + \frac{\partial v}{\partial x} \tag{7}$$

In the FEM the displacement u has to be determined to calculate the stresses and strains. This can be done by the use of shape functions (given as N usually). For the discretization the geometry has to be divided into elements and transferred from the global in a local coordinate system

$$\{x_{(\xi,\eta)}\} = \sum_n N_{n(\xi,\eta)}\{x\}_n \tag{8}$$

where n shows the number of nodes of an element and ξ and η form the new local coordinate system that is aligned with the elements.

When the same shape function is used for the element as well as for the displacement, this kind of elements are so-called isoparametric elements. Therefore, the displacement is approximated as:

$$\{u_{(\xi,\eta)}\} = \sum_n N_{n(\xi,\eta)}\{u\}_n \tag{9}$$

With the known displacement vector $\{u\}$ the strains can be calculated in the next step, when equation (9) is used:

$$\varepsilon_x = \sum_n \frac{\partial N_{n(\xi,\eta)}}{\partial x}\{u\}_n \qquad \varepsilon_y = \sum_n \frac{\partial N_{n(\xi,\eta)}}{\partial y}\{v\}_n \tag{10}$$

$$\gamma_{xy} = \sum_n \frac{\partial N_{n(\xi,\eta)}}{\partial y}\{u\}_n + \sum_n \frac{\partial N_{n(\xi,\eta)}}{\partial x}\{v\}_n \tag{11}$$

So the B-Matrix can be formed with the derivatives of the shape functions:

$$[B] = \begin{bmatrix} \frac{\partial N_1(x,y)}{\partial x} & 0 & \frac{\partial N_2(x,y)}{\partial x} & 0 & \dots & \frac{\partial N_n(x,y)}{\partial x} & 0 \\ 0 & \frac{\partial N_1(x,y)}{\partial y} & 0 & \frac{\partial N_2(x,y)}{\partial y} & \dots & 0 & \frac{\partial N_n(x,y)}{\partial y} \\ \frac{\partial N_1(x,y)}{\partial x} & \frac{\partial N_1(x,y)}{\partial y} & \frac{\partial N_2(x,y)}{\partial x} & \frac{\partial N_2(x,y)}{\partial y} & & \frac{\partial N_n(x,y)}{\partial x} & \frac{\partial N_n(x,y)}{\partial y} \end{bmatrix} \tag{12}$$

Hence, the strain vector is given by

$$\{\varepsilon\} = [B]\{u\} \tag{13}$$

and the stress vector:

$$\{\sigma\} = [D][B]\{u\} \tag{14}$$

Next step is converting the functions of the B-Matrix into the local coordinate system within ξ and η. Therefore, the Jacobian matrix $[J]$ is needed which is formulated as:

$$[J] = \begin{bmatrix} \frac{\partial x}{\partial \xi} & \frac{\partial y}{\partial \xi} \\ \frac{\partial x}{\partial \eta} & \frac{\partial y}{\partial \eta} \end{bmatrix} \tag{15}$$

Then the determinant of the Jacobian matrix $\left|J\right|$ is needed:

$$dV = \left|J\right| d\xi d\eta \tag{16}$$

With the principle of minimum potential energy it is possible to obtain the stiffness matrix. The total potential energy is defined as the sum of the potential energy of the inner system U and the potential energy of the external loads V:

$$\Pi = \Pi_U + \Pi_V = \frac{1}{2}\int_{-1}^{1}\int_{-1}^{1}\{\varepsilon\}^T\{\sigma\}dV + \{p\}\{u\} = \frac{1}{2}\int_{-1}^{1}\int_{-1}^{1}\{\varepsilon\}^T\{\sigma\}\left|J\right| d\xi d\eta + \{p\}\{u\} \tag{17}$$

The equation system can be solved when the minimum of potential energy is obtained by deriving equation (17) and set it zero:

$$\frac{\partial \Pi}{\partial \{u\}} = 0 \tag{18}$$

The differentiation of the potential energy is presented in following form:

$$[k]\{u\} = \{p\} \tag{19}$$

Where $[k]$ is the stiffness matrix, $\{u\}$ is the displacement vector and $\{p\}$ is the load vector. Each element has its own stiffness matrix, where all of them are assembled to receive a solution for a global system.

2.2 Structural dynamics [3, 4]

For the calculation of the seismic response of a dam some fundamentals of structural dynamics are needed and therefore the principles of vibrating systems are explained shortly.

2.2.1 Dynamic motions [3]

There are two kinds of dynamic motion, the periodic motion and the nonperiodic motion. A periodic motion is a motion with uniform periods and amplitudes. One kind is called a simple harmonic motion, which has the shape of a sinus function. The nonperiodic motion is not moving uniformly, it may be caused by impulsive loads like explosions, or by transient loads such as earthquakes. In Figure 1 are given examples of the described motions.

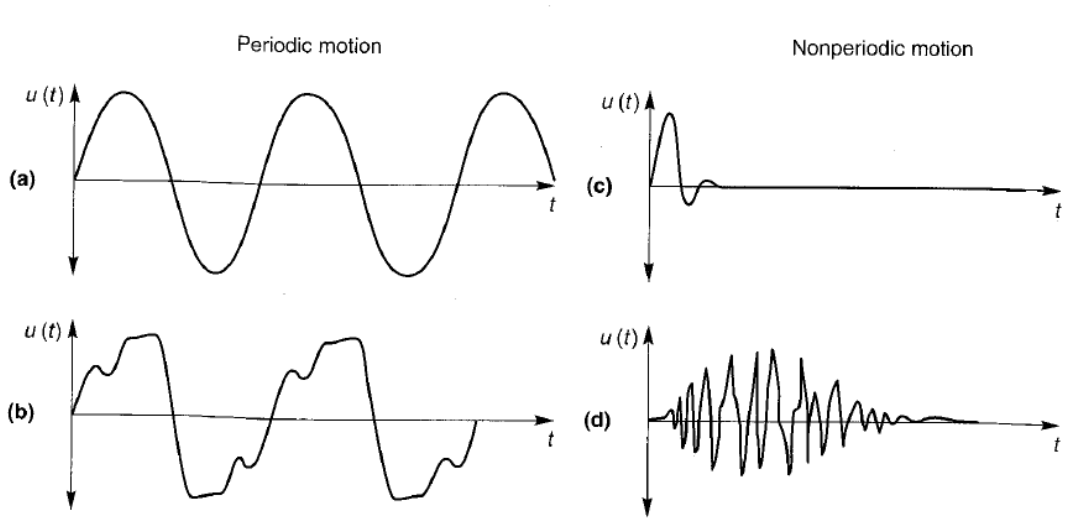

Figure 1: Types of motion: (a) harmonic motion, (b) periodic motion, (c)+(d) transient motions [3]

2.2.2 Single-degree-of-freedom systems [3, 4]

A single-degree-of-freedom (SDOF) system is an idealized system which can be characterized by one single movement, the relative position according to the original position, the degree of freedom. It is defined by the mass m, the stiffness k and the damping coefficient c. In Figure 2 shows a SDOF system as a system with its mass, a spring and a dashpot in (a). In (b) the forces acting on the body are visible with the force in the spring ku and in the dashpot $c\dot{u}$ as well as an external force $p(t)$ and the force of inertia mg. In (c) the free-body figure shows the equilibrium forces with the D'Alembert's principle. Commonly u is used as a variable for displacement in the structural dynamics, therefore, the differentiation of the displacement is the velocity that is written as $\dot{u}$ and after double differentiating the acceleration $\ddot{u}$ is obtained.

The fundament of dynamics is based on Newton's second law of motion:

$$m\ddot{u} = f(t) \tag{20}$$

In a damped SDOF the inertial force of the mass, the forces of the dashpot and the spring are represented in the force equilibrium:

$$f_{Mass}(t) + f_{Dashpot}(t) + f_{Spring}(t) = p(t) \tag{21}$$

The equation of motion for a SDOF can be reformulated in terms of the structure response as:

$$m\ddot{u} + c\dot{u} + ku = p(t) \tag{22}$$

The formulas are given with the mass m, the damping coefficient c of a dashpot, the stiffness k of a spring and the external force $p(t)$. The form of the equation of motion depends on the following conditions:

- Undamped free vibrating system: $c = 0 \; and \; p(t) = 0$

- Undamped forced system: $c = 0 \; and \; p(t) \neq 0$
- Damped free vibrating system: $c \neq 0 \; and \; p(t) = 0$
- Damped forced system: $c \neq 0 \; and \; p(t) \neq 0$

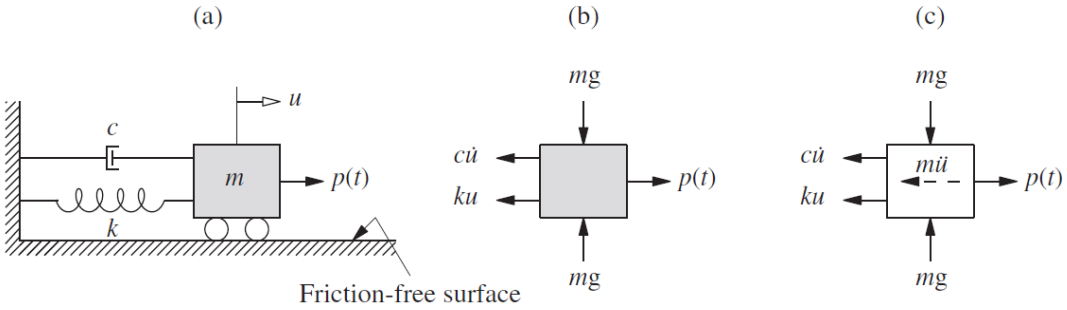

Figure 2: (a) Single-degree-of-freedom system (b) acting forces (c) forces with D'Alembert's principle [4]

2.2.2.1 Undamped free vibrating single-degree-of-freedom systems

When there is no load acting on a SDOF system, it is an unforced system. Setting the $p(t) = 0$, it gives the differential equation for an undamped system ($c = 0$):

$$m\ddot{u} + ku = 0 \tag{23}$$

With the undamped natural circular frequency

$$\omega_0 = \sqrt{\frac{k}{m}} \; [rad/s] \tag{24}$$

and the natural frequency f_0 and the natural period of vibration T_0

$$f_0 = \frac{\omega_0}{2\pi} = \frac{1}{2\pi}\sqrt{\frac{k}{m}} \; [Hz] \tag{25}$$

$$T_0 = \frac{1}{f_0} = 2\pi\sqrt{\frac{m}{k}}\ [s] \tag{26}$$

The approach for a solution of a homogenous, second-order differential Equation (23) is given as:

$$u = e^{\lambda t} \tag{27}$$

The constant λ has to be found and by solving the differential equation it comes to:

$$\lambda_{1,2} = \pm i\omega_0 \ \ with \ \ i = \sqrt{-1} \tag{28}$$

After substitution the solution is:

$$u(t) = a_1 e^{i\omega_o t} + a_2 e^{-i\omega_o t} \tag{29}$$

With the help of the Euler relations, the equation can be formulated as:

$$u(t) = A * cos\omega_0 t + B * sin\omega_0 t \tag{30}$$

A and B are unknown constants, which can be solved by differentiating the equation and set the time to zero. This is the complementary solution part of a differential equation.

2.2.2.2 Damped free vibrating single-degree-of-freedom systems

A damped SDOF system is more common in nature, the vibration decreases with time. For this kind of system without an external force, the equation of motion is given by:

$$m\ddot{u} + c\dot{u} + ku = 0 \tag{31}$$

Dividing the equation by m and inserting ω_0 which is given by Equation (24):

$$\ddot{u} + 2\xi\omega_0\dot{u} + \omega_0^2 u = 0 \tag{32}$$

$$\xi = \frac{c}{2\sqrt{km}} = \frac{c}{2m\omega_0} = \frac{c\omega_0}{2k} = \frac{c}{c_{cr}} \tag{33}$$

The solution for the differential equation depends on the damping ratio ξ, so there are three cases:

- $\xi < 100\%$ *($c < c_{cr}$)* *system is underdamped*
- $\xi = 100\%$ *($c = c_{cr}$)* *system is critically damped*
- $\xi > 100\%$ *($c > c_{cr}$)* *system is overdamped*

The critical damping coefficient c_{cr} is the smallest damping coefficient, where the system gets fully damped. Figure 3 shows examples for an underdamped system, a critically damped system and an overdamped system. The solution of the damped SDOF system depends on the form of damping and has to be calculated in different ways.

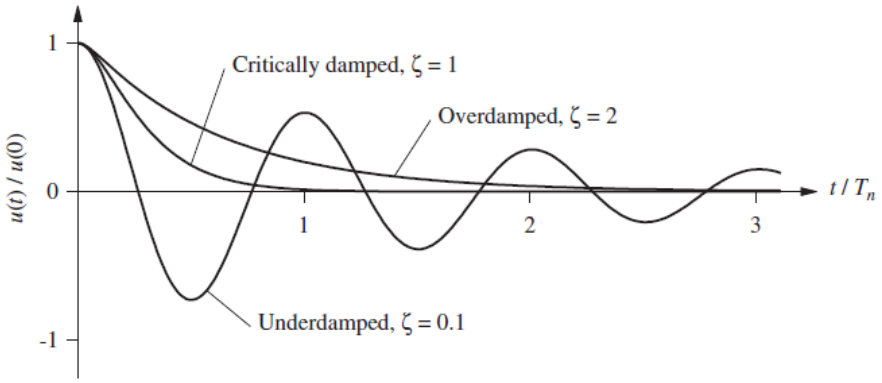

Figure 3: Examples of different damping ratios [4]

2.2.2.3 Undamped forced single-degree-of-freedom systems

For the undamped forced vibration ($p(t) \neq 0$), the particular solution for the inhomogeneous case has to be determined additionally. The particular solution consists of the external load, while the complementary solution is the part of the equation without an external load. The complementary solution has been defined before:

$$u_c(t) = A * cos\omega_0 t + B * sin\omega_0 t \tag{34}$$

The external load can be a sinusoidal load, given as:

$$m\ddot{u} + ku = p_0 \sin \omega t \tag{35}$$

The particular solution can be formed like the complementary one, which can be formulated with $\omega \neq \omega_0$:

$$u_p(t) = U_0 \sin \omega t = \frac{p_0}{k} \frac{1}{1 - (\omega/\omega_0)} \sin \omega t \tag{36}$$

So the general solution of the differential equation results in:

$$u(t) = u_C(t) + u_P(t) \tag{37}$$

2.2.2.4 Damped forced single-degree-of-freedom systems

A harmonic sinusoidal load acting on a system can be described with following equation:

$$m\ddot{u} + c\dot{u} + ku = p_0 \sin \omega t \tag{38}$$

Dividing the equation by m and inserting ω_0, it can be obtained:

$$\ddot{u} + 2\xi\omega_0\dot{u} + \omega_0^2 u = \frac{p_0}{m}\sin\omega t \tag{39}$$

The complementary solution has to be written for the damping case of a system, the particular solution can be assumed the same way as the complementary one.

2.2.3 Multi-degree-of-freedom systems [3, 4]

A multi-degree-of-freedom system (MDOF) system is defined by a finite number of degrees of freedom, like most systems in nature. An example is given in Figure 4, which has two degrees of freedom, where in (a) the system is built up of two masses that are coupled with springs and dashpots with two external forces and (b) is the free-body diagram. With the use of Newton's law the equilibrium equation for j masses is given as:

$$m_j\ddot{u}_j + f_{Dj} + f_{Sj} = p_j(t) \tag{40}$$

Example for a two-degree-of-freedom system with $j = 1{,}2$:

$$\begin{bmatrix} m_1 & 0 \\ 0 & m_2 \end{bmatrix}\begin{Bmatrix} \ddot{u}_1 \\ \ddot{u}_2 \end{Bmatrix} + \begin{Bmatrix} f_{D1} \\ f_{D2} \end{Bmatrix} + \begin{Bmatrix} f_{S1} \\ f_{S2} \end{Bmatrix} = \begin{Bmatrix} p_1(t) \\ p_2(t) \end{Bmatrix} \tag{41}$$

This can be written in a matrix equation and for all degrees-of-freedom j:

$$[m]\{\ddot{u}\} + [c]\{\dot{u}\} + [k]\{u\} = \{p_{(t)}\} \tag{42}$$

Where $\{u\}$ is the displacements vector, $\{\dot{u}\}$ the velocity vector, $\{\ddot{u}\}$ the acceleration vector, $[c]$ is the damping matrix, $[k]$ is the stiffness matrix and $[m]$ the mass matrix. $\{p_{(t)}\}$ is the external load vector.

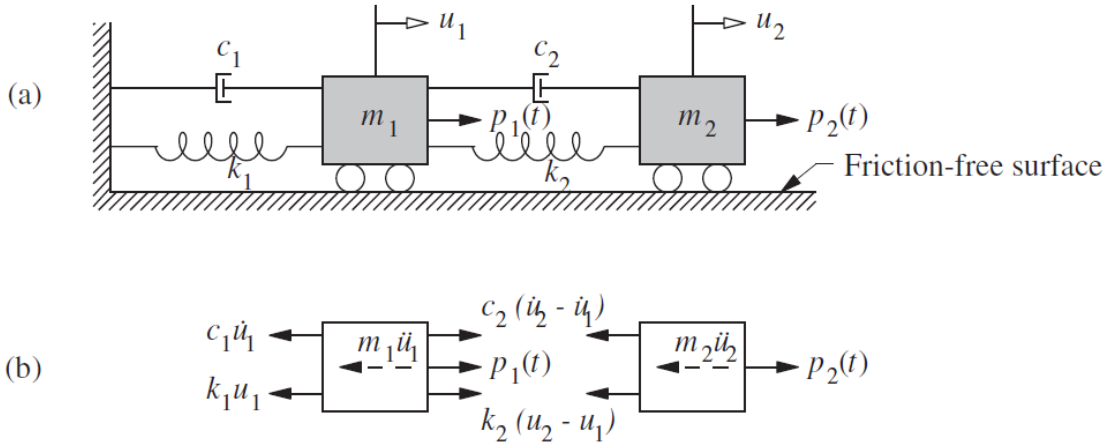

Figure 4: (a) system with two degrees of freedom and (b) its acting forces [4]

2.2.3.1 Undamped multi-degree-of-freedom systems

A MDOF system without an external force acting on it, this means free vibration and $p(t) = 0$, without damping it is given by:

$$[m]\{\ddot{u}\} + [k]\{u\} = \{0\} \tag{43}$$

The equation of an undamped MDOF system can be formulated as:

$$\{u_{(t)}\} = \{q_{(t)}\}\{\phi\} \tag{44}$$

$$\{u_{(t)}\} = \{\phi\}(\{A\}cos\omega t + \{B\}sin\omega t) \tag{45}$$

The vectors $\{A\}$ and $\{B\}$ are constants that have to be figured out. $\{\phi\}$ is the deflected shape. Inserting this in Equation (43), it results in

$$(-\omega^2[m]\{\phi\} + [k]\{\phi\}) = \{0\} \tag{46}$$

$$([k] - \omega^2[m])\{\phi\} = \{0\} \tag{47}$$

for the homogeneous part of the equation. The solution $\{\phi\} = \{0\}$ makes no sense, because it means there is no movement of the system. So there are suitable solutions given by:

$$det|[k] - \omega^2[m]| = 0 \tag{48}$$

A polynomial is received of the order n. ω^2 are the eigenvalues. Equation (48) is named the characteristic equation. There are n eigenvectors $\{\phi\}$ (natural modes of vibration) with n solutions. Next step is putting the n eigenvalues and the n natural modes into matrices, where the n eigenvectors can be listed in the so-called modal matrix Φ:

$$\Phi = [\phi_{jn}] = \begin{bmatrix} \phi_{11} & \cdots & \phi_{1n} \\ \vdots & \ddots & \vdots \\ \phi_{n1} & \cdots & \phi_{nn} \end{bmatrix} \tag{49}$$

The n eigenvalues ω^2 can be listed in a diagonal matrix, the spectral matrix Ω^2:

$$\Omega^2 = \begin{bmatrix} \omega_1^2 & & \\ & \ddots & \\ & & \omega_n^2 \end{bmatrix} \tag{50}$$

With the spectral matrix and the modal matrix the equation in connection of all eigenvalues and eigenvectors can be formed:

$$[k][\Phi] = [m][\Phi][\Omega^2] \tag{51}$$

The orthogonality relations of the natural modes and the related natural frequencies are given as following, if $\omega_n \neq \omega_r$:

$$\{\phi_n\}^T[k]\{\phi_r\} = 0 \tag{52}$$

$$\{\phi_n\}^T[m]\{\phi_r\} = 0 \tag{53}$$

Due to orthogonality the matrices are diagonal,

$$[K] \equiv [\Phi]^T[k][\Phi] \;\; and \;\; [M] \equiv [\Phi]^T[m][\Phi] \tag{54}$$

with their diagonal elements of the stiffness matrix k and the mass matrix m:

$$\{K_n\} = \{\phi_n\}^T[k]\{\phi_n\} \;\; and \;\; \{M_n\} = \{\phi_n\}^T[m]\{\phi_n\} \tag{55}$$

The solution of the undamped MDOF system can be written as:

$$\{u_{(t)}\} = \sum_{i=1}^{n} \phi_n q_n\,(t) \tag{56}$$

$$\{u_{(t)}\} = \sum_{i=1}^{n} \phi_n (A_n \cos \omega t + B_n \sin \omega t) \tag{57}$$

A_n and B_n are constants that have to be determined.

2.2.3.2 Damped multi-degree-of-freedom systems

For a damped MDOF system with free vibration and $p(t) = 0$, the differential equation is the following

$$[m]\{\ddot{u}\} + [c]\{\dot{u}\} + [k]\{u\} = \{0\} \tag{58}$$

All the n differential equations are given as

$$M_n\ddot{q}_n + C_n\dot{q}_n + K_n q_n = 0 \tag{59}$$

The orthogonality relations can be applied for the damping matrix $[c]$ as well:

$$\{\phi_n\}^T[c]\{\phi_r\} = 0 \tag{60}$$

$$[C] \equiv [\Phi]^T[c][\Phi] \tag{61}$$

$$\{C_n\} = \{\phi_n\}^T[c]\{\phi_n\} \tag{62}$$

Normally the damping matrix C is diagonal when it can be expressed proportionally to stiffness and mass. The diagonal matrices $[M]$ and $[K]$ were shown in Equation (60). Including the damping the solution is obtained in the same way as in the undamped systems.

2.2.3.3 Rayleigh Damping

The Rayleigh Damping is one way to build a damping matrix for a certain system. Therefore, modal damping ratios are needed, which can be used due to already existing data from recorded earthquakes that were acting on the structure or from similar structures. Depending on the type of structure and when there is no data available, usually a 5% value is used for the damping ratio.

It starts first with introducing the mass-proportional damping and stiffness-proportional damping:

$$[c] = a_0[m] \ and \ [c] = a_1[k] \tag{63}$$

The coefficients a_0 and a_1 are constants and concerning the orthogonality properties, the damping matrix is diagonal. Therefore, the Rayleigh Damping is defined by

$$[c] = a_0[m] + a_1[k] \tag{64}$$

Then for a certain index n, which specifies the mode, the damping ratio ξ_n is given as

$$\xi_n = \frac{a_0}{2}\frac{1}{\omega_n} + \frac{a_1}{2}\omega_n \tag{65}$$

Above is the equation with the angular speed ω_n for mode n, with $\omega_n = 2\pi f_n$ this equation can also be formulated as:

$$\xi_n = \frac{a_0}{4}\frac{1}{\pi f_n} + a_1\pi f_n \tag{66}$$

Therefore, the parameters a_0 and a_1 can be calculated with ξ_i and ξ_j, which can be written like

$$\frac{1}{2}\begin{bmatrix} 1/\omega_i & \omega_i \\ 1/\omega_j & \omega_j \end{bmatrix}\begin{Bmatrix} a_0 \\ a_1 \end{Bmatrix} = \begin{Bmatrix} \xi_i \\ \xi_j \end{Bmatrix} \tag{67}$$

The given indices i and j are the modes. When both modes have an equal damping ratio ξ (e.g. 5%), then the two coefficients can be solved.

$$a_0 = \xi \frac{2\omega_i \omega_j}{\omega_i + \omega_j} \quad and \quad a_1 = \xi \frac{2}{\omega_i + \omega_j} \tag{68}$$

A suitable damping ratio for two specific modes has to be determined to calculate the coefficients a_0 and a_1 that shows the horizontal line of ξ (or ζ) in Figure 5. For each angular speed ω_n exists one damping ratio. It is visible that the mass-proportional part dampens the lower frequencies and the stiffness-proportional part dampens the higher frequencies.

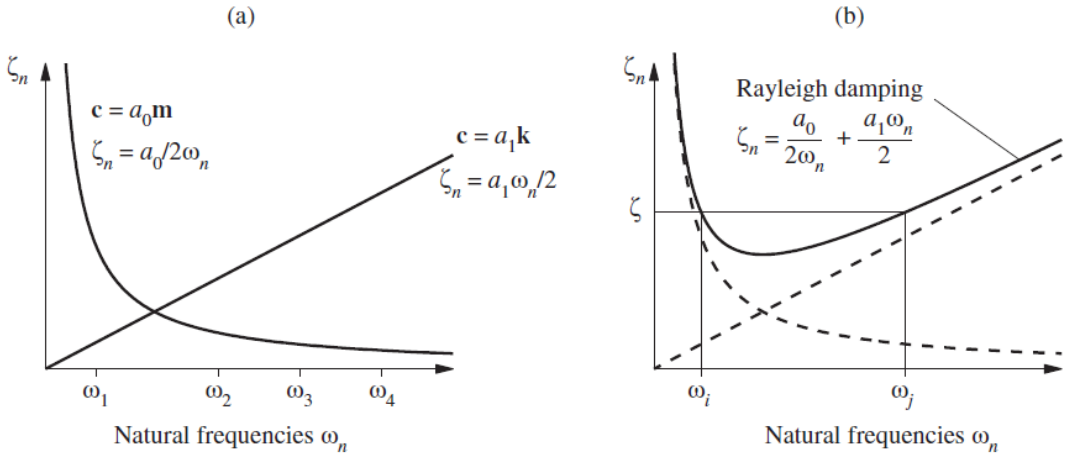

Figure 5: Rayleigh Damping [4]

2.2.4 Seismic assessment of concrete gravity dams [5]

Usually FEM is used for seismic calculation of concrete gravity dams. After Wieland [5], there are some steps to take into account in a preliminary analysis of a dam. First the geometry of the dam has to be modelled and then discretized with a sufficient number finite elements to obtain a proper mesh of the construction. Afterwards the stiffness matrices, the damping matrices and the mass matrices are needed to establish the equation of motion for a MDOF system. At least the seismic response has to be calculated with a suitable method such as the conventional pseudo-static method or the response spectrum method. The time-history analysis can also be used for more detailed designs of concrete gravity dams and in general for all other dam types, as well as hydraulic structures in the field of hydraulic engineering.

Two-dimensional models suit better for a FEM calculation of gravity dams, because plain strain conditions can be assumed. Therefore, the 2D model is considered as a cut-out section of a longer concrete gravity dam, where stresses can occur in longitudinal direction, but no strains [1]. Most arch dams need a three-dimensional model due to its occurring stresses. For the dynamic analysis it is necessary to include the foundation rock in the modelling, as there can occur correlations and difficulties in an earthquake analysis, for example. In the static analysis the idealized foundation block might not be that important. The dynamic behavior of the systems depends on the size of the foundation rock, which is taken into account.

2.2.4.1 Seismic loads [5]

In earthquake engineering on gravity dams a combination of several loads has to be used. The seismic loads consist of the inertia force, dynamic water pressure or earth pressure, while the static loads include the hydrostatic water pressure, dead load, uplift force etc. In chapter 6 the used loads and boundary conditions of the performed calculation of Koyna Dam are explained.

2.2.4.2 Time history analysis [4, 5]

The time history analysis – more specifically the time-step integration – is used in the transient analysis of the numerical calculation, therefore, this method is explained in detail.

The time history analysis is a dynamic analysis that shows the time-dependency of the response of a system. The calculation of a MDOF system depends on the equation of motion:

$$[m]\{\ddot{u}\} + [c]\{\dot{u}\} + [k]\{u\} = \{p_{(t)}\} \tag{69}$$

For the differential equation there are two possible methods to obtain the solution: the modal solution and the direct integration. But the first one is only applicable

on linear systems. Furthermore, Equation (69) can be solved through direct integration (time-step integration - Figure 6). Therefor exist implicit (e.g. Newmark) and explicit (e.g. central difference method) solution methods.

For the time-stepping integration exist following starting conditions at $t = 0$:

$$\{u\} = \{u_{(0)}\} \; and \; \{\dot{u}\} = \{\dot{u}_{(0)}\} \tag{70}$$

So the displacement vector $\{u_{(t)}\}$ can be determined. Then time scale is split into steps with a fixed length Δt. The external load is given with a vector $\{p_i\} \equiv \{p_{(t_i)}\}$ at a certain time $t_i = i\,\Delta t$ at t_i. The following results are displacement $\{u_i\} \equiv \{u_{(t_i)}\}$, velocity $\{\dot{u}_i\} \equiv \{\dot{u}_{(t_i)}\}$ and acceleration vectors $\{\ddot{u}_i\} \equiv \{\ddot{u}_{(t_i)}\}$. Then there is the equation at time *i:*

$$[m]\{\ddot{u}_i\} + [c]\{\dot{u}_i\} + [k]\{u_i\} = \{p_i\} \tag{71}$$

Next step is the response $\{u_{i+1}\}$, $\{\dot{u}_{i+1}\}$ and $\{\ddot{u}_{i+1}\}$ of the system at time $i + 1$:

$$[m]\{\ddot{u}_{i+1}\} + [c]\{\dot{u}_{i+1}\} + [k]\{u_{i+1}\} = \{p_{i+1}\} \tag{72}$$

The starting condition $i = 0$ has to be known. For the three vectors $\{u_{i+1}\}$, $\{\dot{u}_{i+1}\}$ and $\{\ddot{u}_{i+1}\}$ three equations are needed. One of these equations is Equation (69) at a certain time step at which the response is solved for. If this time step is *i*, it is called an explicit method, whereas the time step is *i+1*, it is known as an implicit method.

For the numerical procedure, the important requirements after Chopra [4] are:

1. The more precise the solution is approximated, the smaller the time step *Δt* becomes, this means it converges.

2. When round-off errors appear, the solution should still work in a proper way.

3. The results of the numerical analysis should avoid too much errors and reach the correct solution.

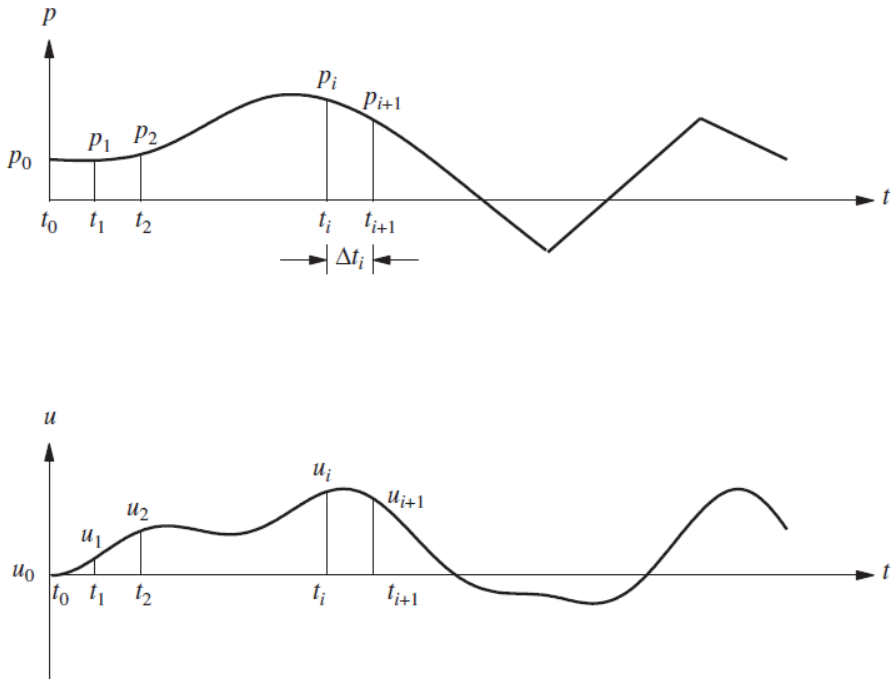

Figure 6: Time-stepping method: above the external force at a certain time step, below the displacement vectors [4]

3. Reinforcement of concrete gravity dams

This chapter deals with the reinforcement of dams with steel anchors. There exist passive and prestressed anchors, they can be installed as a cable or strand and they can also be arranged in rows in the section of a dam. Most efficiently used are prestressed anchors, which are able to be tested to verify the prestressing force. [6, 7]

3.1 Passive anchors [6]

To improve the strength of the concrete structure of dams, several of them are built with passive anchors to endure static loads as well as dynamic loads. In case of large dams, which have already been subjected to earthquake forces for example, it is common to reinforce them with prestressed anchors, whereas smaller dams can be built newly with implemented anchors. One important issue is the reliability against external loads, where the yield strength of an anchor should be higher than the applied forces. Figure 7 shows an example of a typical small gravity dam in (a) and a selected section in (b). In the selected section of a passive reinforced dam (Figure 7 (b)) the eccentricity y is given for the force P. The stress σ_z can be calculated with the equilibrium of forces as follows:

$$\sigma_z = \frac{P}{A} + \frac{M_x}{I_x} * y \tag{73}$$

Stefan and Léger [6] present in their paper three variants for calculating this system of a reinforced section of a dam. Since this would go beyond the scope of the master thesis, it will not be discussed more detailed here. Furthermore, the FEM can be needed to perform an analysis of an anchored dam with a connected reservoir and rock mass.

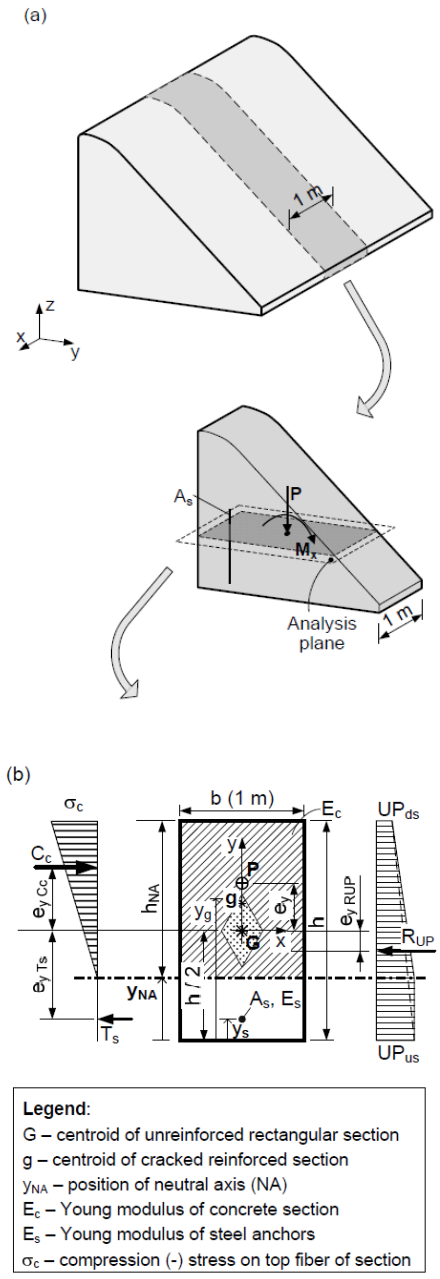

Figure 1: Flexural analysis for dams:
(a) computational model, and (b) sectional analysis

Figure 7: Model of a small gravity dam with passive reinforcement (a) and its section (b) [6]

In addition the paper explains the performance of a dam with an applied hydro-static pressure, when it is reinforced with a passive anchor. In comparison the same dam without any reinforced is represented. As the water level rises of the reservoir, cracking of the unreinforced concrete is possible since the stresses exceed the bearable tensile strength of the dam. On the other hand with a passive

anchor the maximum stresses of the concrete and steel are still in their acceptable limit of yield strength even with a rising water level of the reservoir. In conclusion the passive reinforcements can reduce the uplift pressure as well as ensure stability against sliding and overturning.

3.1.1 Failure causes of passive anchors [6, 7]

There are some failure causes which can appear during the life span of a passive anchor caused by dynamic loads or other external forces. To guarantee reliability of the reinforcement, some failure causes have to be taken into account during the calculation a suitable system. For passive anchors (and also for prestressed anchors, explained in chapter 3.2.1), tensile or tensile-shear failure of the anchor, shear failure between the grout and tendon or between grout and rock or concrete can occur. Also uplift of the rock mass where the anchor is placed into, is possible due to a low weight of the rock cone.

Figure 8 shows the cross-section of an anchor in (a), in (b) the different tensile and shear failure causes and in (c) a diagram with the shear force and the shear displacements of an anchor. Corrosion is also an important topic for passive anchors as well as post-tensioned anchors. With special tests it is possible to determine the remaining strength of a corroded anchor. In newly built concrete dams there should be implemented some removable testing anchors for regular check of corrosion, so the pH-value of the concrete cover is important. Passive anchors cannot be tested to verify the pretension force in comparison to prestressed anchors.

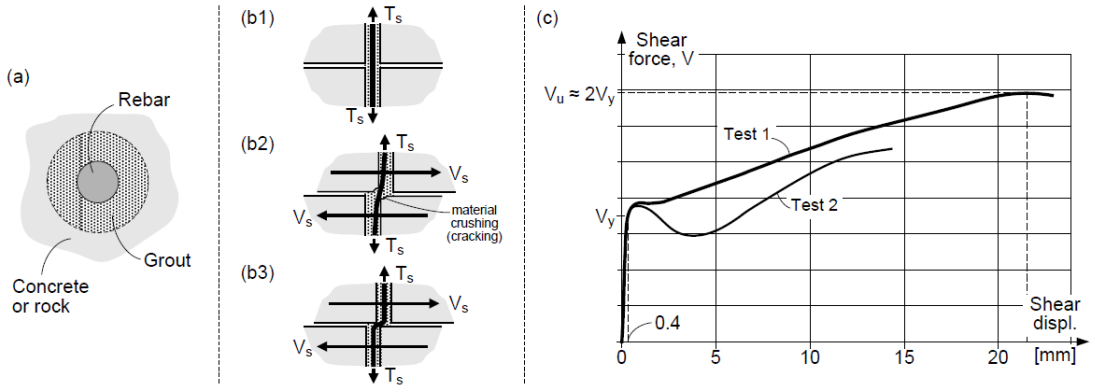

Figure 8: (a) grouted anchor in concrete, (b1) tensile failure, (b2) cracking of material, (b3) tensile-shear failure and (c) shear force-displacement diagram of a passive anchor [6]

3.2 Prestressed anchors [7]

Prestressed anchors (also called post-tensioned anchors) are mainly installed in dams for reinforcing the already existing concrete structure in terms of safety requirements. Figure 9 shows a post-tensioned anchor installed in a dam with its individual components. Parts of it are a grouted and a free length of the anchor, an anchor head and it has a protection attribute against corrosion as well.

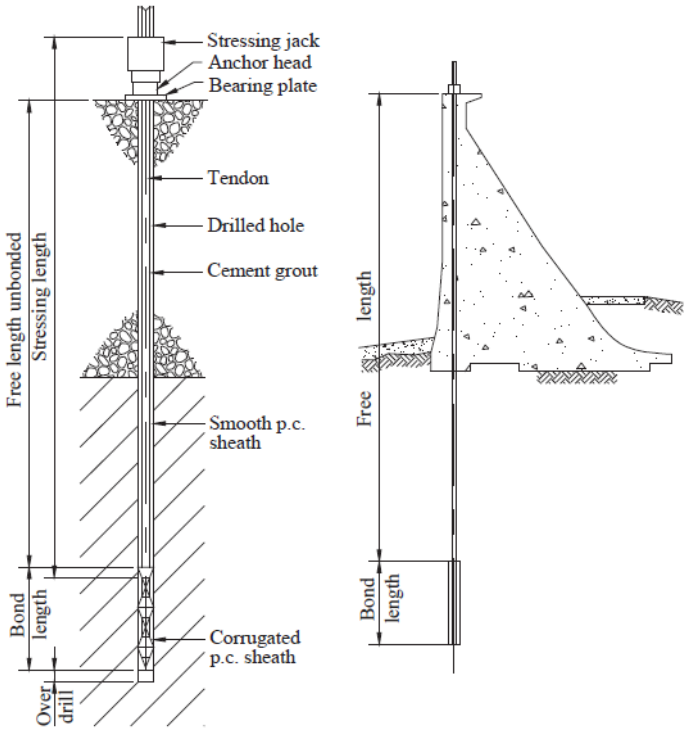

Figure 9: Prestressed anchor in a concrete dam [8]

E. T. Brown used in his report [7] various sources of literature from several authors to provide this overview of the utilization of post-tensioned anchors. Some practical uses of anchors are assembled for concrete gravity dams. One important point is the use against overturning of the dam or sliding in downstream direction due to the water pressure in case of a concrete dam. Also slopes and erosion areas are secured with highest efficiency with additional reinforcement of prestressed anchors. The resistance to earthquakes can be increased with anchors in dams that were not built with suitable concrete to withstand seismic loading.

For the first two cases of overturning and downstream sliding, the typical location and inclination of the installed prestressed anchors in a concrete gravity dam is depicted in Figure 10. The necessary pretension force in the anchor can be determined by using the available forces given in a 2D system of the dam. Therefore, a minimum required force can be defined at which the dam is not moving regarding the factor of safety and the moment equilibrium. Generally a calculation of a concrete gravity dam is performed in a numerical 2D analysis, where the forces are determined for 1 m slices of monoliths cut out of the dam. Then the loads are applied in the analysis, such as static (dead load or hydrostatic pressure) and dynamic forces (earthquakes) acting on the structure.

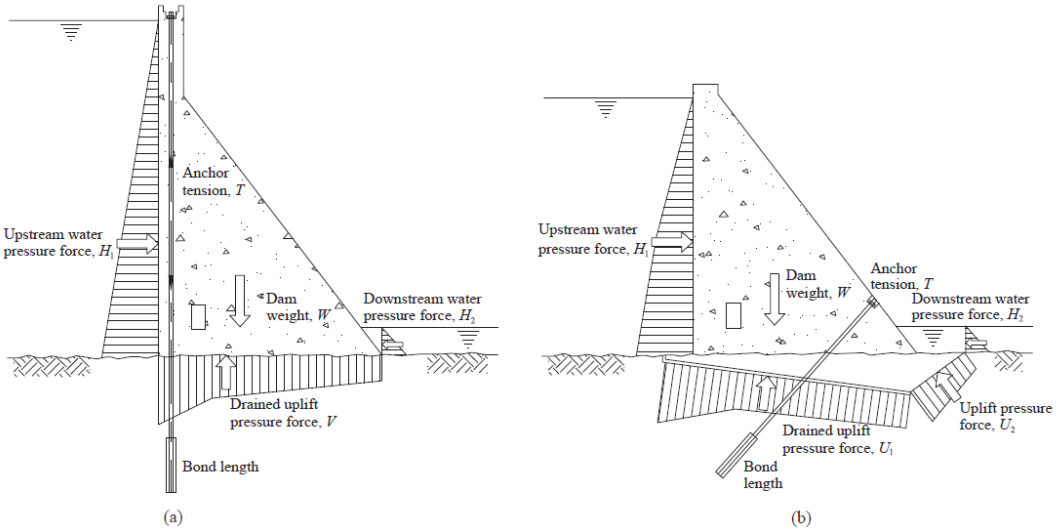

Figure 10: Reinforcement to withstand (a) overturning and (b) downstream sliding [9, 10]

3.2.1 Failure causes of prestressed anchors

There are four causes, which can happen at installed prestressed anchors due to incorrect installation or poor material properties. Brown [7] listed the following causes of anchor failure:

- *"Steel tendon tensile failure"*
- *"Grout-tendon bond or interface failure"*
- *"Rock-grout bond or interface failure"*
- *"Shear or uplift failure within the surrounding rock mass"*

The four causes of failure behavior are depicted in Figure 11. The grouted length of an anchor is generally determined in terms of preventing (b), (c) and (d). Furthermore, the shear failure is important to mention that can occur at passive anchors as well as post-tensioned anchors, shown in Figure 8.

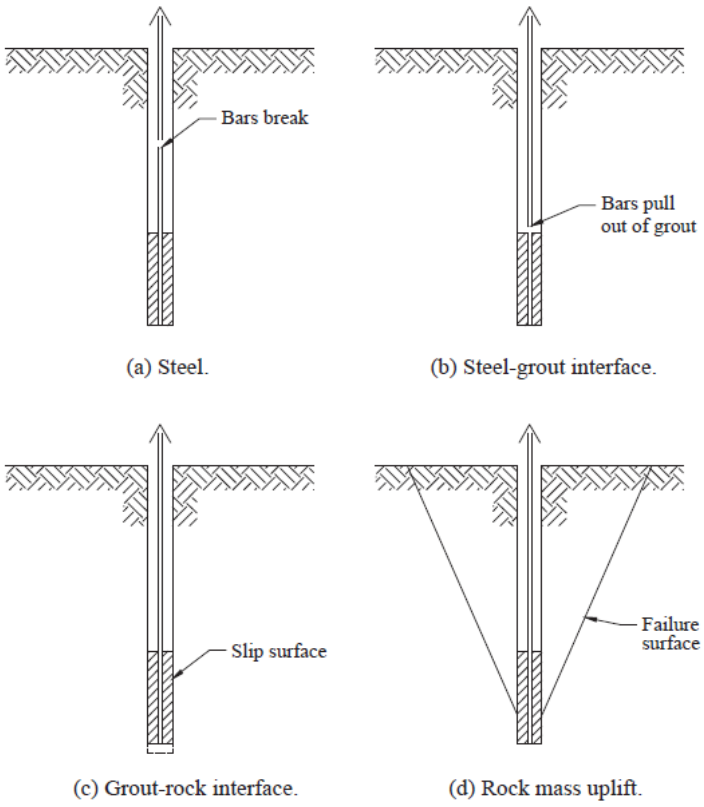

Figure 11: Four failure causes of post-tensioned anchors – (a) tensile failure of the steel tendon, (b) failure of the interface between steel tendon and grout, (c) failure of the interface between rock and grout and (d) uplift failure of the rock mass [11]

In the failure mechanism of (a) the steel tendon is broken, which happens when the maximum bearable force of the installed anchor is lower than the pretension force, then the material cracks.

The case of (b) can occur, when there is not enough frictional resistance respectively shear resistance available between the grout and the steel. So the pretension force can be responsible for pulling out the anchors of the grout by a too high load and too less connection between the grout and the steel.

Failure (c) is very similar to (b), but more problematic usually. The whole bond section of the anchor system gets pulled out by the applied pretension force due to the lack a shear resistance between the grout and the surrounding soil or rock.

To prevent failure cause (d), the shear resistance of the rock surrounding the anchor-grout system, should be able to withstand the uplift caused by the pretension force. This happens due to sufficient weight of the rock cone as well as the counteracting shear resistance against uplift failure. For the failure cause it is important to consider more than one anchor installed next to each other, where the uplift failure can affect the whole series of grouted anchors.

3.2.2 Installation of anchors

One main issue is the geological investigation of the ground, which serves as the foundation of a concrete dam. Therefore, the occurring stresses in the rock need to be determined as well as the friction angles, probably existing faults and the strength of the rock foundation. Before the initial installation of anchors can be started, some prototype anchors for testing reasons are needed and implemented in the rock or concrete required to reinforce. Thereby failure causes described before can be excluded and the drilled borehole, in which the anchors are placed, is tested on stability. The mixture of grout applied in the borehole undergoes many attempts to find a suitable grout strength and consistency. To ensure durability and provide the necessary safety the anchors should get a proper stressing and after some lifetime the ability of applying pretension once more should be given. Also most of the components of the anchored system should be accessible for maintenance and examination if there are already corroded parts.

3.2.3 Strand anchors [12]

For numerical studies presented in this thesis, seismic retrofit by anchors is investigated. Therefore, the data of DYWIDAG systems for a strand anchor is used, so the concept is described.

With the prestressed DYWIDAG anchors (Figure 12) it is possible to counteract displacements and stresses occurring in the ground which is required to reinforce.

As mentioned before, corrosion is an important topic in anchoring systems, therefore, the described anchors here have a suitable protection system against corrosion. There exist three parts of an anchor, the grouted length, the non-grouted length and the head of the anchor. The first part of a strand anchor is fixed with cement, which ensures the necessary force transmission in the ground. In the middle part there is the free length, in this part the pretension works. The anchor head serves for applying the force in the soil and the whole system. Figure 12 shows the strand anchors and the specification of the individual components:

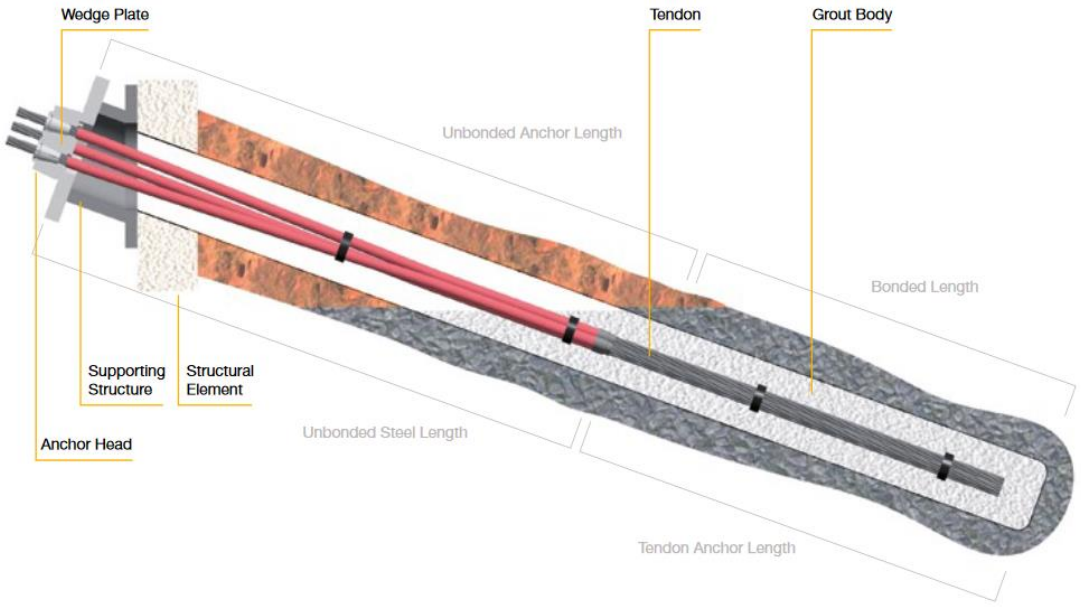

Figure 12: Design of a strand anchor [12]

4. Koyna Dam

Koyna Dam is the main topic of this thesis, as its dimensions and the data of the 1967 earthquake are used for the numerical analysis. In this chapter the geology and seismicity of the region are described as well as the section of Koyna Dam with its related values. Concerning the US system that Chopra and Chakrabarti used in their reports of Koyna, all values had to be changed in the metric system in the text and also before starting the calculation. This system is used in all the reports of Koyna Dam, so the needed conversion factors are following:

- Length: $1\ mile = 1.609\ km$, $1\ foot = 0.3048\ m$ and $1\ inch = 2.54\ cm$
- Pressure: $1\ psi = 0.006895\ MPa$
- Force $1\ kips = 4.4482\ kN$

4.1 Koyna Dam region [13, 14]

Koyna Dam got its name from the River Koyna in this region and is situated in the Krishna river basin in the western part of the Indian peninsula. It was constructed to gain electricity from hydropower in the state Maharashtra. In this region most of the rainfalls per year occur during the monsoons between June and September. Therefore, it was necessary to store the excess water obtained in the wet season to store it for the dry season.

Koyna Dam is situated about 193 km south of Mumbai. In Koynanagar, a small town near the dam, was used as the organization point during its construction between 1954 and 1963.

4.1.1 Geology

The Koyna River flows into the Krishna River about 5 kilometers south from the dam which leads to the Bay of Bengal on the East Indian coast.

Koyna Dam lies next to a continental divide, the Western Ghats, which has heights up to 1700 m.a.s.l, the plateau level is about 600 m.a.s.l. It is located in

the so-called Deccan Traps, which are thick dried lava flows made out of basaltic rocks and cover about 500.000 km² of the Indian peninsula. Due to the Koyna Earthquake on December 11, 1967 some superficial investigations started in order to gain data about the seismic conditions of the Koyna area. As far as it was known, no active faults were existing, but many hot springs in the Western Ghats with smaller earthquakes could have led to a higher seismicity. [15, 16]

Rock samplings were taken from the ground, where Koyna Dam is located, which pointed out three different minerals, tuff breccia, vesicular basalt and massive basalt. Brecciated rock has the lowest compressive strength in comparison to the other minerals and is also unreliable. The terrain had been improved to provide a foundation made of mainly massive basalts which guarantees a suitable ground. [17] The Modulus of elasticity and the compressive strength of the existing rock types are listed in the table below:

Table 1: Properties of different rock types in the Koyna foundation [18]

	Compressive strength	Modulus of Elasticity
Tuff Breccia	High: 17.24 MPa Low: 10.34 MPa	8.9e3 MPa
Vesicular Basalt	High: 68.95 MPa Low: 16.55 MPa	3.45e4 MPa
Massive Basalt		> 6.9e4 MPa

4.1.2 Seismic activity of Koyna region

The following map of India (Figure 13) shows the seismic zones of the whole country. Obviously, the northern part of India is more vulnerable to earthquakes than the south, the Indian peninsular. According to former data it has turned out

that between years 1594 and 1967 about twenty stronger earthquakes were recognized in West India. These are shown in Figure 14. Relating to the magnitude, one earthquake of August 1764 was close to the Koyna Earthquake in 1967. The earthquakes happening in the past were small and the fact the Indian peninsula was seen as rather seismically inactive was the main reason for wrong judgement of seismicity for the constructions in this area. [19]

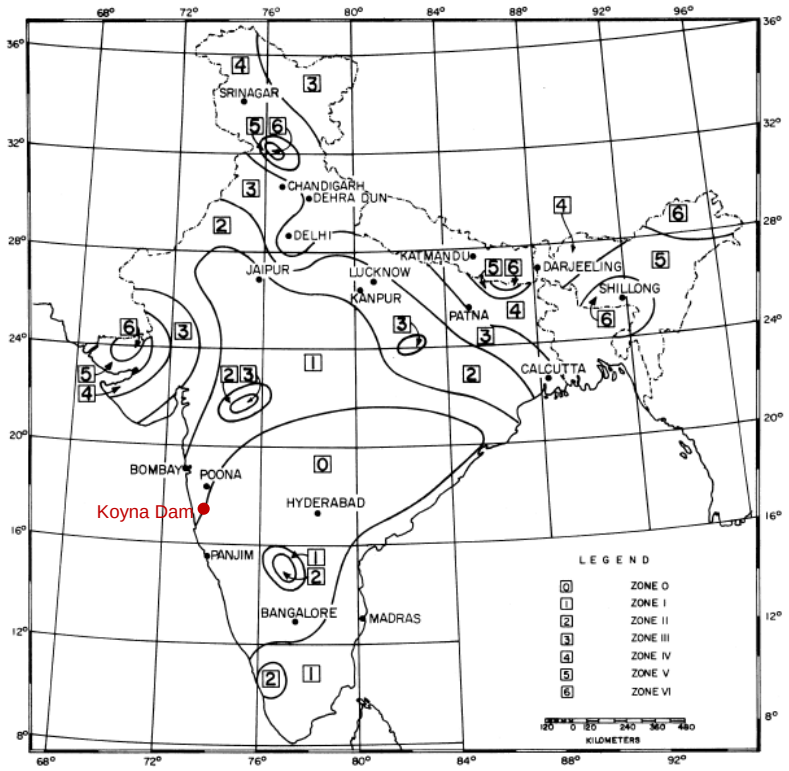

Figure 13: Seismic zones in the Indian country [20]

As shown in Figure 13, the most seismic active areas are located in the north of India, where the mountain range of Himalaya and Karakorum regions stretch along the borders. Also some parts in the north-west of India are assumed to be more vulnerable to ground motion. The peninsula in the south is marked with zones 0 up to 3, which indicates a seismic stable zone. As this map was published in the 1960s, nowadays the seismic zones may be relocated to the respective regions after the Koyna Earthquake along with other strong earthquakes.

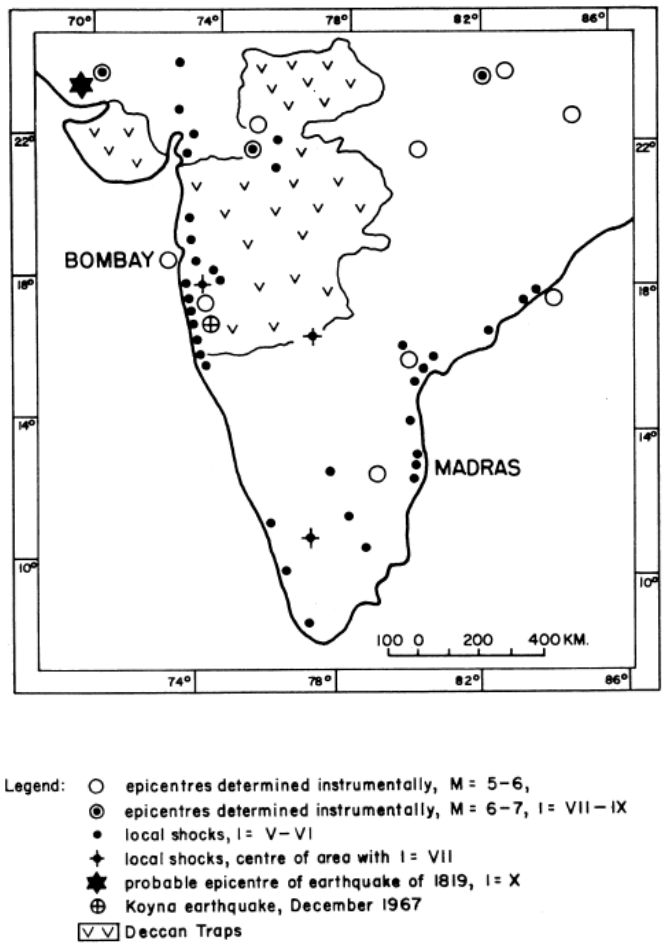

Figure 14: Earthquakes from the past [16]

In 1962 during the wet season was the first filling of the Shivajisagar lake, the reservoir inbounded by Koyna Dam. Then some small earthquakes was recognized, so four seismographs were positioned around and at the dam itself. [21] The seismic activity was growing in 1963, so many smaller earthquakes occurred and some epicenters of these are depicted in Figure 15.

Three months before the Koyna Earthquake, two earthquakes of higher magnitudes 5.0 to 5.5 were felt. It came along with many fore- and aftershocks with epicenters nearby the dam.

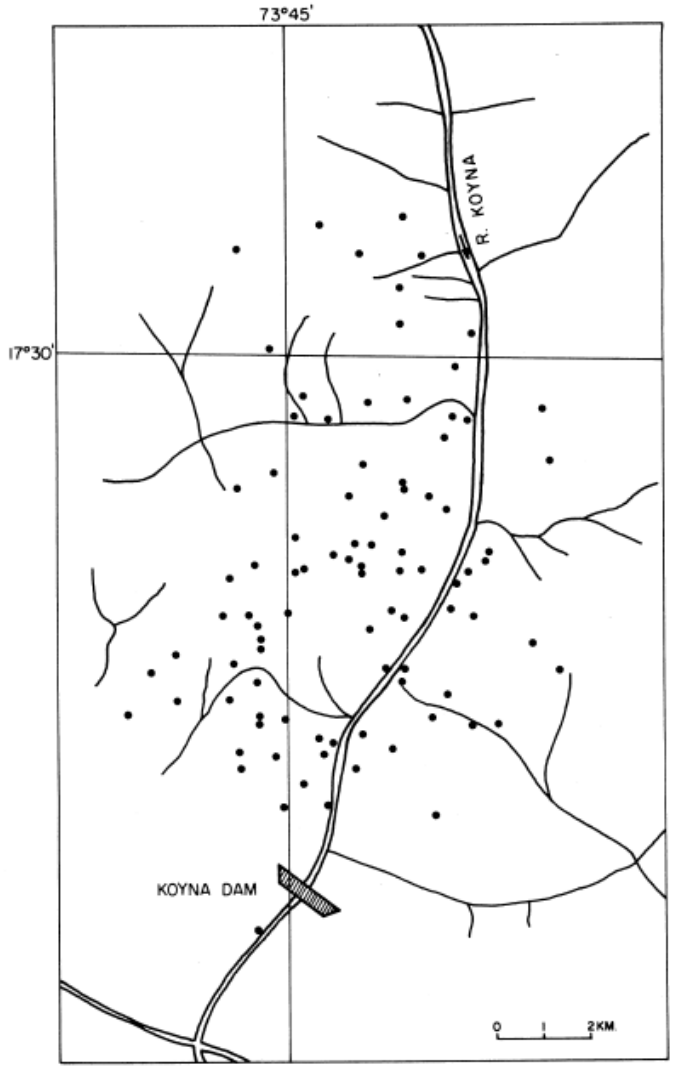

Figure 15: Epicenters of earthquakes in the Koyna region since initial filling of the reservoir [22]

On December 11, 1967 the small town Koynanagar was shocked by an earthquake of magnitude 6.5 with the epicenter not far from Koyna Dam and a depth of the hypocenter from 8 to 20 kilometers. It was recognized 600 kilometers away from the epicenter. This was the first earthquake in the region, which was responsible for damaging Koyna Dam and also destroyed many buildings in its surrounding, thus 180 people lost their lives. The earthquakes occurring in a period of around the Koyna Earthquake are depicted in Figure 16. After the main earthquake very high magnitudes of 5.5 to 6.2 were felt.

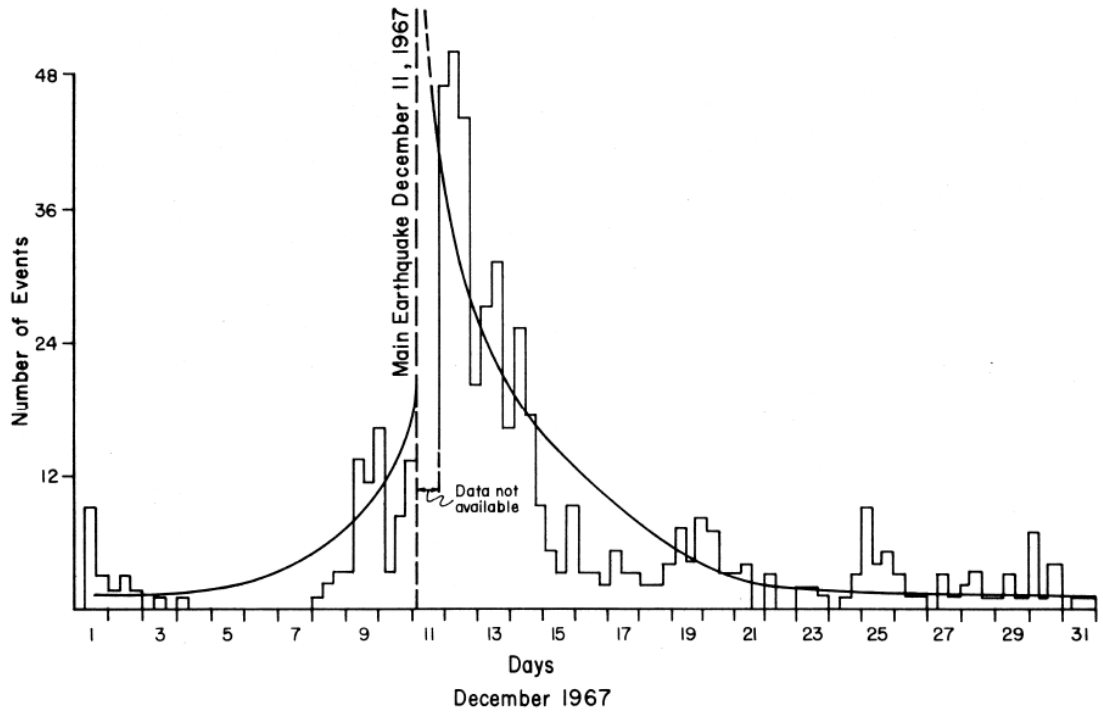

Figure 16: Tremors around the earthquake of December 11, 1967 [22]

It is possible that the reservoir induced seismicity due to an originally not existing reservoir, as it is the Shivajisager, can cause the development of seismic activity in a region. This was also noticed earlier in other regions on different continents. But there are also concrete dams on the Indian peninsula with a foundation of the same rock composition as the Koyna foundation without any occurrence of earthquakes. [23]

In Figure 17 the relation between the frequencies of earth tremors in the Koyna area, the water level of the reservoir and the discharge in a period of 1963 - 1967 is clearly visible.

The possible reason why a strong earthquake of magnitude 6.5 at the dam site can be caused by filling a reservoir, is described more precisely in chapter 4.2. [5]

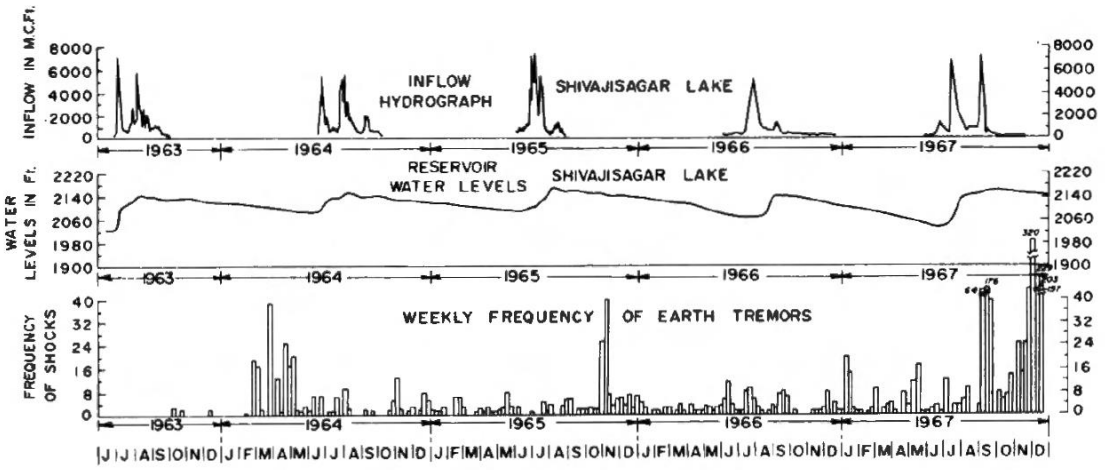

Figure 17: Correlation between the inflow hydrograph, water level of the Shivajisagar lake and frequency of earth tremors [24]

4.2 Dam-reservoir-induced seismicity [5, 25, 26, 3]

Induced seismicity can cause considerable damage on dams, like Koyna Dam or the Hsinfengkiang buttress dam in China.

For comparison, the Hsinfengkiang dam has a height of 105 m and was shocked by a 6.1 tremor in 1962 and its reservoir started filling 3 years before. While the 103 m high Koyna Dam experienced an earthquake with 6.5 magnitude in 1967, the impoundment of water started in 1962.

Actually dam-reservoir-induced tremors can occur in regions with a higher seismicity as well as in regions without any history of earthquakes. The Hoover Dam was one of the first dams, where this phenomena was observed in the 1940s. When the dam is higher than 100 m and the reservoir volume greater than 10^9 m^3, an increase of smaller shocks is reported. Currently there are some theories about how the reservoir-induced seismicity works, where Wieland [5] summarized the findings from [26] as follows:

- *The increasing stress conditions triggered by large reservoirs is still too small to set off an earthquake without already existing critical stresses in areas of faults in the foundation rock. If there are already cracks and initial stresses in the rock mass, they have to be large enough to trigger seis-*

micity. Therefore, the reservoir can trigger earthquakes due to the increase of ground water pressure in the cracks. This is also possible when there is an interaction of the additional stresses with the original ones.

- *The increase of ground water pressure leads to decreasing of the friction resistance. Normally this case happens where a strike-slip fault is present, which is shown in Figure 18 (a). Presumably Koyna Dam is located above this kind of fault. Usually one year or several years after filling the reservoir a large magnitude rattles the damsite.*

- *The triggering of an offset caused by interaction of additional stresses with the original ones is assumed to occur on a strike-slip fault shown in Figure 18 (b). There the largest tremor happens short time after filling a reservoir or during the filling process.*

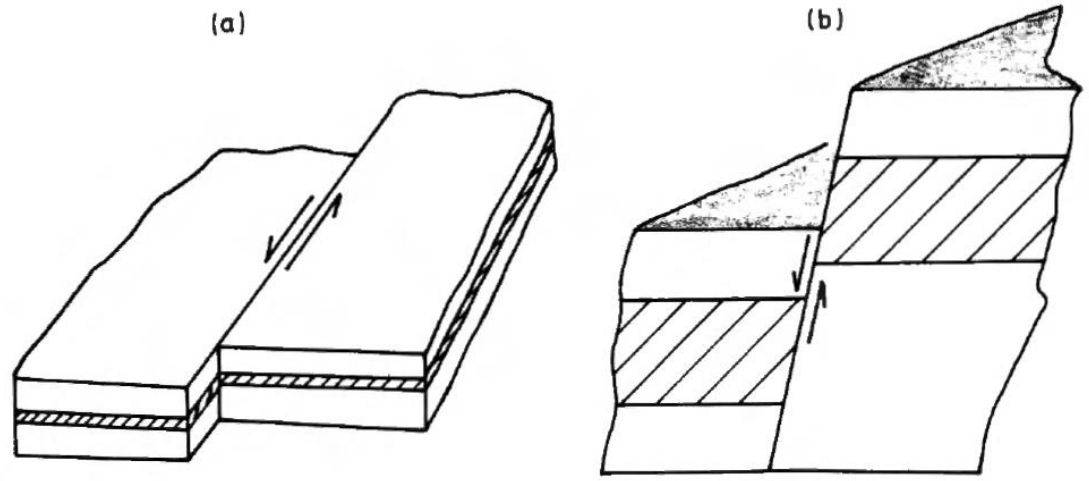

Figure 18: (a) strike-slip fault and (b) normal or reverse fault [5]

In conclusion, the faster a reservoir was filled up, the stronger the earthquake shocks have been. Usually the maximum shock occurs within a short period after the first impounding.

Induced seismicity can be avoided by stepwise or slower filling of reservoirs and seismic investigation and measurements long before the impoundment of the reservoir starts to exclude former seismic activity in the affected area.

4.3 Koyna Dam section [14]

There are several factors which caused the construction of a storage power plant in 1950. On the one hand there falls 3800 – 6300 mm of rain during the wet season in the summer months due to its position in the tropical climate area. This means the water level of the river was permanently high without any use for the excess water in the raining season. Also the geology, as it is described before, served as a good argument for the design of a storage power-plant.

Primarily Koyna Dam was considered to be built in two steps, but due to a high demand of electricity in the Maharashtra state the whole dam was decided to be built at once. So the dam was built from an elevation of 561.5 m.a.s.l up to 664.5 m.a.s.l.

Koyna Dam is divided in monoliths with a width of 15.28 m. In Figure 19 the plan and the elevations (in ft) are depicted along with the galleries, where two of them provide the installation points of strong motion accelerographs. They are situated in monolith 1A respectively in monolith 13. The parameters of the dam are following:

- Height of highest monolith: 103 m
- Block width of monolith: 15.28 m
- Crest length of dam: 854 m
- Length of spillway: 91.44 m
- Reservoir capacity: ~ 2.8 billion m^3

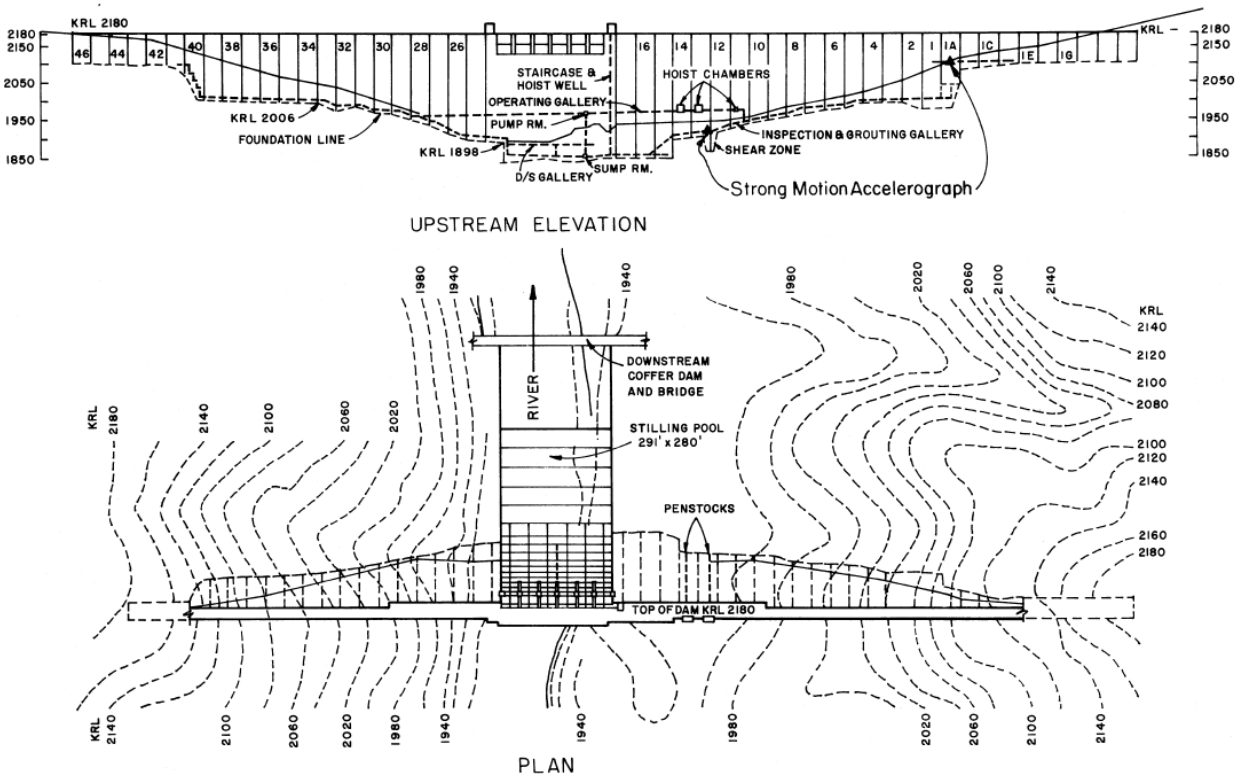

Figure 19: General plan of Koyna Dam [14]

The material used for Koyna Dam is rubble concrete with rubbles of sizes between 0.1 and 0.4 meter. Conventional concrete was used additionally for a waterproof layer. In Figure 20 the cross sections of both non-overflow and overflow monoliths are shown. [17, 27]

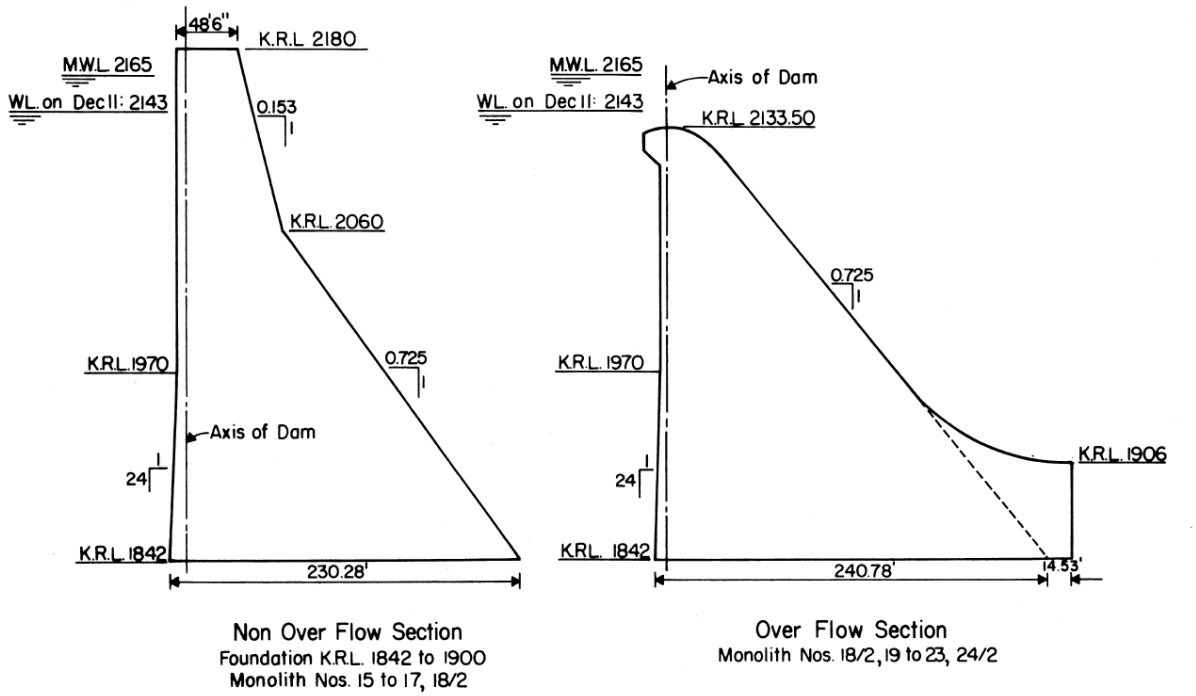

Figure 20: Koyna Dam overflow and non-overflow cross sections [14]

There were some requirements for designing Koyna Dam concerning the stresses, where especially the compressive stresses should stay within the range of the bearable stresses of the concrete.

In the year 1966 the West Indian part, where Koyna Dam was constructed was assigned as seismic zone 1 (see Figure 13), hence the seismic coefficients are 0.00, 0.02 and 0.04. For the entire dam a seismic coefficient of 0.05 was set.

Figure 21 shows the non-overflow section of Koyna Dam in comparison to a section of a typical concrete gravity dam. It resulted in a deviation of the cross section design by constructing the dam at once. Therefore, the crest part of the dam is higher und thicker than it would be in any other concrete gravity dam, whereas the bottom part is narrower in its base width. However, it was considered to fulfill the safety requirements as normal dam sections would do. [17, 28, 29]

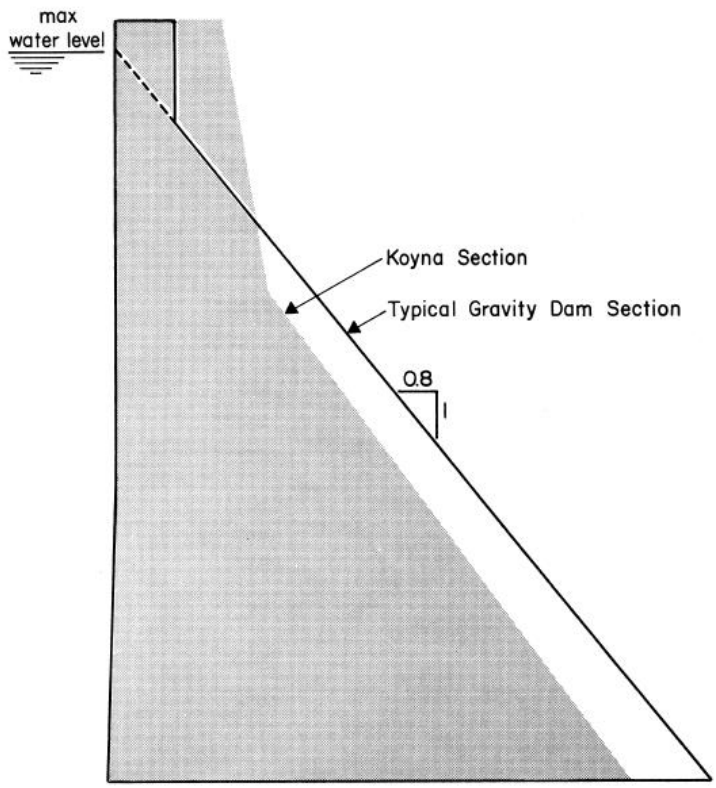

Figure 21: Comparison of Koyna Dam to a typical gravity dam section [14]

4.3.1 Concrete strength of Koyna Dam

For Koyna Dam, four concrete mixtures were used for the construction, where three of them, which were mainly used, are given in Table 2. The tensile strength is a 1/10th of the allowable compressive stresses for concrete.

Table 2: Concrete mixes used in the Koyna sections [29]

Mix No.	Parts of the Dam	Compressive Strength (MPa)	Tensile Strength (MPa)	Allowable Compressive Stress (MPa)	Allowable Tensile Stress (MPa)
2	Up to 579.1 masl	28.27	2.827	7.067	1.413
3	579.1 – 658.4 masl	24.13	2.413	6.033	1.206
4	Above 658.4 masl	20.00	2.00	5.00	1.00

In India it is quite normal that gravity dams are designed and constructed with different concrete mixes of varying compressive and tensile strength. The aim of this method is to counteract stresses occurring from standard loadings such as the hydrostatic water pressure, the dead load or the uplift pressure and still built the dam in an economically favorable way. So the lower part consists of concrete with better quality, whereas the upper parts of the dam have concrete of lower quality. The stresses due to the mentioned static loads reduce with the height of the dam, so this method seems to be useful. But after the dynamic analysis of Chopra and Chakrabarti, they indicated that most stresses develop in the crest part of the dam due to seismic loading, such as earthquakes. Therefore, all parts of a dam should be constructed with concrete of suitable conditions.

5. Koyna Earthquake

Several seismographic stations in different countries recognized Koyna Earthquake on December 11, 1967 and came to the conclusion for a 6.5 magnitude [22, 30, 31]. In this chapter the acceleration, the damage and the reinforcement of Koyna Dam are described.

5.1 Earthquake acceleration [14]

The depth of the hypocenter is located in a depth about 8 to 20 kilometer below the earth's surface and about 13 kilometers away from Koyna Dam. In this case, when the strength of the earthquake decreases the further away the seismographic station is recording from the epicenter, this is usually occurring at earthquakes with a shallow hypocenter. But actually the earthquake was recognized in cities about 650 kilometers away from the epicenter, which means the earthquake included the behavior of a deep hypocenter as well.

The placed accelerographs in two monoliths of the dam (described in chapter 4.3) were assumed to record the earthquake on December 11, 1967. The device located in monolith 13 was not working during that time, so there is only one accelerogram available from monolith 1A, which is shown in Figure 22. It includes the horizontal, the vertical and the longitudinal component. [32]

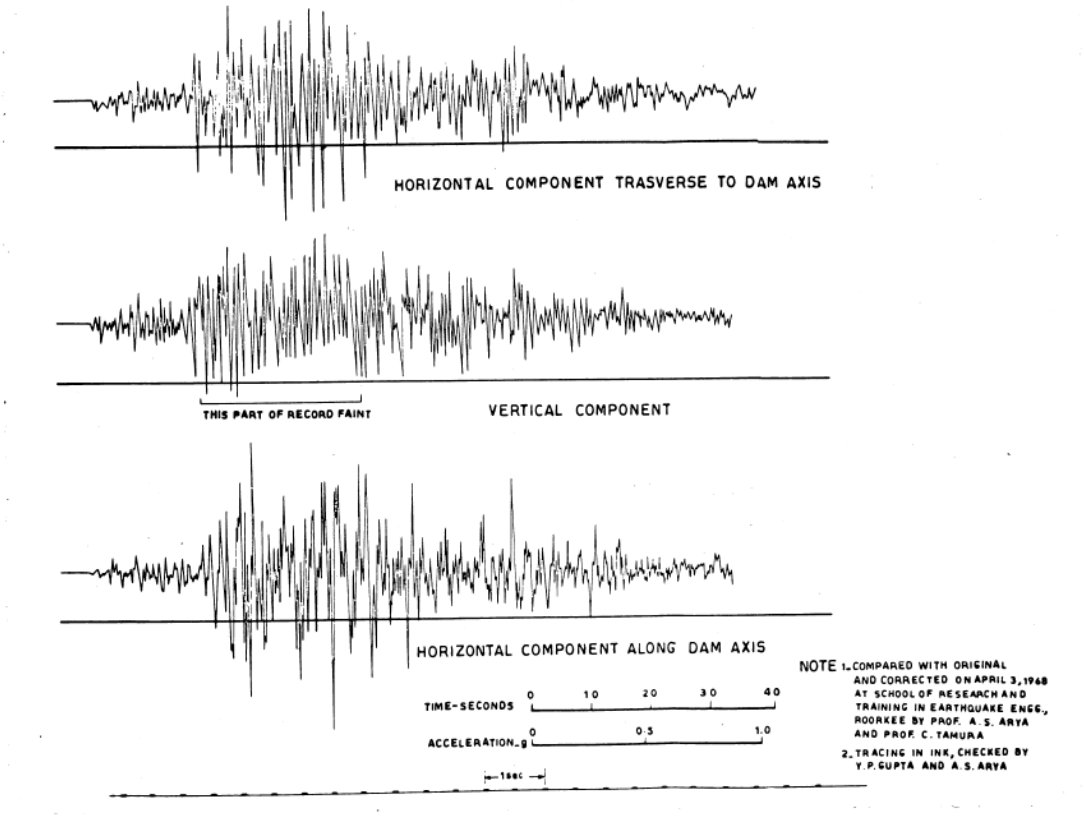

Figure 22: Accelerogram of the Koyna earthquake 1967 [30]

In the recorded accelerogram the maximum accelerations were determined. For the longitudinal movement – cross valley direction - it resulted in 0.63g, for the horizontal acceleration 0.47g in flow direction and for the vertical one 0.31g. In comparison, the strong El Centro earthquake in California in 1940 only had a maximum of 0.33g or the Parkfield earthquake with a maximum acceleration of 0.5g and the San Fernando earthquake with almost 1g.

5.2 Damage of Koyna Dam [14, 5]

The Koyna Earthquake was responsible for some severe damage on houses in Koynanagar, other buildings and Koyna Dam itself. In Koynanagar buildings of rubble masonry were more vulnerable and some of them were broken, while most of the timber frame houses withstood the earthquake. The spillway bridge, the intake structure and the power plant were affected significantly by the Koyna

Earthquake. Besides the auxiliary structures were damaged and Koyna Dam suffered some structural damage with spalling of concrete and water leakage.

The cracks observed on the dam are depicted in Figure 24. These cracks stretching along the monoliths in horizontal direction are the most significant damage on the non-overflow monoliths on both faces upstream and downstream. The overflow part has almost no cracks respectively did not suffer much destruction. In the vicinity of KRL 2060 (627.9 m.a.s.l.) – KRL means Koyna Reduced Level - a longer crack is observed and many small cracks are visible between the levels KRL 2040 (621.8 m.a.s.l.) and KRL 2080 (634.0 m.a.s.l.). Most of the cracks are around the area where on the downstream side the inclination changes.

This is the reason why the crack in the FEM analysis was decided to be located in KRL 2050 (624.8 m.a.s.l.), which is the average elevation of the most significant cracking of the concrete on the non-overflow monoliths. It is described in the further chapters of this thesis.

Due to its special form which means it is half overflow half non-overflow section, monolith 18 has the most cracks. Due to the vibration of the shocks relative displacements between the connected monoliths occurred, which caused spalling of concrete in vertical direction in the joints.

The contact between foundation rock and dam was not subjected to any damage. As it is shown as well in Figure 24, the overflow monoliths were not as damaged as the non-overflow monoliths. Figure 23 shows the elevation plan with the indicated area of the observed cracks, which are given in the illustration below. [30, 33]

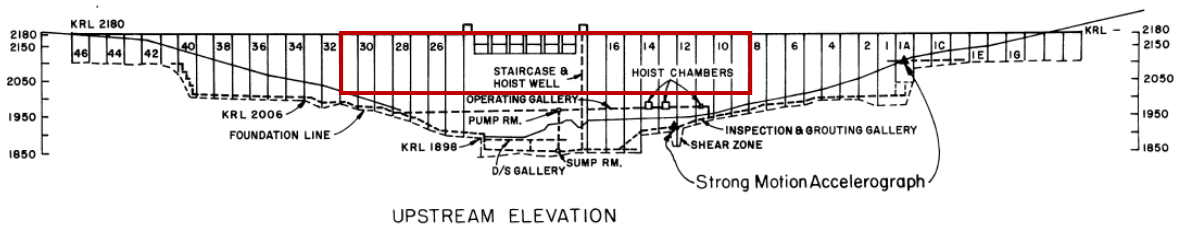

Figure 23: Location of the main cracks of Koyna Dam [14]

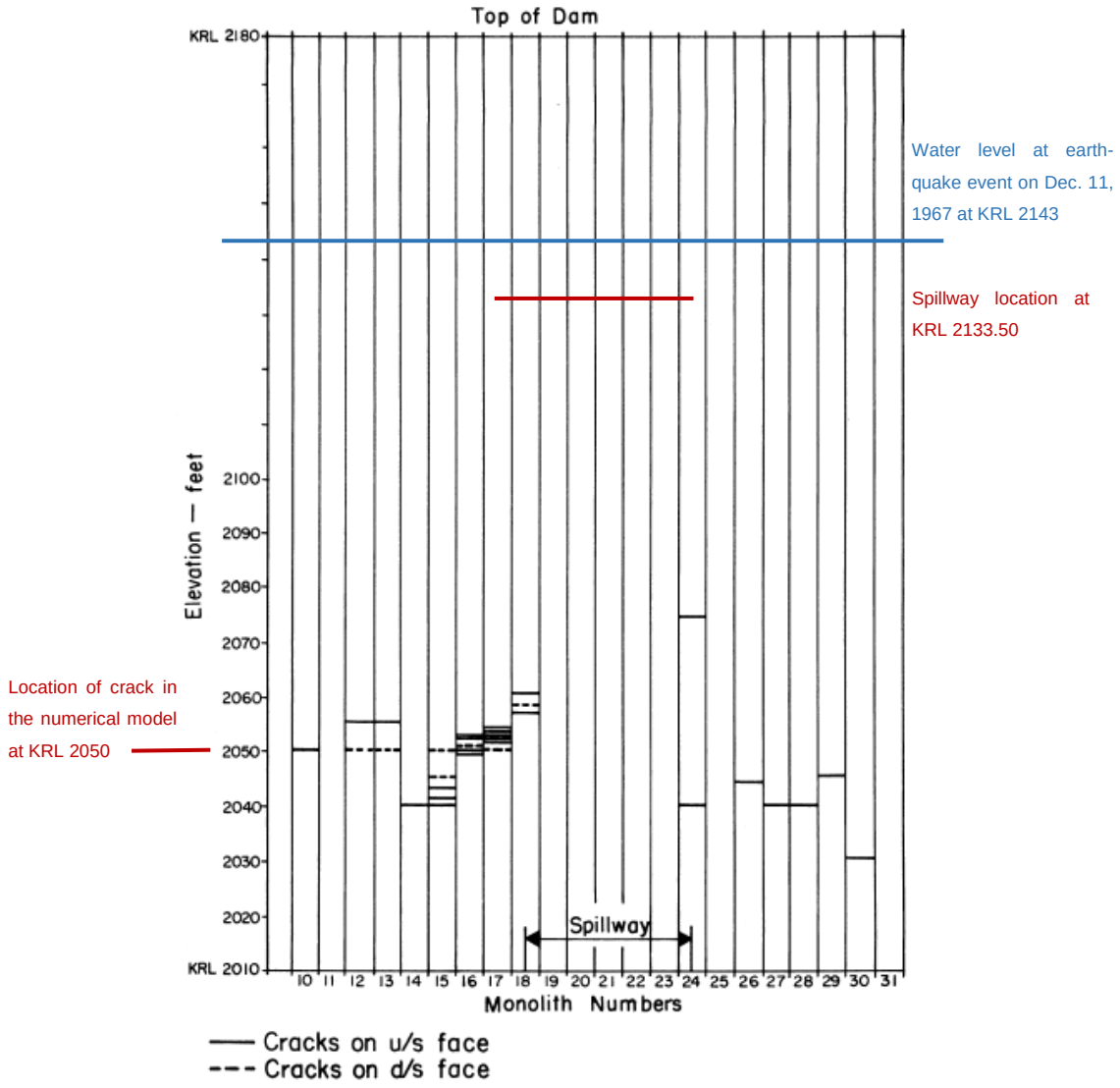

Figure 24: Cracks in Koyna Dam on upstream and downstream face [30]

5.3 Reinforcement of Koyna Dam [14, 33]

After the earthquake in 1967 Koyna Dam had to be reinforced as fast as possible. The cracks described in the chapter above were filled with epoxy resin and then the non-overflow monoliths had to be tensioned with cables. Eight or ten cables per monolith were installed from the top at KRL 2180 (664.5 m.a.s.l.) down to KRL 1990 (606.5 m.a.s.l.). One of this cables is able to withstand a force of 2450 kN or 250 tons. Therefore, in holes with diameters of 150 mm the cables were placed in 64 parallel wires of 8 mm. Figure 25 and Figure 26 show the plan of the cables.

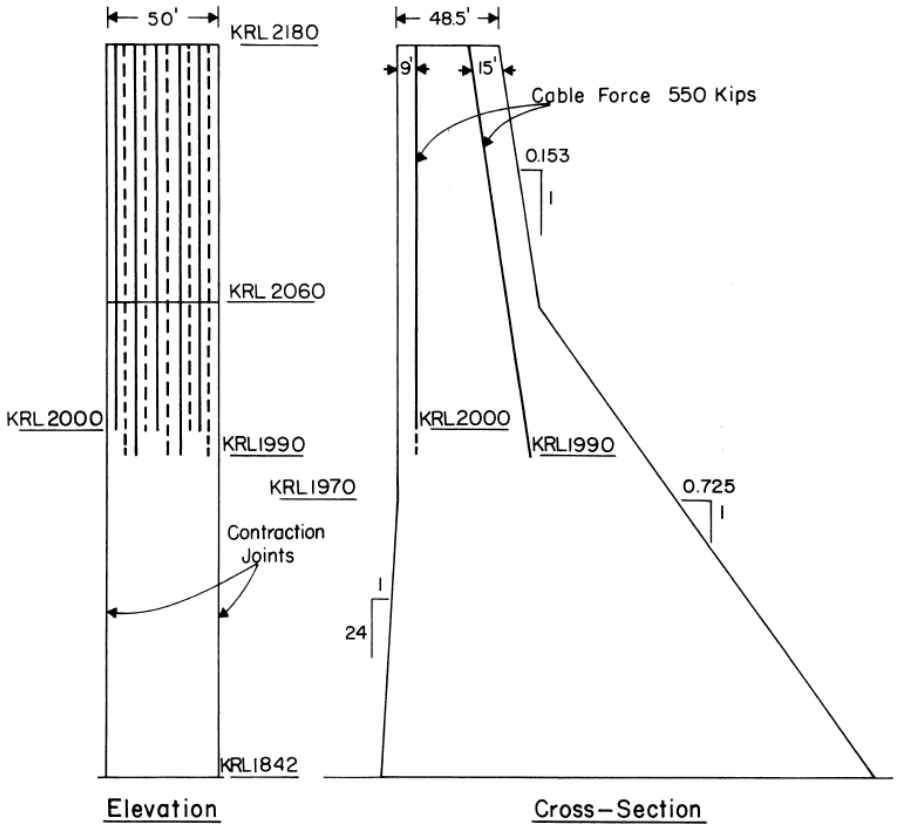

Figure 25: Implemented cables – elevation plan [14]

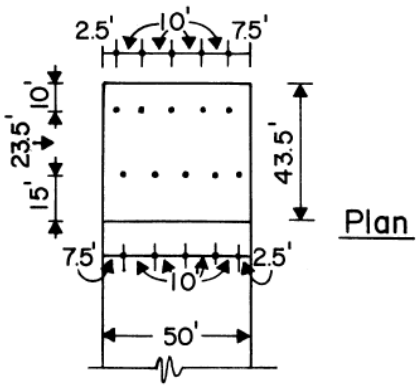

Figure 26: Plan view of cables [14]

Furthermore, it was decided to reinforce the whole Koyna Dam length regarding the stronger earthquakes in the past. The cross sections from the foundation level to KRL 1970 (600 m.a.s.l.) got widened from the non-overflow monoliths, then a supporting pillar up to KRL 2145 (653.5 m.a.s.l.) was constructed. This is shown of monolith 17 in Figure 27. Hence, the unusual section of Koyna was converted

in a typical gravity dam section. The cross section of the overflow monoliths was not changed in any way as there was almost no damage.

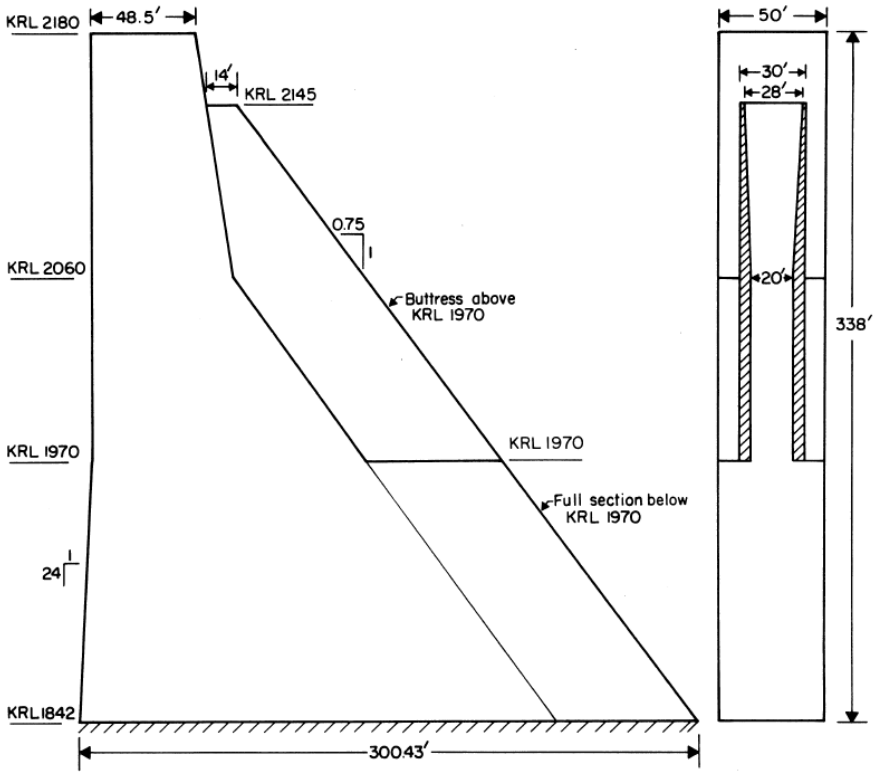

Figure 27: Expanded cross section of monolith 17 [14]

6. Realization in ANSYS

In this part the modelling of Koyna Dam reinforced and unreinforced with several load cases is described. For the modelling and the dynamic analysis ANSYS Workbench was used. Koyna Dam figures are created with AutoCAD and the diagrams are made with Python. All necessary information and theory concerning the program included in this chapter originate from ANSYS Help [34].

6.1 Parameters

The needed parameters for the modelling of Koyna Dam such as the geometry, the loads and material properties of the dam are given by the report of Chopra and Chakrabarti [14].

As already mentioned at the beginning of chapter 4, all values for the geometry as well as stresses and forces have to be changed from the US customary units to the metric system. In Figure 28 Koyna Dam with its dimensions is shown.

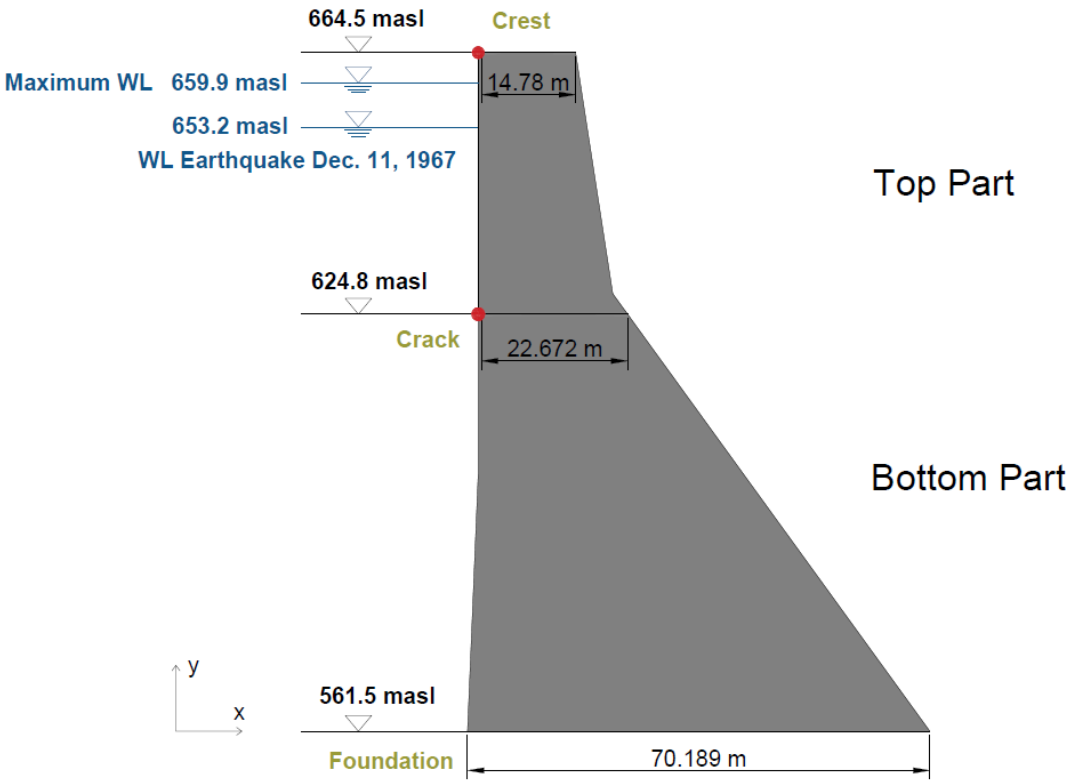

Figure 28: Koyna Dam dimensions in metric system

The location of the crack was a decision based on the data from chapter 5.2 and is assumed to go through the entire cross section of the model. In the red points of crack and crest located on the upstream side of the dam the results of deformations are extracted from ANSYS. Koyna Dam has a height of 103 m, a base width of 70.189 m and a crest width of 14.78 m. The crack length is 22.672 m. In all models the x-axis is the horizontal direction and the y-axis is the vertical direction. The maximum water level of the dam is shown as well as the water level at the event of the Koyna Earthquake on December 11, 1967, which is only 6.7 m lower than the maximum can reach.

6.2 Modelling and discretization

In comparison to arch dams using 3D models, concrete gravity dams are modelled as a 2D system usually. For the implementation of the geometry the ANSYS DesignModeler and for the further steps ANSYS Mechanical was used. Ultimately 9 models of Koyna Dam, which are indicated in Table 3, were set up:

Table 3: Numerical models of Koyna Dam

Koyna Model	Foundation	Reservoir	Linear with closed crack	Non-linear with open crack	One anchor	Two anchors
1	✗	✗	✓	✗	✗	✗
2	✓	✗	✓	✗	✗	✗
3	✓	✓	✓	✗	✗	✗
4	✓	✗	✗	✓	✗	✗
5	✓	✓	✗	✓	✗	✗
6	✓	✗	✗	✓	✓	✗
7	✓	✓	✗	✓	✓	✗
8	✓	✗	✗	✓	✗	✓
9	✓	✓	✗	✓	✗	✓

The intention of all models is to keep them as simple as possible and to realize the mesh as precise as possible. Quadratic elements are used for all parts. The mesh should be as fine as possible as well, but the smaller the elements the longer the program needs to calculate the results.

6.2.1 Mapping from 2D to 3D

All models without anchors were designed as a two-dimensional cross section, which means the individual parts are surfaces. With starting the implementation of the anchors in the Koyna model, a problem arises that it is not possible to integrate a LINK element for the anchor in a two-dimensional model as ANSYS does not support this. Furthermore, a plane strain behavior is needed as the model of Koyna is only an idealized section cut out of the 854 m long concrete gravity dam, where stresses may occur in the longitudinal direction. The plane strain conditions are following:

$$Stresses: \quad \tau_{xz} = 0 \quad \tau_{yz} = 0 \tag{74}$$

$$Strains: \quad \varepsilon_z = 0 \quad \gamma_{xz} = 0 \quad \gamma_{yz} = 0 \tag{75}$$

To replicate this plane strain conditions, the anchor models were implemented as 3D models with the same cross section and a total thickness of one meter with the anchors as link/truss element located in a plane offset 0.5 m from the exterior faces that are parallel to the x-y plane. Additionally for the 3D models there has to be set a boundary condition to lock the displacement in the longitudinal direction, in z-direction of the model. After several test models it is possible that with this method the plain strain behavior of the 2D models are mapped to 3D.

6.2.2 Modelling of the dam and foundation

For the dam the geometry was taken from the reports, the size of the foundation was chosen to get a height of 150 m and a length of 200 m each side from the upstream and downstream edge. Both dam and foundation are modeled as PLANE elements in 2D, as SOLID elements in 3D. The concrete of the dam remains in a linear-elastic range in all models.

6.2.3 Modelling of the fluid [34]

For the reservoir there exist so-called acoustic elements that have pressure as only degree of freedom. So it can be modelled as a separate body or surface at the upstream side of the dam. Its height corresponds to the water level of the earthquake of Dec. 11, 1967. For the 2D models FLUID29 is used, for 3D models FLUID220, where both can simulate the fluid medium and the interface between the fluid and the structure, therefore, the activation of the fluid-structure interaction (FSI) is possible. In the interface between fluid and structure, the structure displacement degrees of freedom are coupled to enable FSI. The possible geometries of the acoustic elements are shown in Figure 29 and Figure 30.

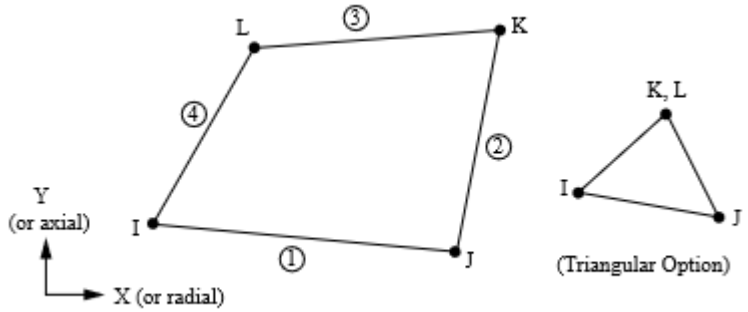

Figure 29: FLUID29 element for 2D analysis [34]

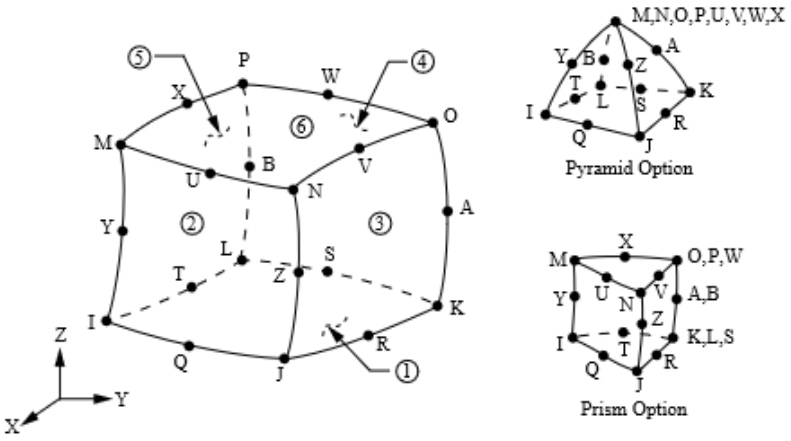

Figure 30: FLUID220 element for 3D analysis [34]

6.2.4 Modelling of the anchors [34]

For the anchors a link or truss is used to replicate the typical behavior of a real anchor. Therefore, the LINK180 element is needed, which is a tension-compression element in axial direction and has degrees of freedom in x-, y- and z-direction and no bending occurs. In all models the anchors remain in a linear-elastic state and furthermore the resistance against shear failure (described in chapter 3.1.1) is not taken into account.

6.2.5 Linear models (bonded crack)

The following Koyna Dam models are linear and its values are used for the Rayleigh damping calculation.

6.2.5.1 Koyna Dam without foundation

This model consists of 390 elements and 1290 nodes. The dam (Figure 31) is modelled with PLANE183 elements in a 2D system.

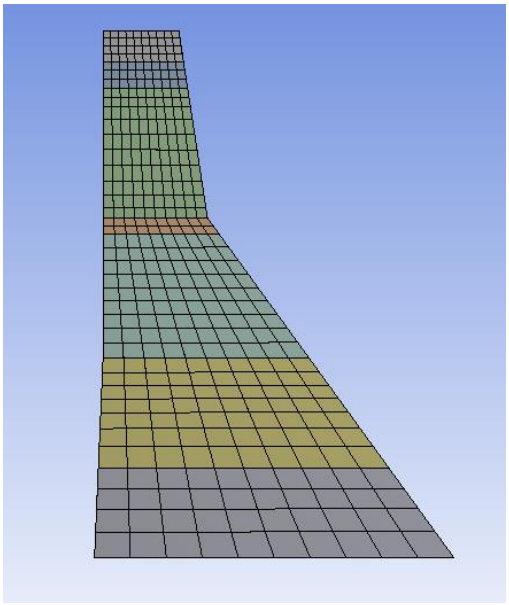

Figure 31: Koyna Dam without foundation and without reservoir

6.2.5.2 Koyna Dam with foundation

With empty reservoir: consists of 4056 nodes and 1420 elements.

With full reservoir: consists of 5115 nodes and 1980 elements.

The foundation and the dam are modelled with PLANE183 elements, the reservoir with FLUID29 element as 2D surfaces. Figure 32 shows the model with a full reservoir.

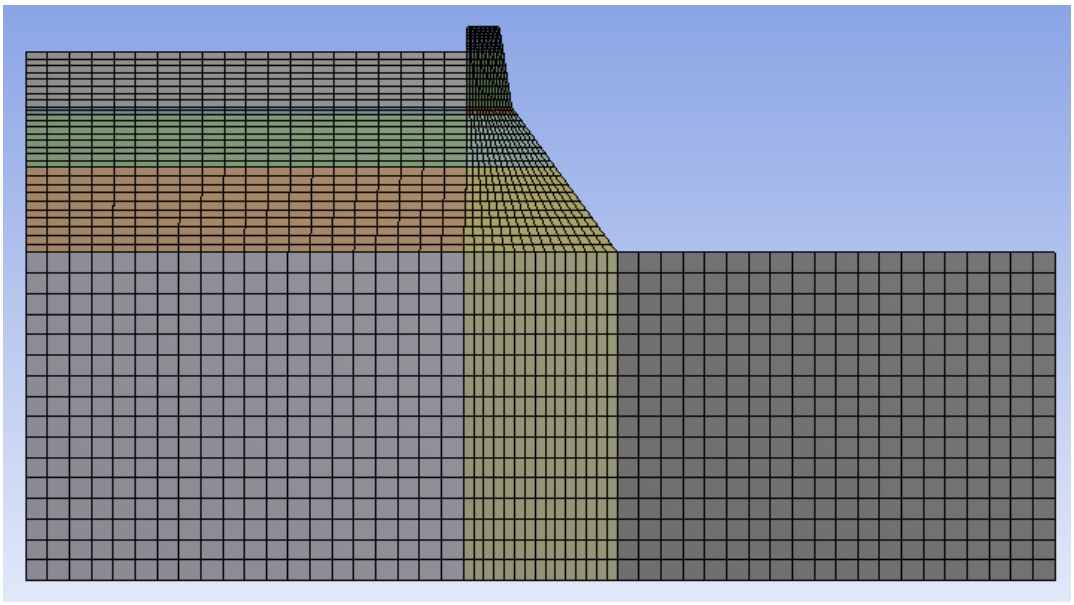

Figure 32: Linear Koyna Dam model with full reservoir

6.2.6 Non-linear models (open crack)

The following Koyna Dam models are the main topic of this thesis, it is evaluated how the crest block behaves in different cases.

6.2.6.1 Koyna Dam with foundation

With empty reservoir: consists of 6024 nodes and 1896 elements.

Full reservoir: consists of 6633 nodes and 2456 elements.

The foundation and the dam are modelled with PLANE183 elements, the reservoir with FLUID29 element as 2D surfaces. These non-linear models have the same geometry as the linear ones, the only difference is the refined mesh in the crack area to reach the convergence. Figure 33 shows the model of Koyna Dam with an empty reservoir.

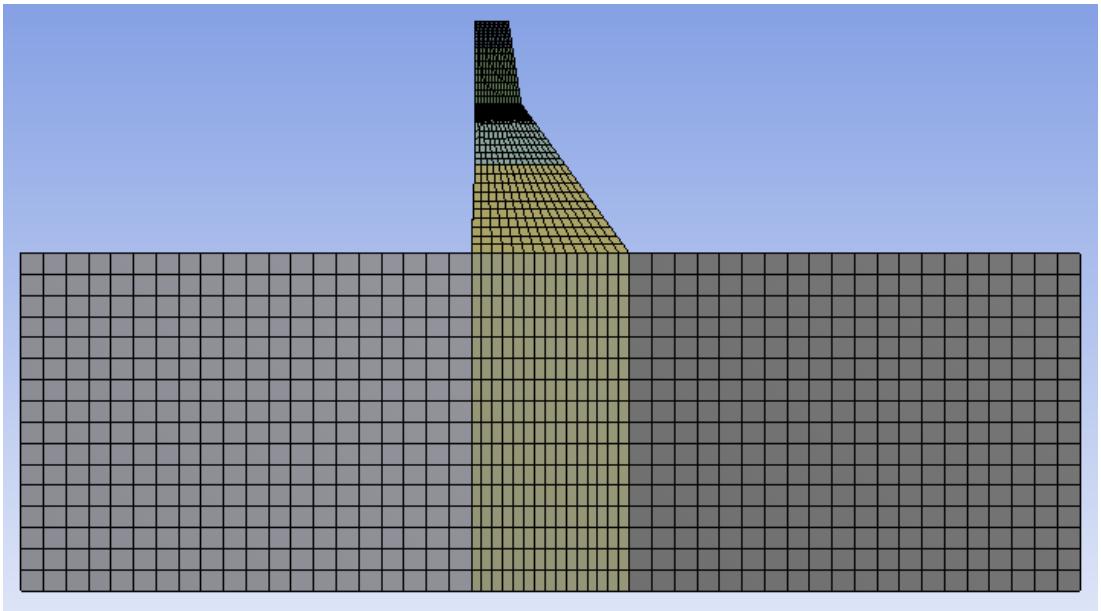

Figure 33: Non-linear Koyna Dam model with empty reservoir

6.2.6.2 Koyna Dam with foundation and one anchor

With empty reservoir: consists of 17127 nodes and 2958 elements.

With full reservoir: consists of 24132 nodes and 4158 elements.

The foundation and the dam are modelled as SOLID186 elements as 3D bodies with a thickness in z-direction of 1 m. The anchor is located in the middle and has a cross section surface of A = 1680 mm² and thus a radius of r = 0.023 m. It is modelled as a LINK180 element. Figure 34 shows the reinforced Koyna Dam with one anchor. The anchor has a length of 58 m.

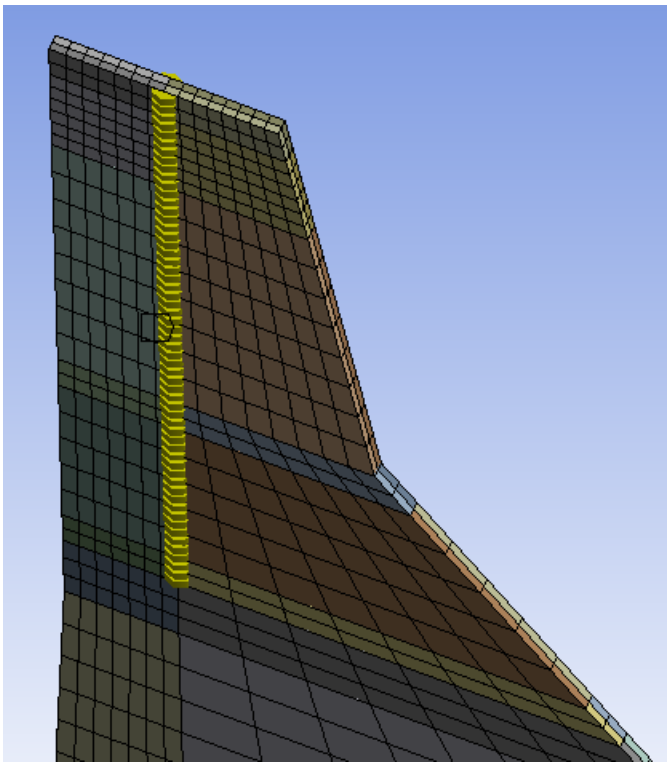

Figure 34: Koyna Dam with one anchor

6.2.6.3 Koyna Dam with foundation and two anchors

With empty reservoir: consists of 17188 nodes and 3017 elements.

With full reservoir: consists of 24193 (23963 for passive anchor model) nodes and 4217 (4102 for passive anchor model) elements. The link elements of the passive anchors in this model with the fluid-structure interaction require a coarse mesh to achieve the force convergence.

This model equals the design of the original reinforced Koyna Dam after the earthquake regarding length and location of anchors. The data for the geometry of all anchors is taken from DYWIDAG [12] to obtain the modern standards of the relationship between diameter and pretension force. For better comparison one anchor in the two anchor model has a cross section A = 840 mm² and thus a radius r = 0.016 m, which is the half cross section area of the one anchor model. Figure 35 shows Koyna Dam with full reservoir and two anchors. The vertical anchor located on the upstream side has a length of 58 m, the inclined anchor located on the downstream side has a length of 58.69 m.

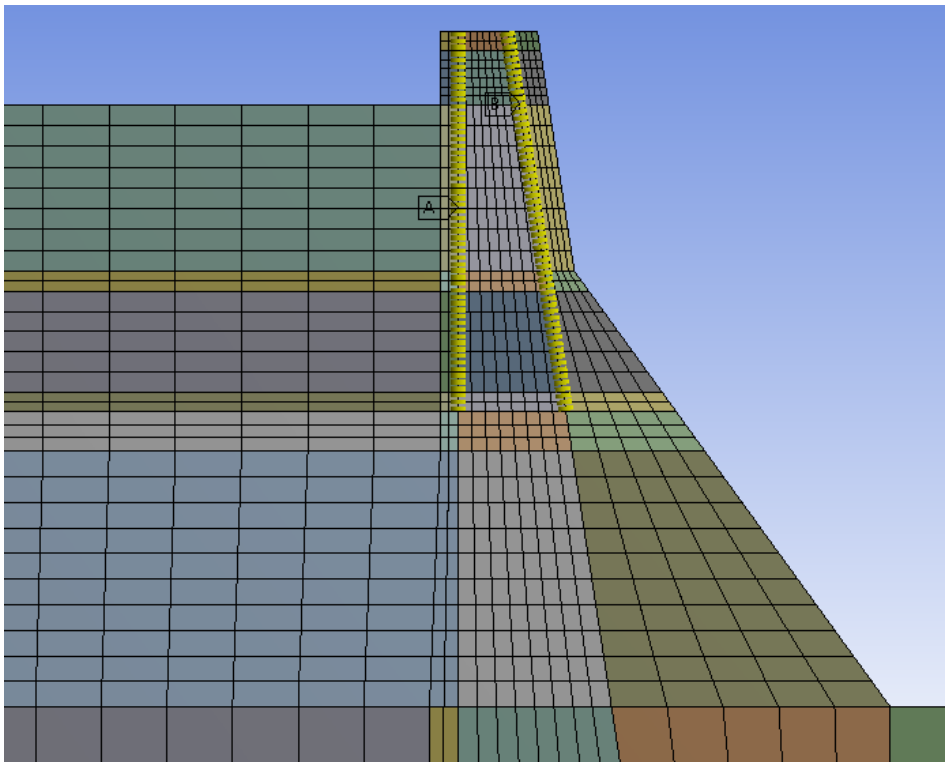

Figure 35: Koyna Dam with reservoir and two anchors (fine mesh)

6.3 Contacts [34, 35]

The definition of a contact is when two surfaces are tangential by touching each other. Through the contact compressive normal forces as well as tangential friction forces can be transferred. The stiffness of two parts is based on the type of contact, like bonded or frictional or any other status available in ANSYS.

Interpenetration in a contact should be avoided, hence, in ANSYS Mechanical are some contact formulations to ensure the contacts cannot overlap. For the Koyna systems in this thesis, the MPC formulation and the Augmented Lagrange formulation are used. The multi-point constraint (MPC) formulation only works at “bonded” contacts or contacts with “no separation”. With constructing constraint equations (restrictions or boundaries) the displacements are restricted between the surfaces. In contrast to the MPC, the Augmented Lagrange can be used for non-linear contacts, such as “frictional” or “frictionless”, because there are controls for decreasing the penetration value. Also in this formulation a certain contact stiffness has to be selected to keep the penetration as small as possible. It can be defined as a certain factor or also as an absolute value in the program.

Another important issue in designing contacts is the choice of which surface (3D) or edge (2D) is taken as the contact surface and which one is the target surface. When symmetric behavior is selected in the Mechanical, the contact surfaces are restricted in overlapping target surfaces and vice versa. When asymmetric behavior is used only contact surfaces are restricted in overlapping target surfaces, which is used in the fluid-structure contact and in the crack contact as well. Following contact regions are implemented in the different Koyna models:

- Bonded contact at crack: with MPC formulation and an asymmetric behavior in which the contact surface is the top part of the dam and the target surface is the bottom part.

- Frictional contact at crack: the friction coefficient is 1 with an asymmetric behavior and the Augmented Lagrange formulation is used in which the unit-less normal stiffness factor is 0.1, which is rather small, but helps to reach the convergence. It is a multiplier of the contact stiffness that is calculated automatically in the program during the iteration process. Contact surface is the top part and the target surface is the bottom part.

- Fluid – structure contact: bonded with MPC formulation and an asymmetric behavior in which the contact surface is the fluid surface and the target surface is the solid surface (foundation + dam).

- Anchor – structure contact: bonded with MPC formulation in which the contact surface is the anchor and the target surface is the edge in the dam where the anchor is meant to be grouted inside. In the design of the one anchor model and the two anchors model all anchors are fixed (grouted) in a length of 3 m at the top (anchor head) and 3 m at the bottom of an anchor. The unfixed part in the middle is assumed to be the unbonded anchor length. The grouting is shown as a constraint equation in Figure 36 and Figure 37 for both designs and also the contacts between fluid and structure and that one in the crack are indicated.

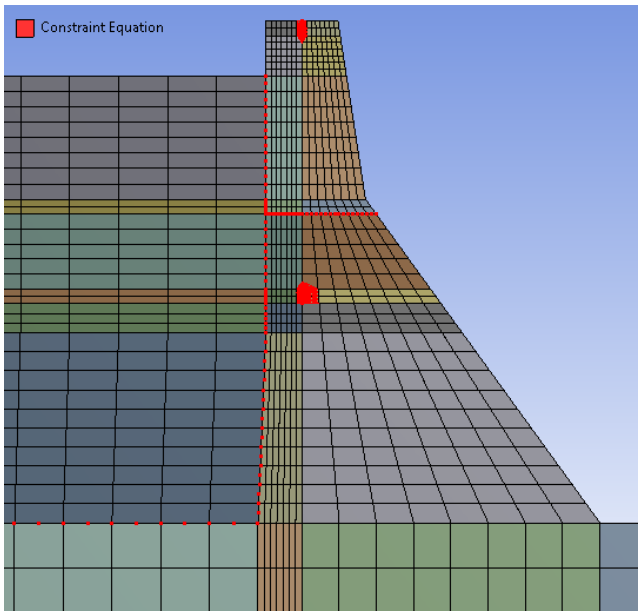

Figure 36: Constraints of Koyna Dam with foundation and full reservoir and one anchor

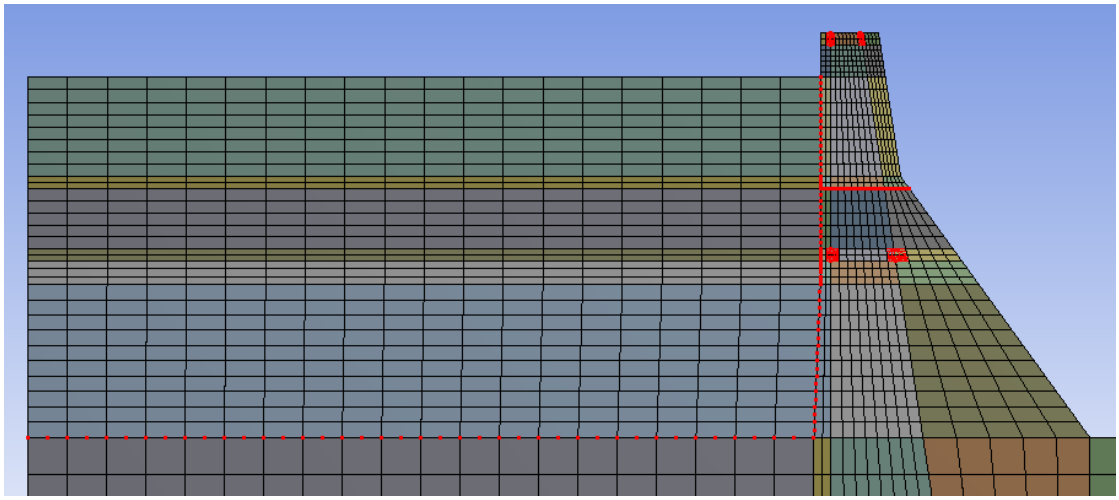

Figure 37: Constraints of Koyna Dam with foundation and full reservoir and two anchors

6.4 Material properties

In Table 4 the linear elastic material properties of the models are defined for the dynamic calculations:

Table 4: Material properties of the models

Part of model	Elastic Modulus [Pa]	Poisson's ratio [-]	Density [kg/m³]	Speed of sound [m/s]	Damping factor [-]
Dam	3.1e10	0.2	2643.3	-	0.5
Foundation	3e10	0.2	1e-10	-	0.5
Fluid	-	-	1000	1440	-
Anchor	2.5e11	0.3	1e-10	-	-

The weight of the foundation and the anchors are neglected in the analysis, so it is assumed zero. As dam is the most important part for calculating the seismic response, a foundation with almost no density is taken, which serves for a simpler model of a fluid-structure interaction system with dam and reservoir. The anchor is considered as weightless as its volume and size does not influence the results in the dynamic analysis. The material properties are implemented with an APDL script in the ANSYS Mechanical.

6.5 Boundary conditions

There are essential boundary conditions for the system, the displacement of the bottom edge in y-direction and the displacement in x-direction of both side edges in the 2D models are locked. For the 3D models the displacement of the bottom surface in y-direction and the displacement in x-direction of both side surfaces are locked and additionally, to obtain the plane strain conditions, all surfaces in the x-y plane on both exterior sides are locked in z-direction.

The fluid needs two important boundary conditions, first the zero pressure at the water surface and also the impedance at the back end edge or surface of the

reservoir, so the acoustic waves in the fluid are absorbed. Figure 38 shows the boundary conditions in a sketch.

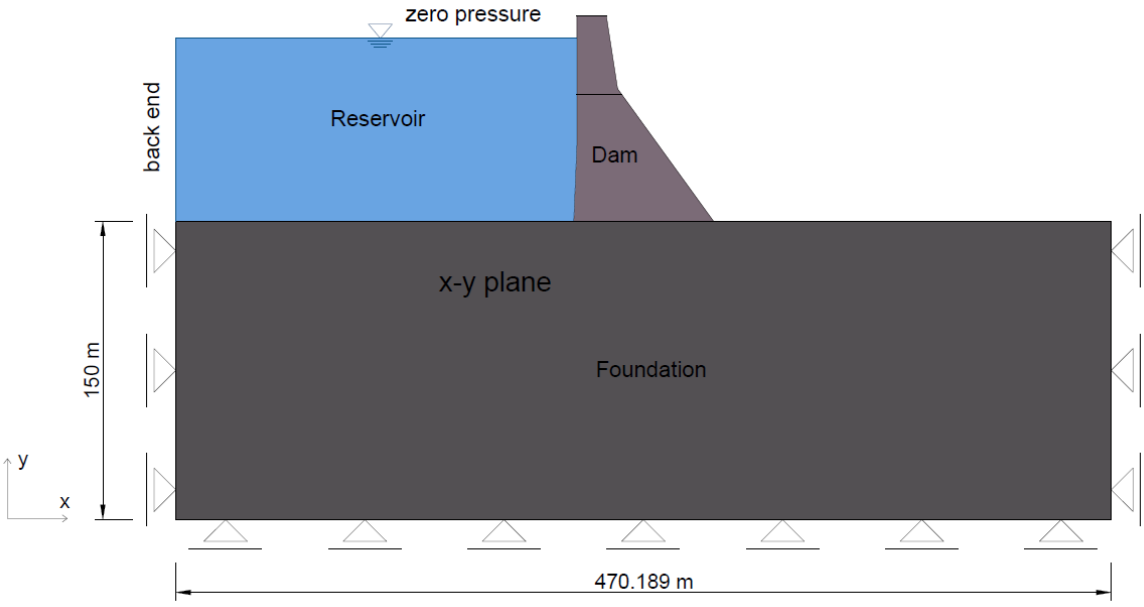

Figure 38: Boundary conditions of the Koyna Dam model

6.6 Fluid-structure interaction [34]

As already explained before, there are acoustic elements such as FLUID29 for 2D simulations and FLUID220 for 3D needed to simulate the fluid medium and the interface of fluid and structure. The acoustic element which is unconnected with the structure has only pressure as degree of freedom, the element at the fluid-structure interface has four degrees of freedom which are the displacements in x, y and z directions and also pressure. The calculation of the fluid-structure interaction (FSI) is based on the Navier-Stokes equation and the continuity equation as well as the fundamentals of dynamics. The Navier-Stokes equation is derived from the law of conservation of the momentum and can be written as following:

$$\rho \frac{d\vec{v}}{dt} = -\nabla p + \nabla . \bar{\bar{S}} + \rho \vec{b} \tag{76}$$

ρ ….. *density*

v ….. *velocity*

p ….. *pressure*

b ….. *body force*

S ….. *viscous stress tensor*

The fluid-structure interface is flagged manually in an APDL script, where surfaces or edges of the interface between the solid part and the fluid part are selected to obtain four degrees of freedom per node.

6.7 Loads

The loads that are listed in this part are applied to the system in the following order. The loads can be switched on or off stepwise in ANSYS Mechanical.

6.7.1 Dead load of Koyna Dam

In the first assumption only the dead load of Koyna Dam was taken into account, the whole foundation was considered without mass. Usually a transient dynamic analysis of a concrete gravity dam works without dead load, because at the time the dynamic load (e.g. earthquake) takes place, the construction time is over and mass of the dam has already settled.

The very first model tests were performed with dead load of the dam, but then it was decided to continue without dead load as it is the common procedure. But with the open crack, which means only frictional contact between the top part and the bottom part of the dam, there is only little or no friction resistance given without mass. This led to the decision to include only the dead load of the crest block (top or crest part) of the dam as it is important to keep the friction resistance in the model and to get more realistic results.

6.7.2 Hydrostatic pressure (full reservoir)

At full reservoir the hydrostatic pressure is applied which depends on the height of the reservoir. This height is considered to be the water level in the Koyna reservoir at the day of the earthquake on Dec 11, 1967. The only model with a hydrostatic pressure applied and without a reservoir is Koyna Dam model without foundation, which was primarily used for testing reasons. In this case the hydrodynamic effects are not present. For this investigation the uplift pressure is neglected in all models.

6.7.3 Anchor pretension

The anchors can be switched on or off in ANSYS Mechanical with Element Birth/Death stepwise. When the elements of the anchor or 2 anchors are switched on, the pretension can be applied with the so-called bolt pretension tool. A pretension force of 2.45 MN is given from the Koyna reports for each anchor. In the first anchor model this value is used as the basis for choosing the further data. As already described in chapter 3.2.3, the data from DYWIDAG [12] is used for the anchor design. For the one anchor model the standard strand anchor is used with 12 strands (A = 140 mm²) and a cross-section of 1680 mm² with an applied pretension force of 2.45 MN, which is within the range of the corresponding yield load. In the two anchor model each anchor consists of 6 strands with a cross section area of 840 mm² and an applied pretension force of 1.225 MN, below the maximum yield force. This results in the same cross-section area and the same pretension load of the whole system to compare both models reasonably. In Table 5 the data is listed.

Table 5: Strand anchor data [12]

Koyna model	Number of strands	Area of cross-section [mm²]	Yield load [kN]	Ultimate load [kN]
With two anchors	6	840	1310	1487
With one anchor	12	1680	2621	2974

6.7.4 Dynamic loads

In the last step the dynamic loads (earthquake load) is applied. The data for the Koyna Earthquake from Dec 11, 1967 is provided from the Abaqus Example Problems Guide [36] and lasts 10 seconds.

As the models are assumed to be 2D systems - or 3D with 1 m thickness - with the main focus on the cross-section of the dam, only the horizontal and the vertical acceleration are needed. For the sake of completeness, it is to mention that the maximum acceleration of the z-direction (cross valley direction) is 6.18 m/s² (0.63g). Figure 39 shows the horizontal acceleration in flow direction and its maximum is 4.61 m/s² (0.47g).

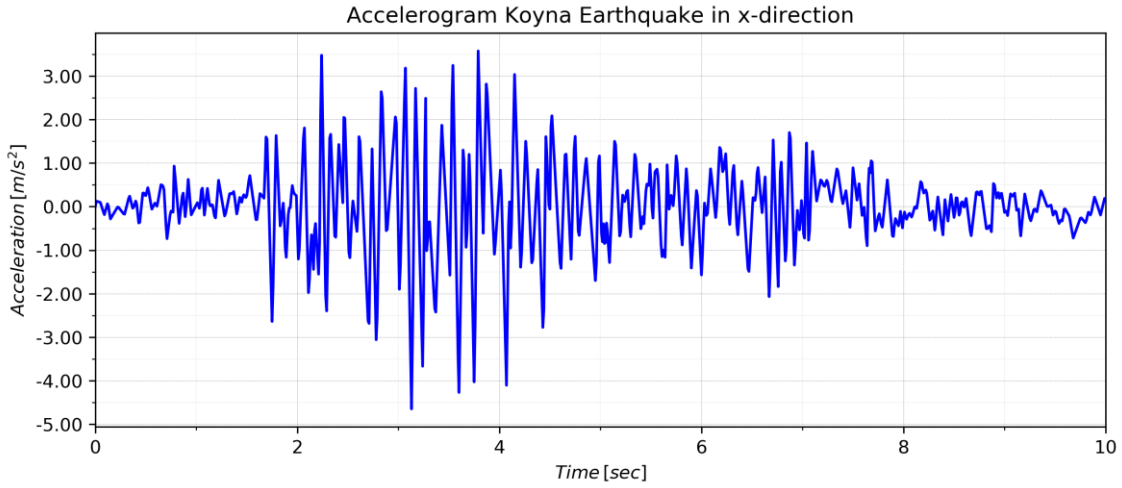

Figure 39: Accelerogram in x-direction

Figure 40 shows the vertical acceleration in the system, which has a maximum of 3.04 m/s² (0.31g).

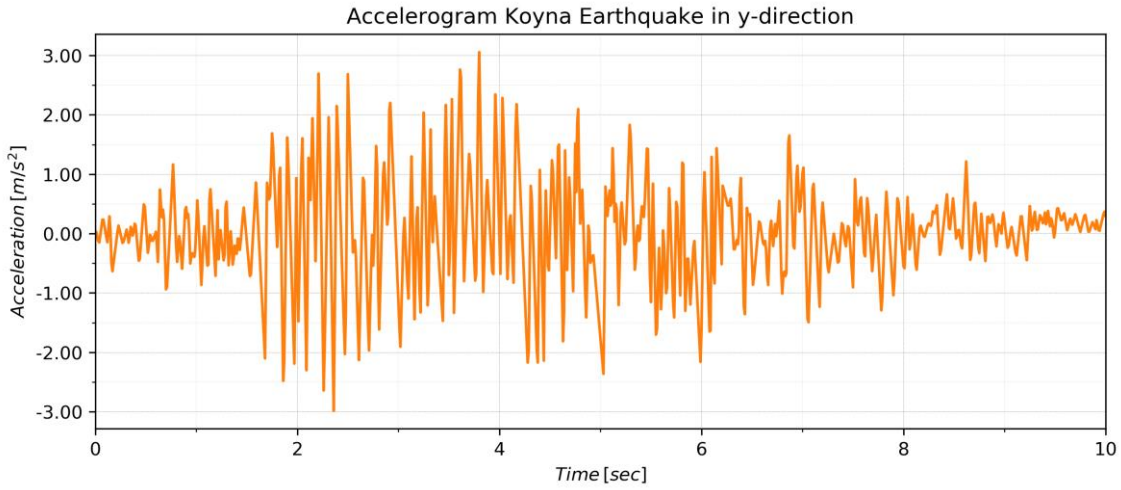

Figure 40: Accelerogram in y-direction

7. Numerical results

The following procedure shown in Table 6 was done to obtain the results:

Table 6: Procedure of the numerical analysis

Step	Procedure
1	Modelling of simple linear Koyna Dam with closed crack and without foundation
2	Static analysis and modal analysis to obtain damping parameters
3	Transient analysis with applied acceleration of Koyna Earthquake
4	Data from first Koyna model and modelling of additional foundation and reservoir
5	Carrying out modal analysis and transient analysis with full and empty reservoir
6	Implementation of frictional contact in the open crack for following non-linear models
7	Transient analysis of non-linear Koyna model with foundation and with full and empty reservoir
8	Mapping from 2D to 3D to implement anchors as link elements
9	Application of pretension force

10	Transient analysis of Koyna model with one anchor as passive and as prestressed anchor
11	Transient analysis of Koyna model with two anchors as passive and as prestressed anchors

The aim of this thesis is to model Koyna Dam under its initial conditions and implement a crack line and then improve it theoretically step by step with anchors. The results plotted as diagrams are done with Python. The final results are implemented with dead load of the crest part of Koyna Dam. The results are extracted from two nodes set in the ANSYS model, in Figure 41 the locations of the crest node and the crack node are shown. The deformations in horizontal and vertical direction were taken and compared in these points.

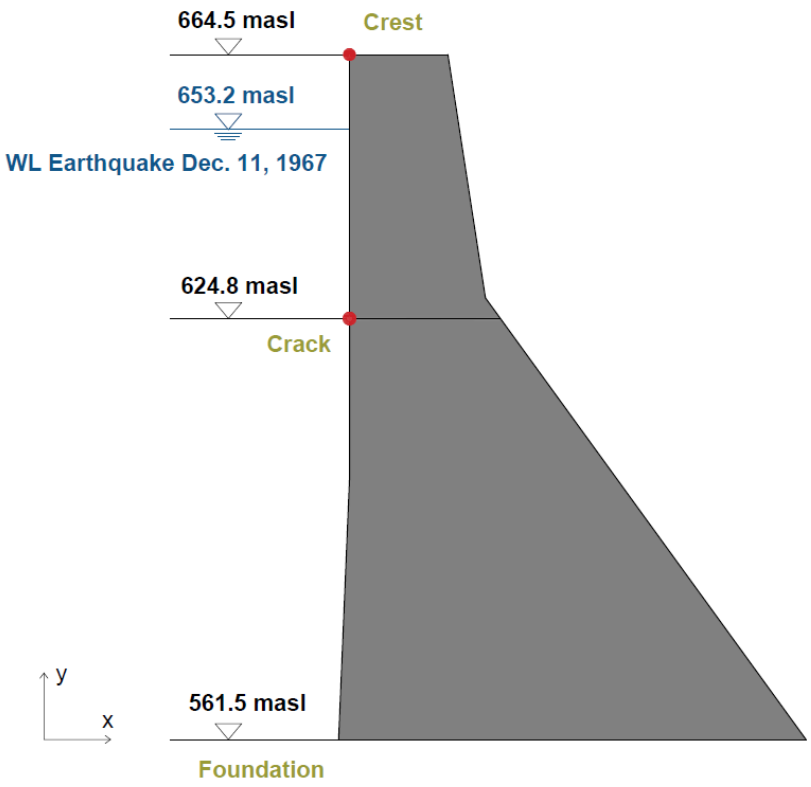

Figure 41: Crest and crack point location in the Koyna model

7.1 Rayleigh damping

In order to calculate the Rayleigh damping parameters, the stiffness-proportional damping and the mass-proportional damping is used. The first 10 eigenmodes are used to represent the system behavior. The damping ratio ξ is set to 5%. The Rayleigh damping calculation is done for the three linear models which is described in chapter 2.2.3.3. In Table 7 the eigenfrequencies obtained from the modal analysis of the three Koyna models are listed.

Table 7: Eigenfrequencies of the linear Koyna models

Eigenfrequencies [Hz]			
Mode	**Dam**	**Dam + Rock**	**Dam + Rock + Fluid**
1	3.1374	2.6459	2.3245
2	8.3478	6.2428	3.9285
3	11.048	6.979	4.9687
4	16.162	11.995	6.3958
5	24.645	18.125	6.9623
6	24.79	19.547	8.5497
7	34.026	27.439	10.692
8	36.109	30.4	11.757
9	38.779	32.345	11.932
10	41.22	36.078	12.762

The eigenfrequencies of the dam with a foundation and a reservoir are smaller than in the other models, but the main issue is the mass contribution to the related eigenfrequency. At the dam with foundation the first 4 eigenfrequencies cover about 95% of the effective mass. With this values the Rayleigh damping parameters α (mass proportional damping) and β (stiffness proportional damping) can

be calculated by assuming a damping ratio of the system of 5%. The total Rayleigh damping is the sum of mass proportional and stiffness proportional damping. The parameters α and β are used in the transient analysis of the corresponding linear and non-linear models.

The Koyna model without foundation has an α-value of 1.651 and a β-value of 0.000825. Due to the effective mass modes 1 and 4 are chosen to calculate these values. Afterwards the Rayleigh diagram (Figure 42) can be plotted with its minimum damping factor of 0.037. The first 5 eigenfrequencies f_i are indicated in the diagram as well.

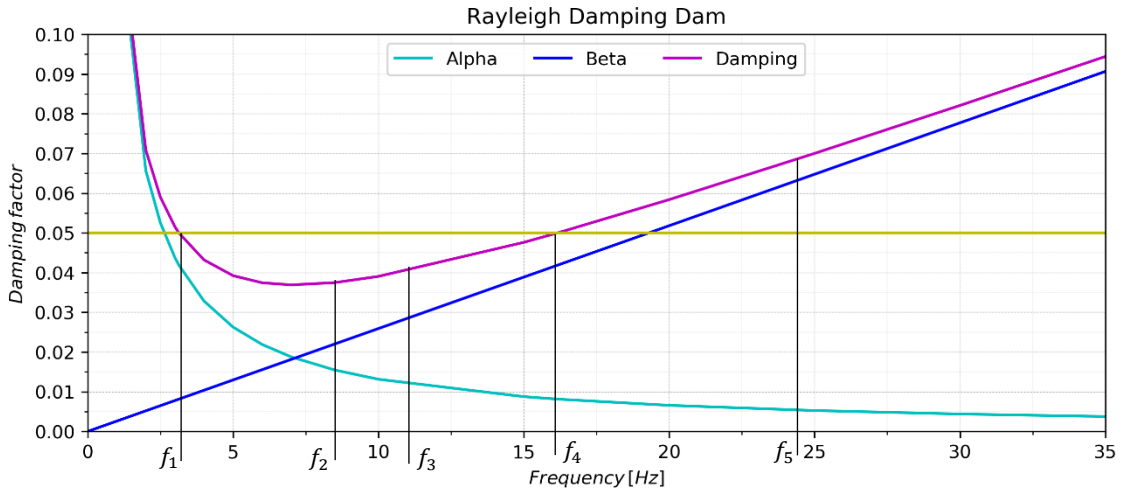

Figure 42: Rayleigh damping of Koyna Dam without foundation

The Koyna model with foundation and empty reservoir has an α-value of 1.362 and a β-value of 0.001087. Due to the effective mass modes 1 and 4 are chosen to calculate these values. Afterwards the Rayleigh diagram (Figure 43) can be plotted with its minimum damping factor of 0.038. The first 5 eigenfrequencies f_i are indicated in the diagram as well.

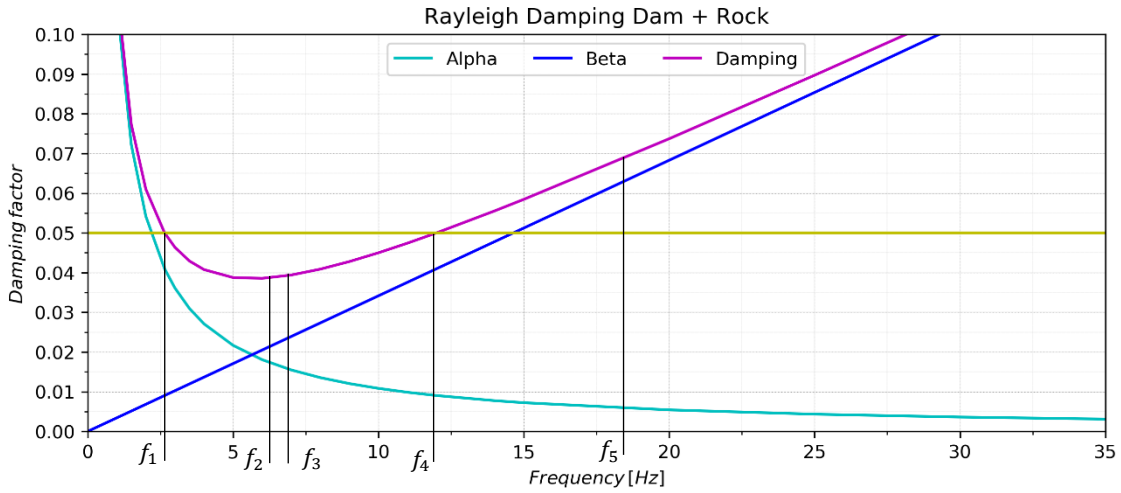

Figure 43: Rayleigh damping of Koyna Dam with foundation

The Koyna model with foundation and full reservoir has an α-value of 2.194 and a β-value of 0.000952. Due to the effective mass modes 3 and 8 are chosen to calculate these values. Afterwards the Rayleigh diagram (Figure 44) can be plotted with its minimum damping factor of 0.0455. Some of the eigenfrequencies f_i are indicated in the diagram as well.

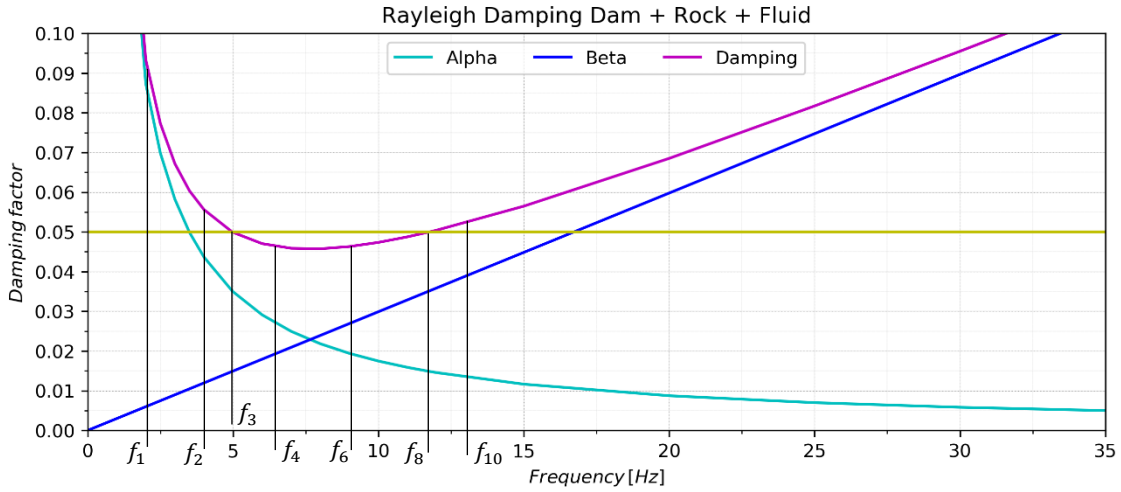

Figure 44: Rayleigh damping of Koyna Dam with foundation and full reservoir

7.2 Linear models with closed crack

The linear models, especially those ones with foundation, are mainly needed for the damping parameters for the following calculations. As the crack is closed in the transient analysis, the results of the node at the crack on the upstream side

remain the same in the top part and the bottom part of the dam. In all the following models, also the non-linear ones, the term FSI (fluid-structure interaction) is used in the diagrams for the results calculated with full reservoir. The results obtained in the calculation with an empty reservoir are defined as “without FSI”.

7.2.1 Koyna Dam without foundation

Koyna Dam without foundation has a hydrostatic pressure applied without a reservoir. When there is no foundation modelled with specified parameters such as in the other models, the structure is meant to be placed on an infinitely stiff ground. This has an effect on the response of a system. Also due to the absence of a reservoir modelled as a separate body, the hydrodynamic effects are not present. In the transient analysis the 10 s earthquake is put in and in the results the displacement in the horizontal and vertical direction is compared between crest and crack node in Figure 45 and Figure 46.

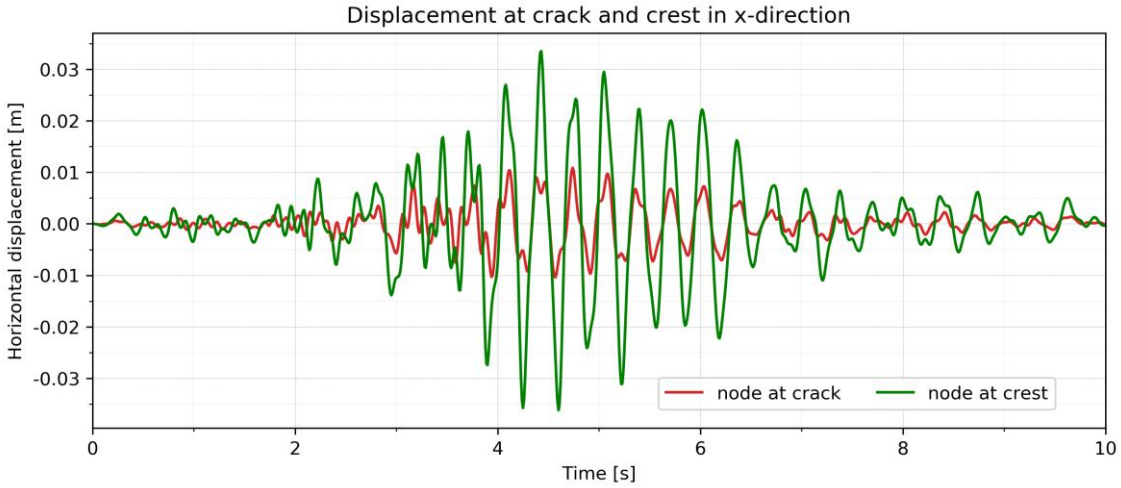

Figure 45: Displacement comparison crack and crest node in x-direction

Due to the effect of amplification of structures response at higher elevations at the upper part of the dam, the displacement in x-direction is about three times larger at the crest node than at the crack node. In y-direction the amplification is lower due to the seismic loading and the layout of the structure. Regarding the natural modes of a system the oscillation in horizontal direction is different from the vertical one and the acceleration caused by the earthquake is smaller in vertical direction as well.

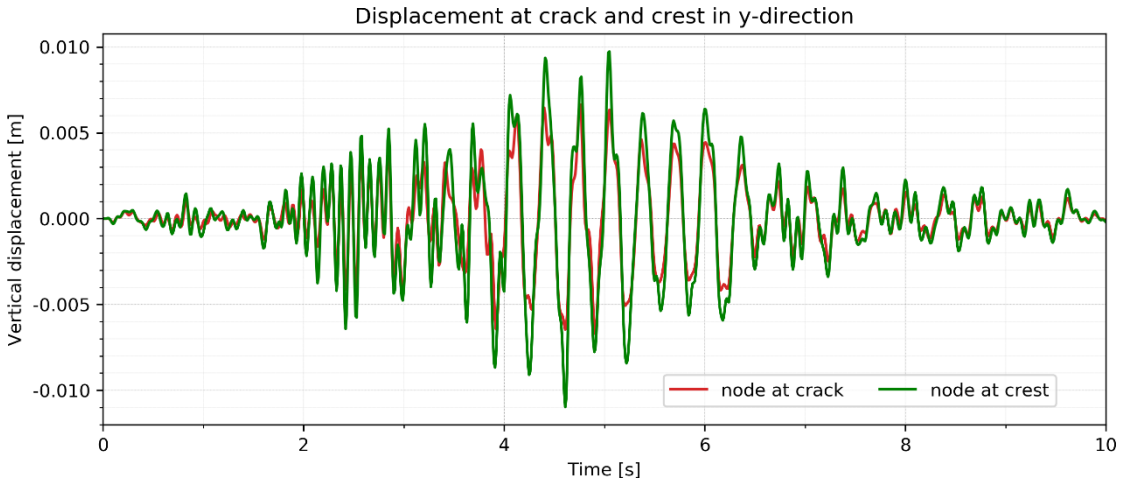

Figure 46: Displacement comparison crack and crest node in y-direction

7.2.2 Koyna Dam with foundation

These linear models include the massless foundation and are subjected to the earthquake as well. In this case the node deformation results at crest and crack are taken separately from the model with full reservoir and with an empty reservoir. Hence, in Figure 47 and Figure 48 the displacement of the crest node in horizontal and vertical direction is shown. The deformation, when the fluid-structure interaction is included at full reservoir, is somewhat larger in both directions at the crest node.

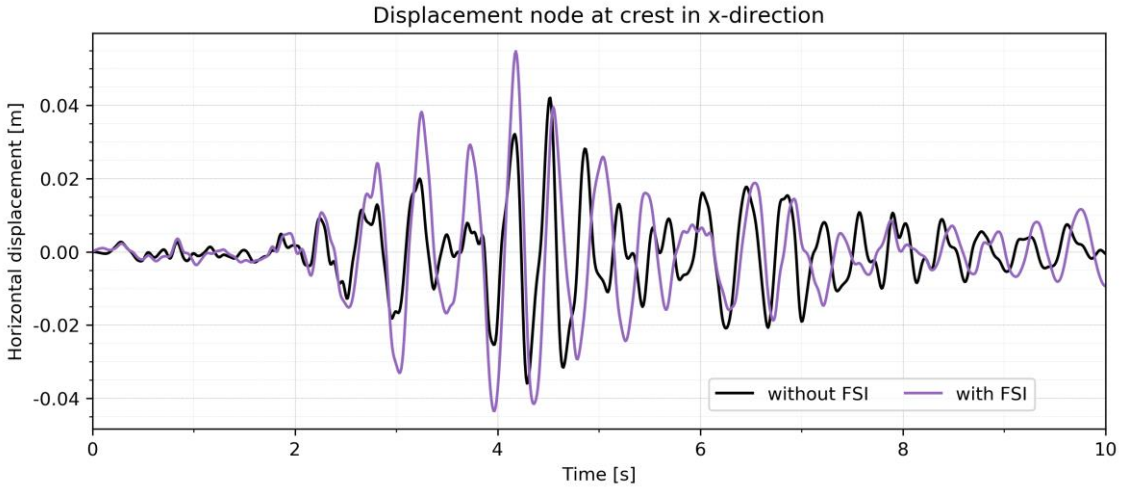

Figure 47: Displacement of crest node in x-direction

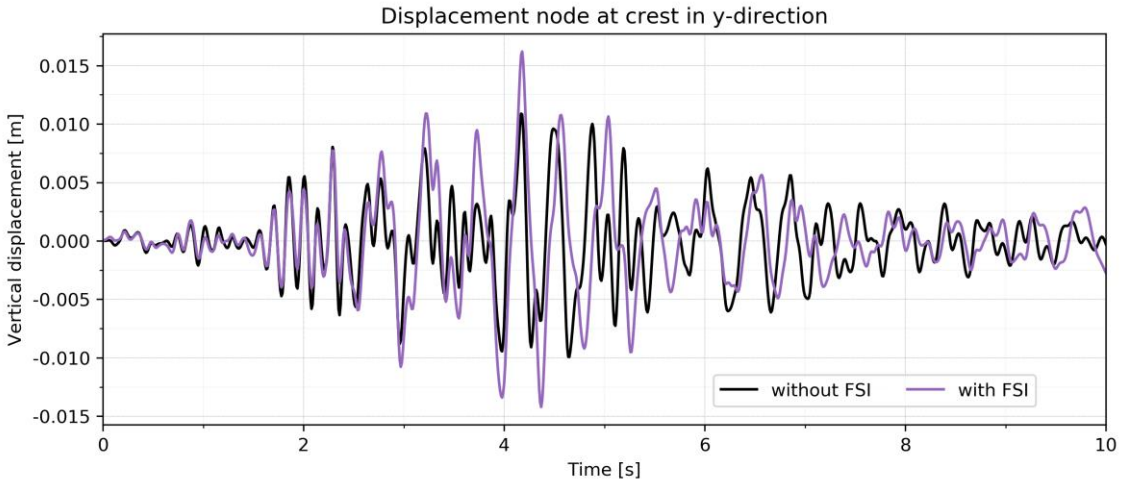

Figure 48: Displacement of crest node in y-direction

Figure 49 and Figure 50 show the displacements of the crack node in horizontal and vertical direction. Also with FSI the absolute deformation is larger, but in comparison with the crest node it is slightly smaller.

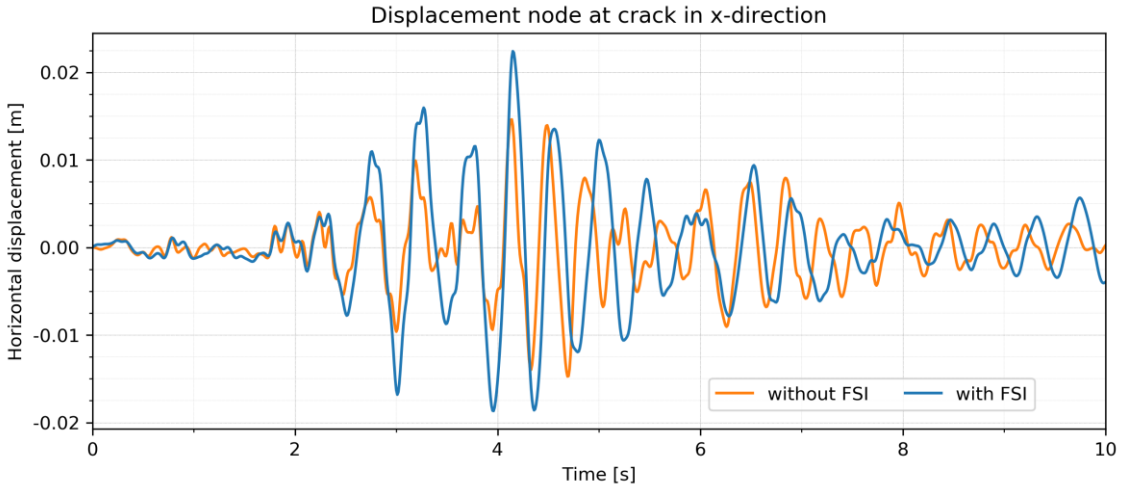

Figure 49: Displacement of crack node in x-direction

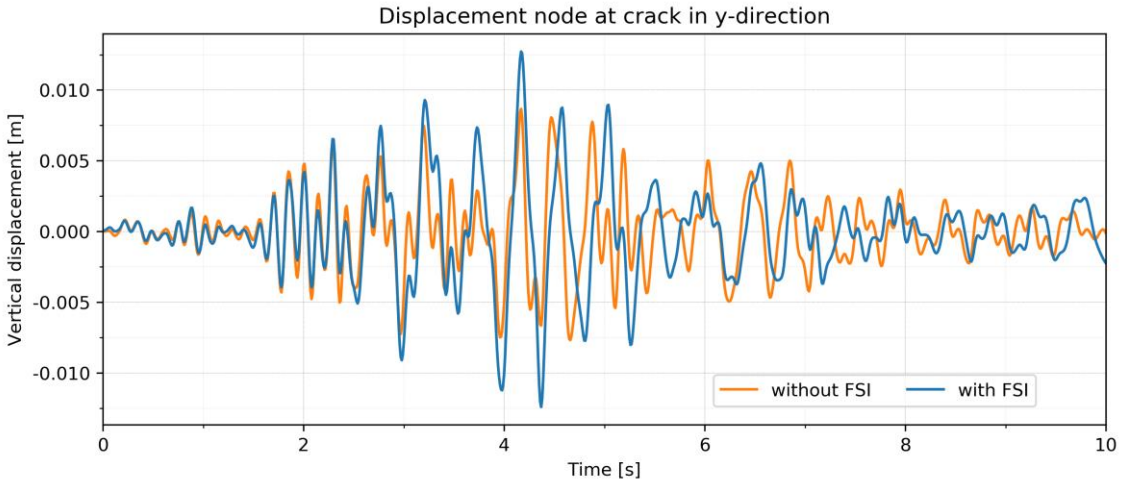

Figure 50: Displacement of crack node in y-direction

7.3 Non-linear models with open crack

In the linear models an additional frictional contact and the corresponding changes of discretization and settings is developed to obtain reasonable results. In the next steps the whole system is mapped in a 3D design to implement the anchors as link elements. Figure 51 and Figure 52 show the Koyna design with one anchor and with 2 anchors. In the first anchor model it is located in the middle of the crest width, in the second anchor model with two pieces the geometry is taken from the Koyna reports (Figure 25). There the left anchor is called anchor 1 which is located on the upstream side, anchor 2 on the downstream side.

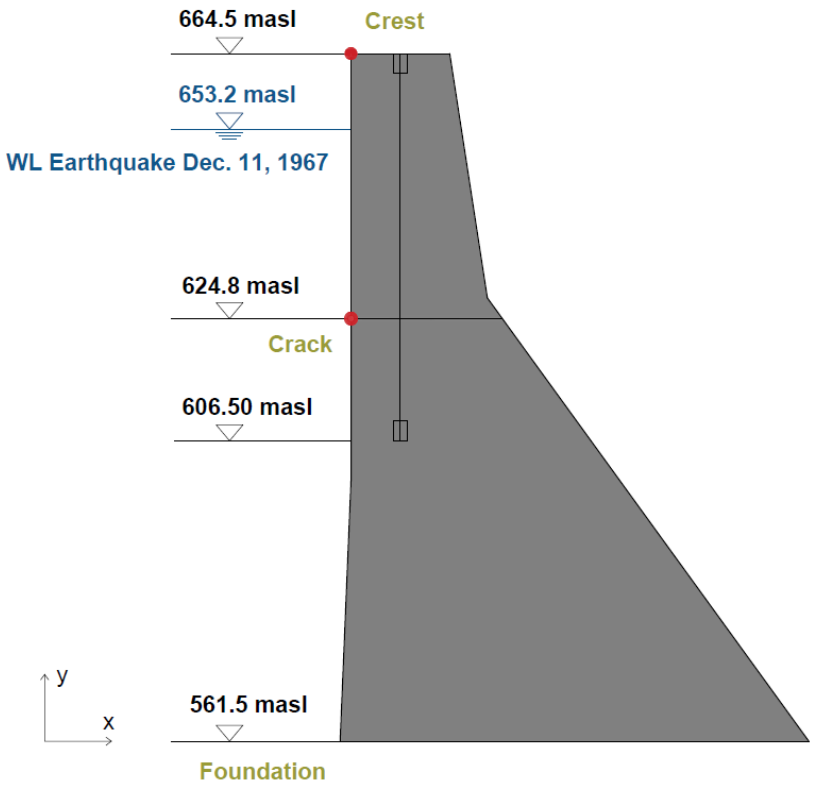

Figure 51: Koyna Dam with one anchor

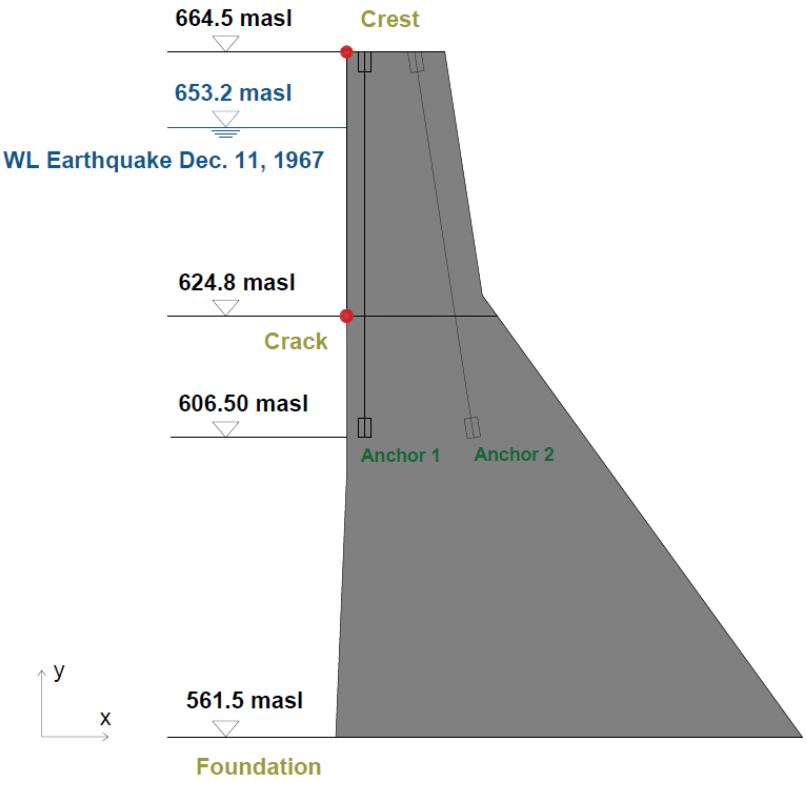

Figure 52: Koyna Dam with two anchors

Now the crack is not bonded anymore, the node at the crack has two sets of results, that one at the top part of the dam, which is only kept by its dead load and friction resistance at its original position and those results of the bottom part of the dam which is bonded with the foundation block. Interesting results for comparing the improvement with anchors with the unreinforced dam are the absolute deformations and the relative deformations of the crest and crack point. Horizontal deformations visible in the diagrams with positive values indicate a movement in downstream direction, with negative values in upstream direction. Furthermore, the contact pressure is determined in selected points of the crack surface and the anchor forces developing during the earthquake period.

7.3.1 Absolute displacements

Figure 53 and Figure 54 show the absolute displacements in x- and y-direction of the crest node for 5 systems with an empty reservoir. The unreinforced systems has an obviously higher deformation than the reinforced ones. Between second 5 and 6 the displacement in x-direction of the unreinforced Koyna system is about 3 times larger than the displacements of the reinforced Koyna systems. The displacement in y-direction of the reinforced systems seems to be slightly larger, but in total the deformation is smaller.

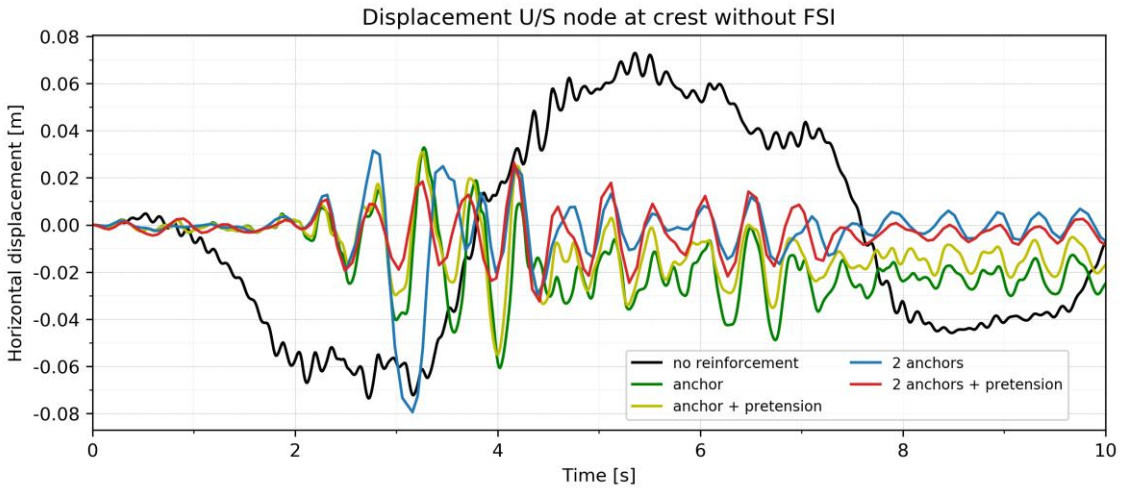

Figure 53: Displacement in x-direction of crest node with empty reservoir

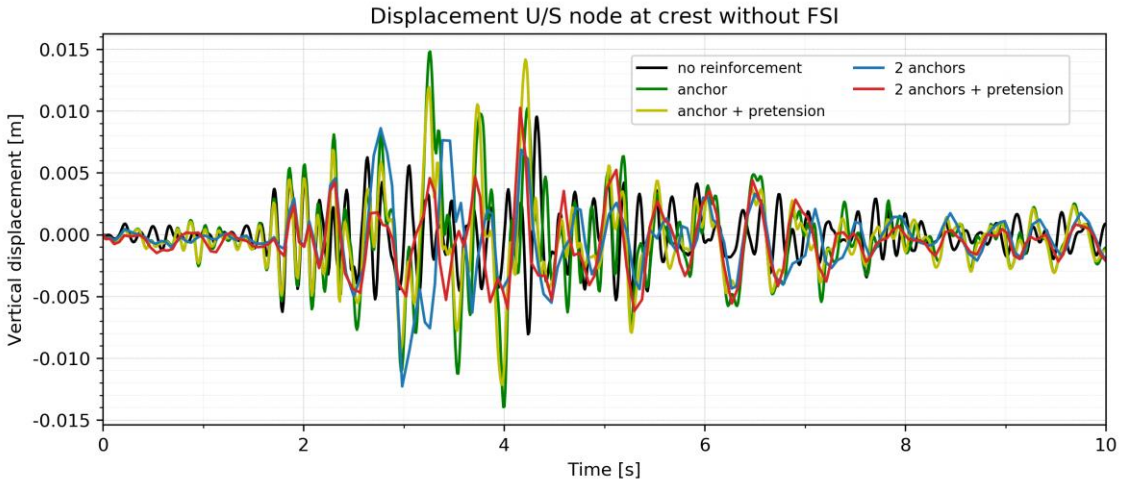

Figure 54: Displacement in y-direction of crest node with empty reservoir

Figure 55 shows the deformation figure of the unreinforced dam, Figure 56 the reinforced dam with two anchors and Figure 57 the reinforced dam with two pre-stressed anchors with scaling at time 3.1 s. The absolute value of horizontal deformation for the unreinforced system is about 7.0 cm, for the passive two anchor system about 8.0 cm and with the two prestressed anchors it is about 1.7 cm in upstream direction. Above in Figure 53 at this time the displacements of the dam with two passive anchors in negative x-direction are slightly higher than that one of the unreinforced dam at the crest node. Also the vertical displacements of the unreinforced model is – also in the following models – smaller than those of the anchored models. In the deformation figures it is visible that the anchored system has conditions of rocking or tilting due to the supporting anchors, which leads to a higher displacement in y-direction and a smaller displacements in x-direction and a smaller total displacement. The higher peak of the two anchors system (blue line) in the crest point shown in Figure 53 is caused by a kind of bending back of the dam, which does not occur anymore in the crack point anymore, which is shown in Figure 58. The scaled deformation figure in Figure 55 shows the crest part sliding in a plane condition in upstream direction.

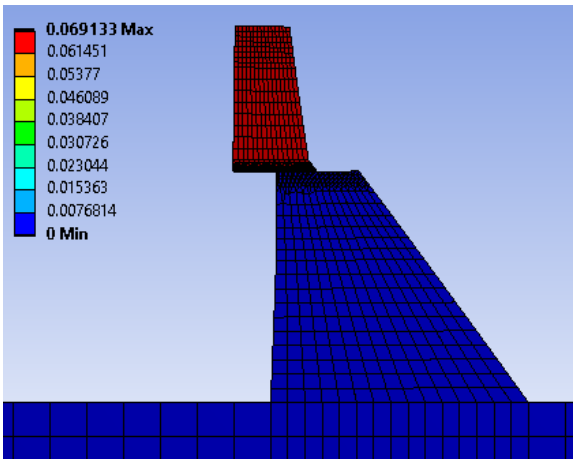

Figure 55: Deformation figure of the unreinforced dam at time 3.1 s with a scaling of 1.7e2

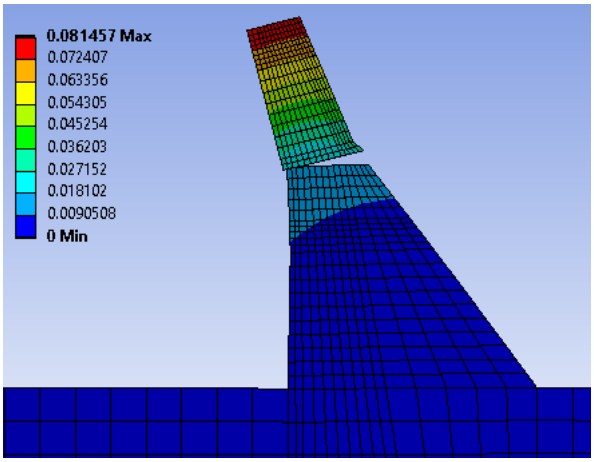

Figure 56: Deformation figure of dam with two anchors at time 3.1 s with a scaling of 1.7e2

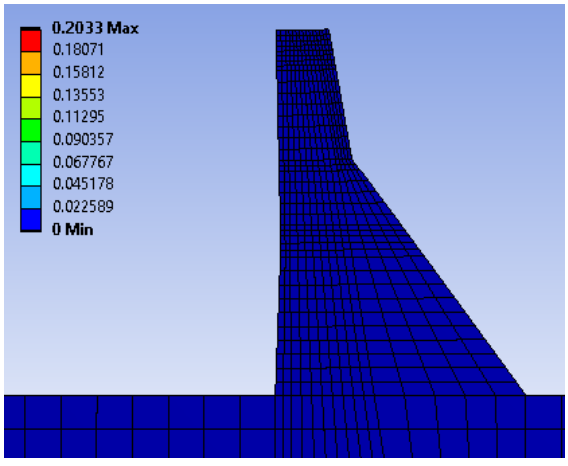

Figure 57: Deformation figure of dam with two prestressed anchors at time 3.1 s with a scaling of 1.7e2

Figure 58 and Figure 59 show the absolute displacements in x- and y-direction of the crack node at the top part for 5 systems with an empty reservoir. The diagrams are similar to those at the crest node, which means the crest block is sliding over the crack surface in upstream (negative x-value) and downstream (positive x-value) direction during the earthquake. The displacement of the unreinforced systems is larger as well than these of the reinforced systems in x-direction.

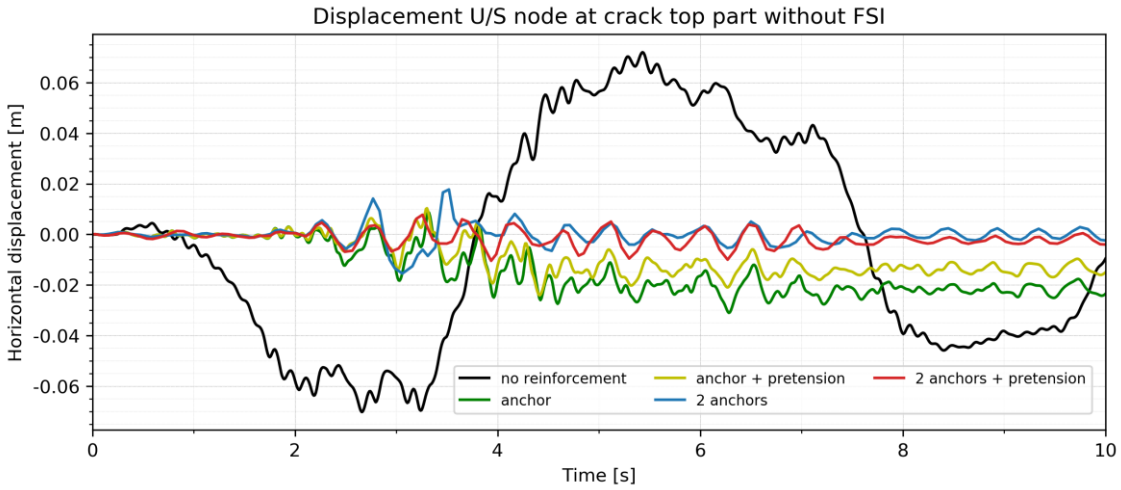

Figure 58: Displacement in x-direction of crack node at top part with empty reservoir

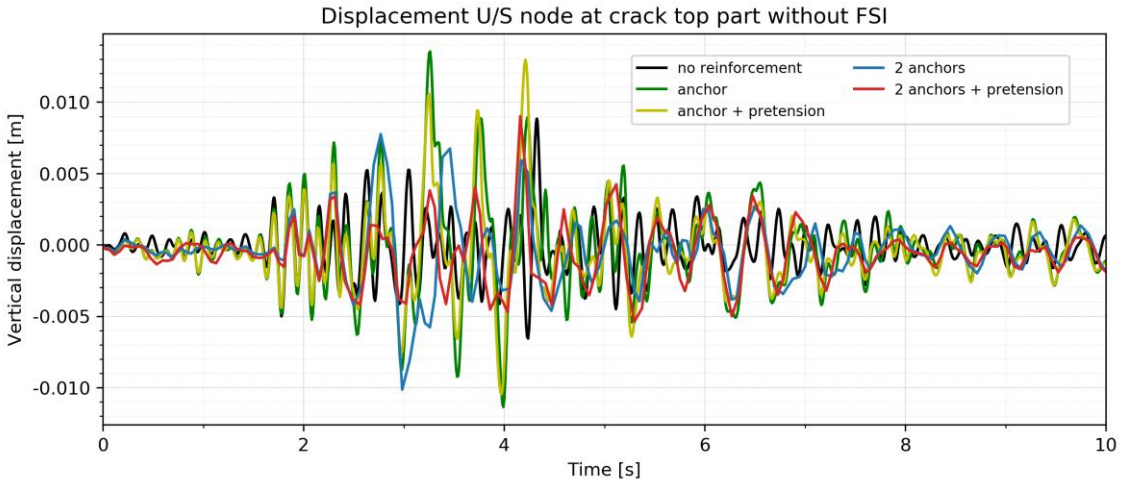

Figure 59: Displacement in y-direction of crack node at top part with empty reservoir

Figure 60 and Figure 61 show the absolute displacements in x- and y-direction of the crack node at the bottom part for 5 systems with an empty reservoir. The

bottom part is bonded with the rock foundation below, therefore, the deformations values are small. In all models it has to be in a similar range.

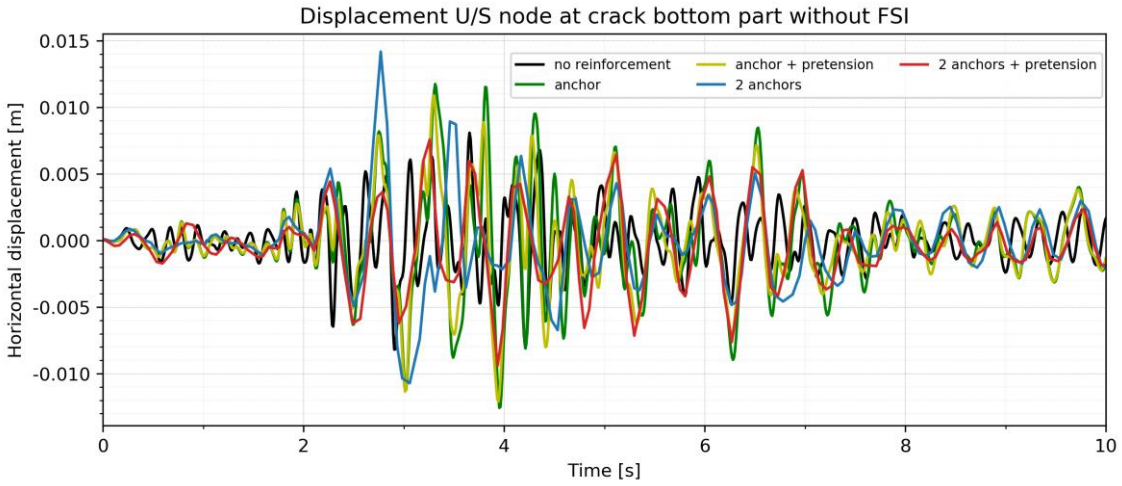

Figure 60: Displacement in x-direction of crack node at bottom part with empty reservoir

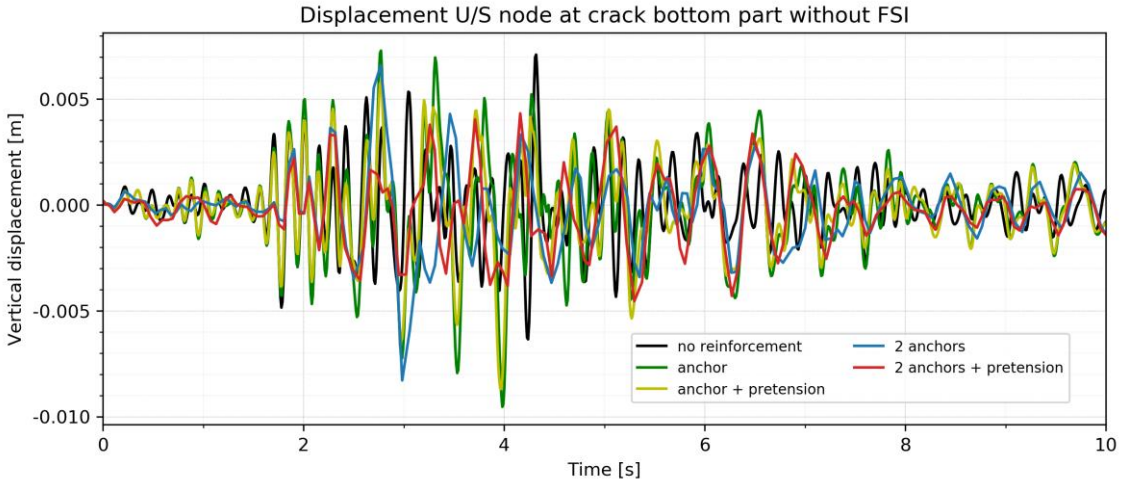

Figure 61: Displacement in y-direction of crack node at bottom part with empty reservoir

Figure 62 and Figure 64 show the absolute displacements in x- and y-direction of the crest node for 5 systems with a full reservoir. Figure 63 shows the displacement in x-direction of the reinforced systems for a better legibility of the values. The deformation of the crest part without anchors is about 9.0 m, when the reservoir is filled up. In comparison the deformations of the systems with anchors are practically not significant compared to the dimensions of the dam. In Figure 63 the small displacements of the crest node of each anchored system is shown

in which the performance of the anchors with pretension seems to be somewhat better than the passive anchors. The last value at second 10 is about 2.5 cm for passive anchors and 1.5 cm for the posttensioned anchor systems. The significant displacements which occur in both models without reinforcement, with and without reservoir, are caused by the modelling of the system. Usually during the construction of a concrete dam, in the vertical contraction joints between the monoliths, shear keys are implemented (described in chapter 7.3.2.1) in order to avoid too large deformations of the cross-section.

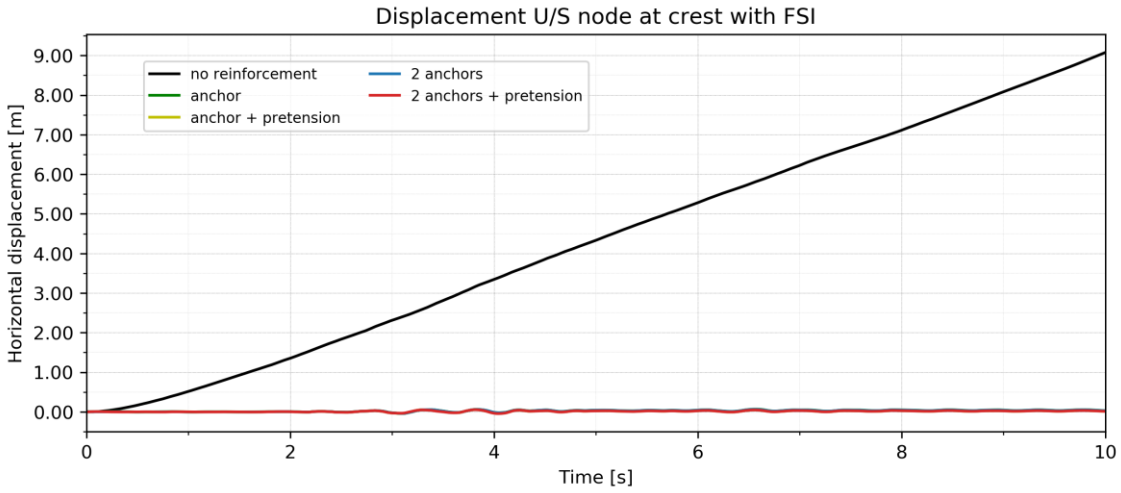

Figure 62: Displacement in x-direction of crest node with full reservoir

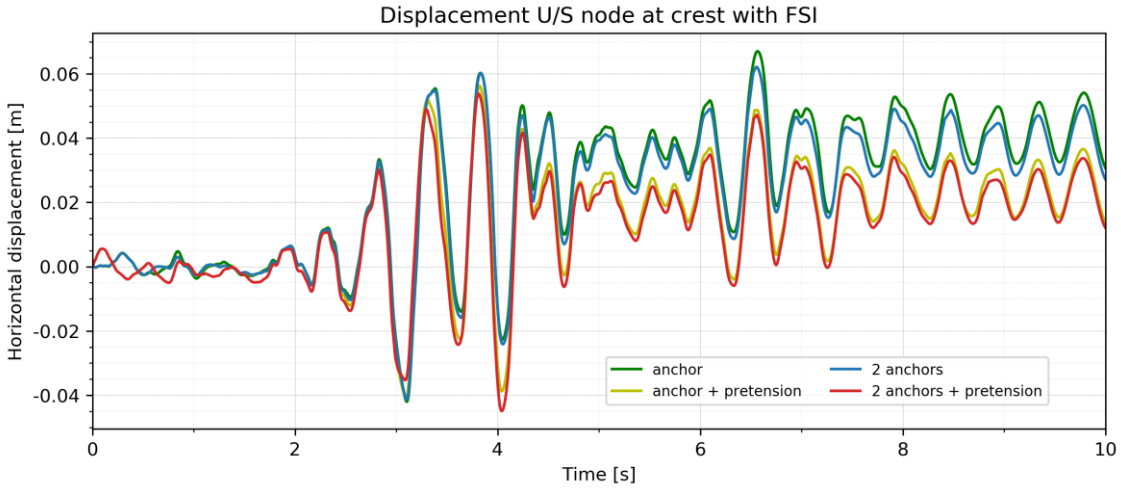

Figure 63: Displacement in x-direction of crest node with full reservoir (reinforced systems)

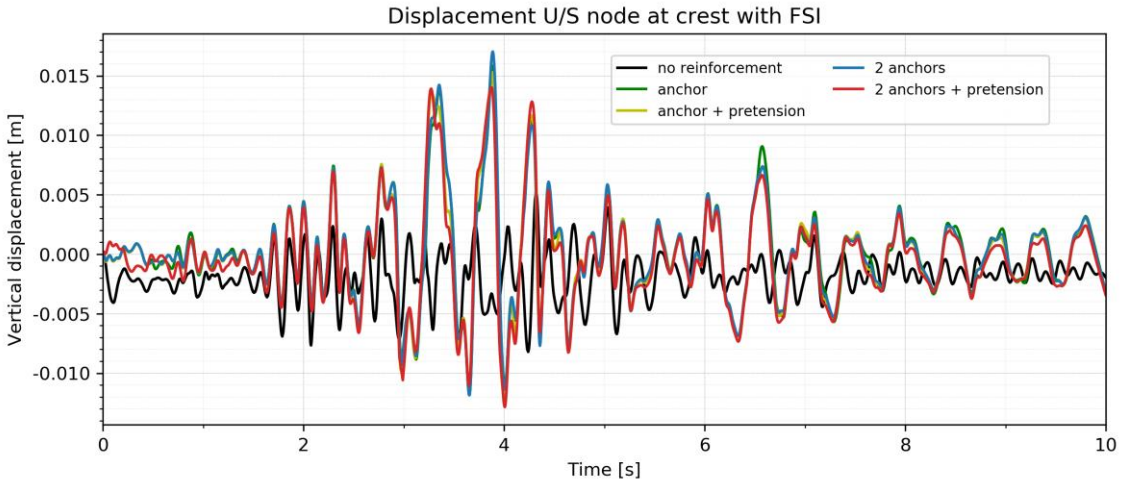

Figure 64: Displacement in y-direction of crest node with full reservoir

Figure 65 shows the deformation figure of the unreinforced dam in a true scale at final time 10 s. The total displacement is about 9.0 m, also depicted in Figure 62. Due to the simplification in the numerical analysis this result is obtained, which is not possible respectively higher than in reality because normally shear keys are implemented between the monoliths of a dam to prevent large deformations. The crest part slides on the plane surface of the bottom part, so there is almost no displacements in vertical direction due to the dead load of the concrete. Figure 66 shows for comparison the scaled deformation figure of the dam with one pre-stressed anchor at the final time. The displacement is also towards downstream side, which is shown in Figure 63 and Figure 68, but noticeably smaller in x-direction.

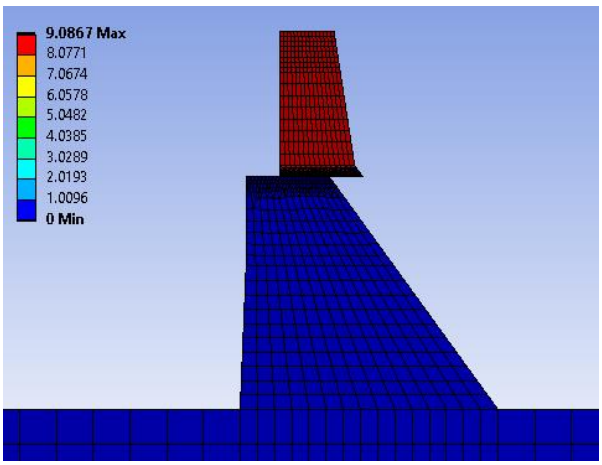

Figure 65: Deformation figure of the unreinforced dam with FSI at time 10 s without scaling (true scale)

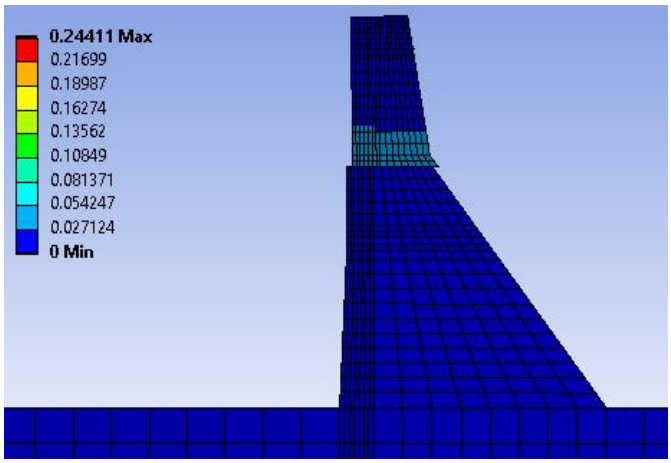

Figure 66: Deformation figure of dam with one prestressed anchor with FSI at time 10 s with a scaling of 65

Figure 67 and Figure 69 show the absolute displacements in x- and y-direction of the crack node at the top part for 5 systems with a full reservoir. Figure 68 shows the displacement in x-direction of the reinforced systems for a better legibility of the values. The deformation of the crack node in the unreinforced system is about 9.1 m unlike to the almost zero value of the reinforced systems. The performance of the posttensioned anchors is again better with a final node displacement among 2 cm than that one of the passive anchors with displacement value of 3.5 cm at second 10.

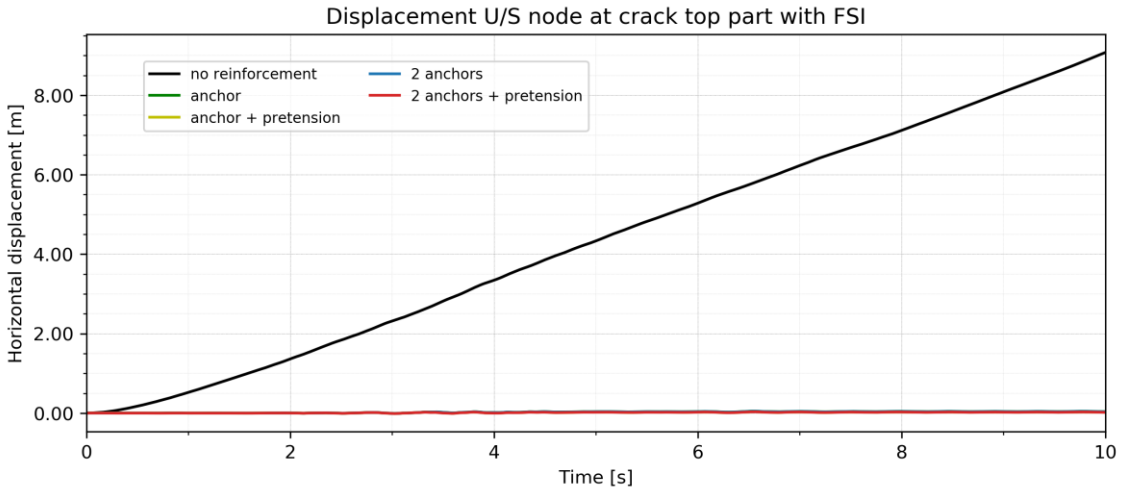

Figure 67: Displacement in x-direction of crack node at top part with full reservoir

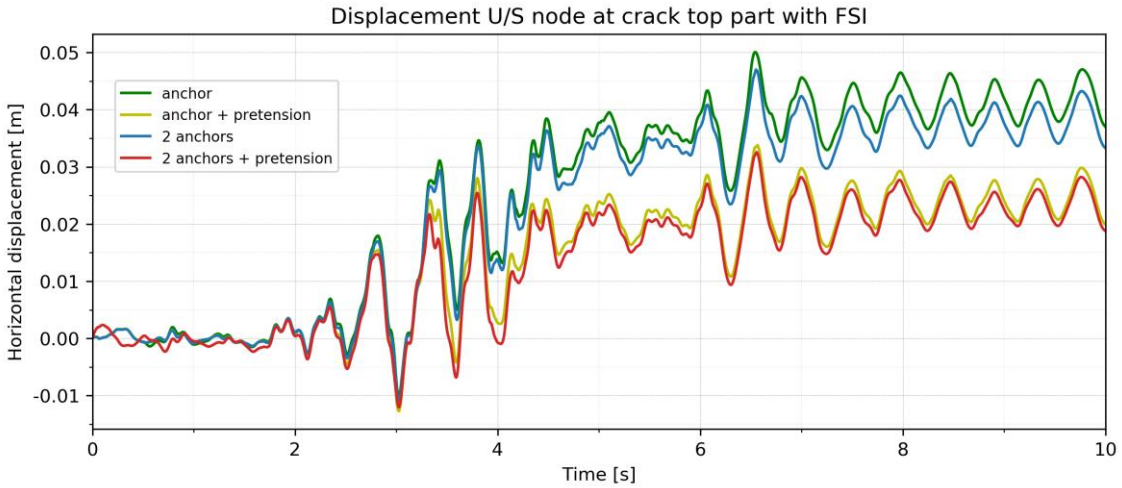

Figure 68: Displacement in x-direction of crack node at top part with full reservoir (reinforced systems)

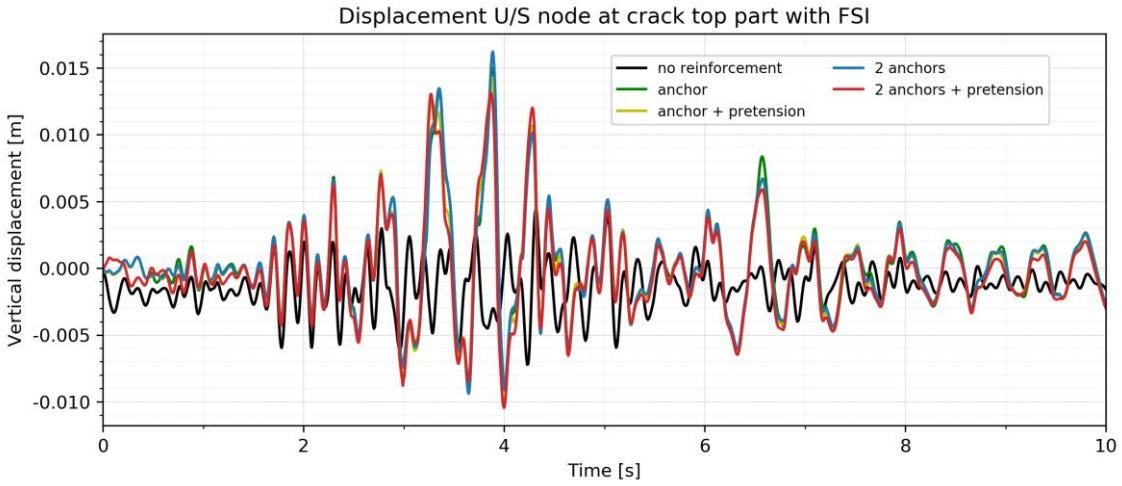

Figure 69: Displacement in y-direction of crack node at top part with full reservoir

Figure 70 and Figure 71 show the absolute displacements in x- and y-direction of the crack node at the bottom part for 5 systems with a full reservoir.

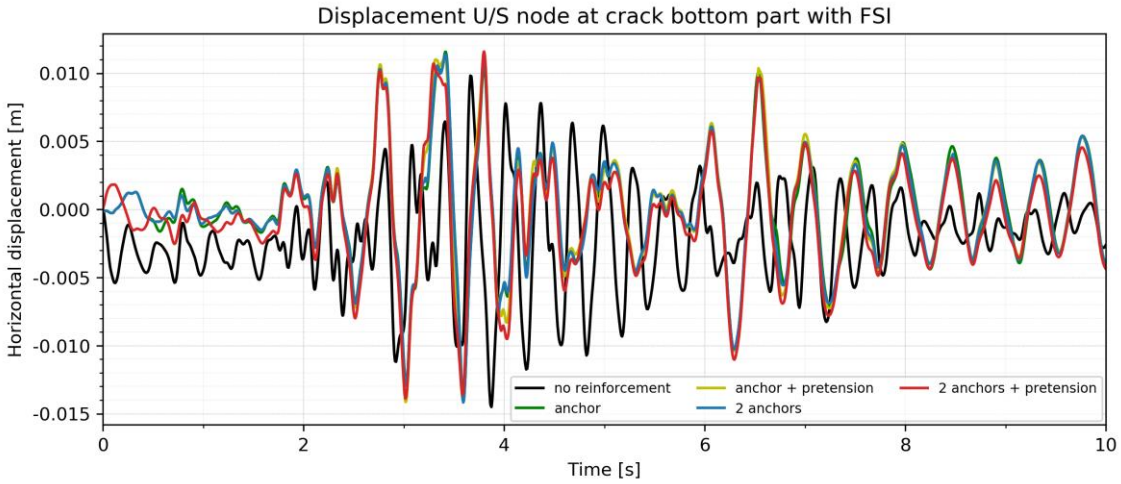

Figure 70: Displacement in x-direction of crack node at bottom part with full reservoir

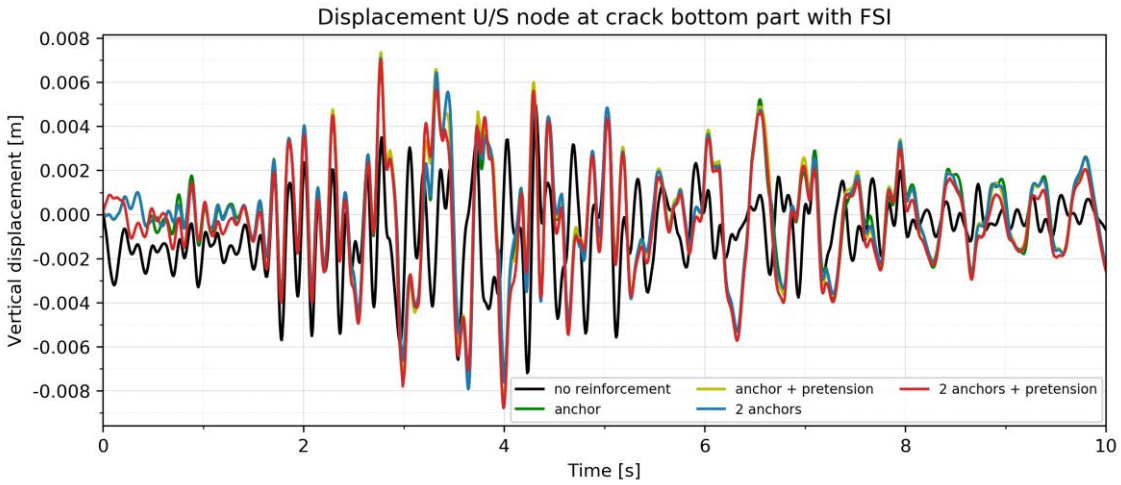

Figure 71: Displacement in x-direction of crack node at bottom part with full reservoir

7.3.2 Relative displacements

The relative displacements are determined in the crack node with following approach:

$$u_{r,crack}(t_i) = u_{r,crack}^{Top}(t_i) - u_{r,crack}^{Bottom}(t_i) \tag{77}$$

Where $u_{r,crack}$ is the relative displacement at a certain time t_i ranging from second 0 to 10. $u_{r,crack}^{Top}$ is the absolute displacement at the crack node of the top part and $u_{r,crack}^{Bottom}$ is the absolute displacement of the crack node at the bottom part of the dam. This means that the higher the deformation of the crest part, a larger amount of relative displacement can be observed. As noticed earlier, the displacement values of the bottom node are only in the range of a few millimeter.

Figure 72 shows the relative displacement in x-direction in the crack area for 5 Koyna systems with an empty reservoir. The displacement peaks of the unreinforced system add up to 7.5 cm, while the final deformation of the one anchor systems with and without pretension sets around 2.0 cm. The passive two anchor model has displacement values around zero, the pretensioned anchor systems creates practically no deformation. This leads to the first assumption that two posttensioned anchors located with different orientations in a dam might perform better during an earthquake situation than one vertical anchor with a larger diameter.

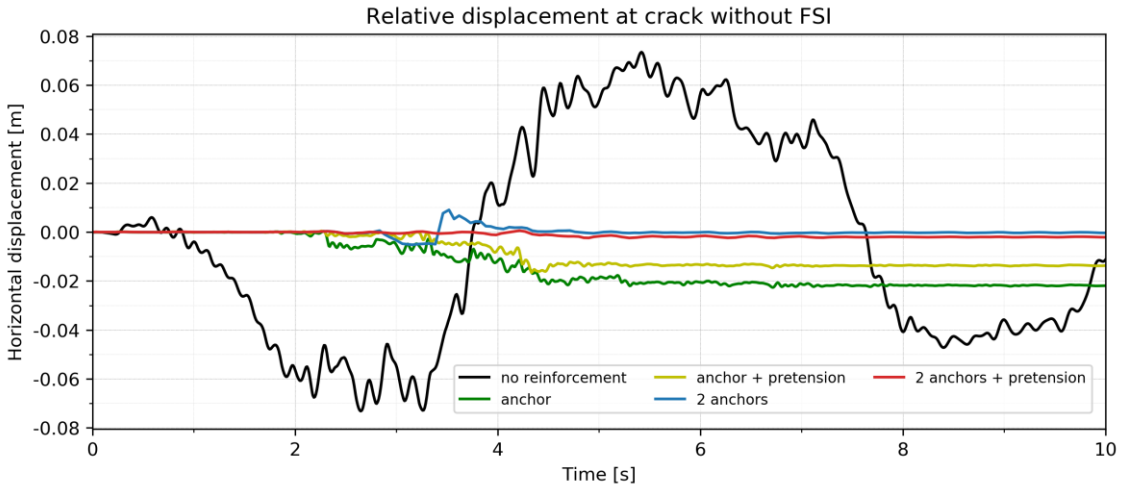

Figure 72: Relative displacement in x-direction in crack node with empty reservoir

Figure 73 shows the relative displacement in y-direction in the crack area for 5 Koyna systems with an empty reservoir. Apparently the relative deformation of the unreinforced system is larger in x-direction, it is virtually non-existent in the y-direction. The relative displacements of the reinforced systems still contains

some peaks up to 1.3 cm during the acceleration peaks of the Koyna earthquake. This refers to a rocking movement due to anchoring of the reinforced crest part as there is a larger vertical displacement than of the unreinforced crest.

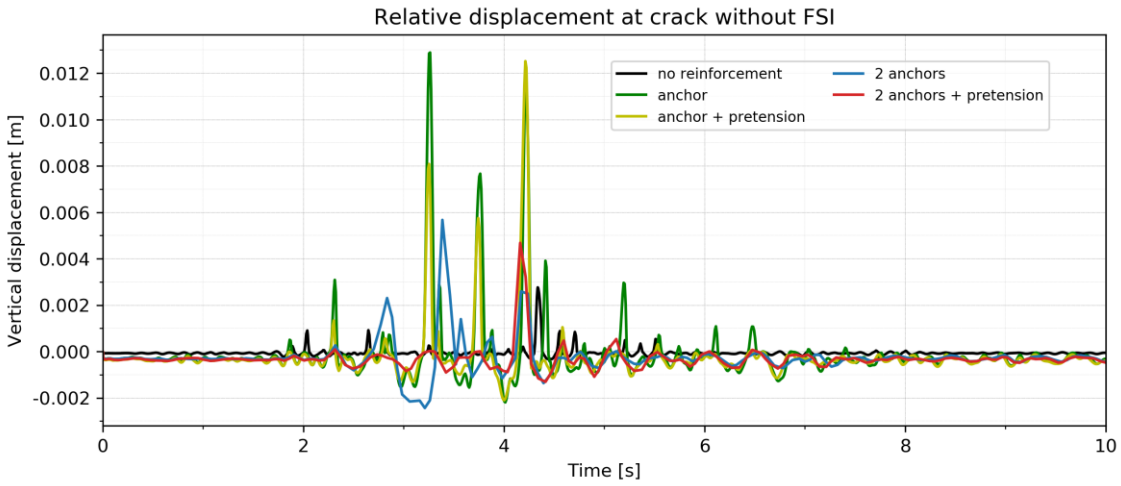

Figure 73: Relative displacement in y-direction in crack node with empty reservoir

Figure 74 and Figure 75 show the scaled deformation figures of the dam with one anchor respectively one prestressed anchor at the time 3.25 s, where a peak in Figure 73 of the green and yellow line occurs. As it is shown in the deformation figures, the crest part is rocking at this point, so the distance between the crack node of the top part and the bottom part is at its highest level.

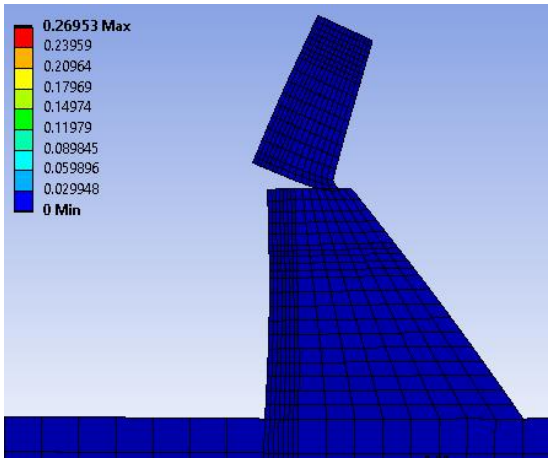

Figure 74: Deformation figure of dam with one anchor at time 3.25 s with a scaling of 5.6e2

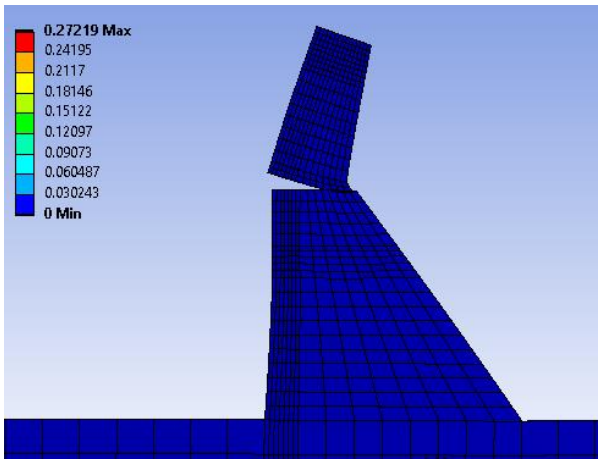

Figure 75: Deformation figure of dam with one prestressed anchor at time 3.25 s with a scaling of 5.6e2

Figure 76 shows the relative displacement in x-direction in the crack area for 5 Koyna systems with a full reservoir. The relative displacement in the crack of the unreinforced systems amounts to 9.10 m. Even with the filled up reservoir the performance of the reinforced systems is still sufficient.

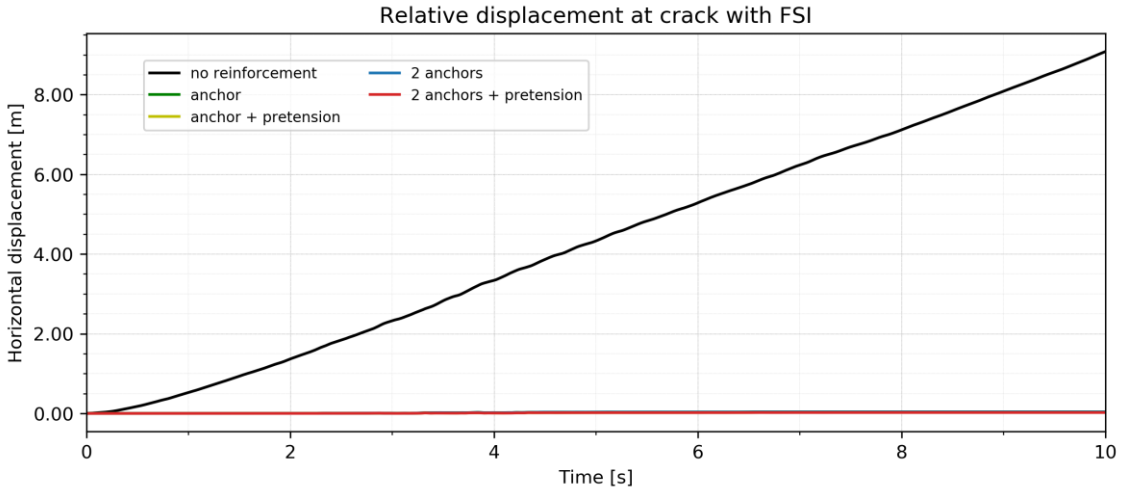

Figure 76: Relative displacement in x-direction in crack node with full reservoir

Figure 77 shows the relative displacement in x-direction in the crack area for the reinforced Koyna systems with a full reservoir for a better legibility of the values. With the smallest deformation of 2.3 cm at second 10 the two anchor system with pretension has the best performance, but the one anchor system with pretension is almost equally good. The relative final deformation of the two anchor model is 3.7 cm which is about 38% more than this one of the posttensioned

systems. The final relative deformation of the one anchor model is 4.2 cm which is about 45% more than this one of the posttensioned systems. This leads to the assumption that posttensioned anchors work better than passive anchors in an earthquake situation with a full reservoir. The shape of all reinforced deformation figures is similar.

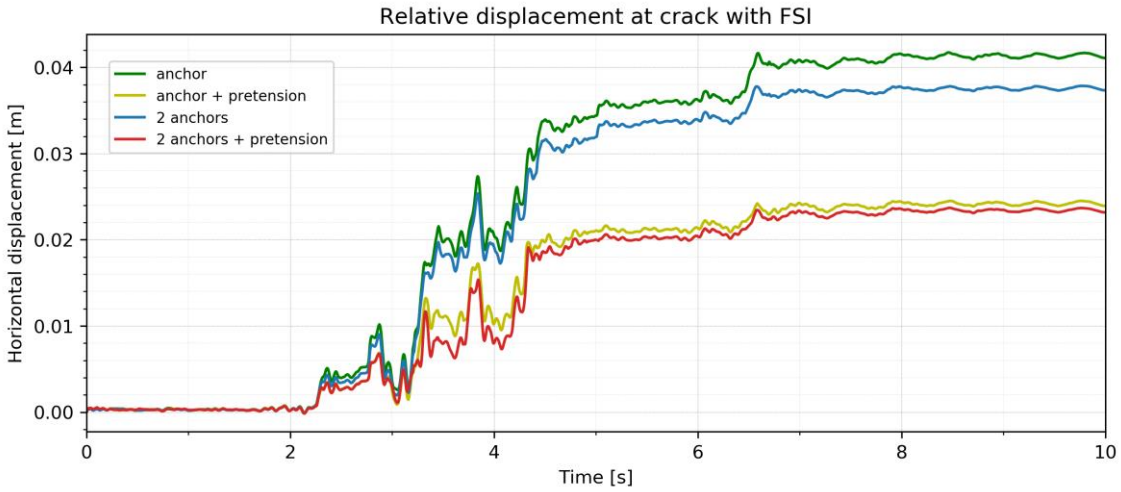

Figure 77: Relative displacement in x-direction in crack node with full reservoir (reinforced systems)

Figure 78 shows the relative displacement in y-direction in the crack area for 5 Koyna systems with a full reservoir. The relative displacements of the reinforced systems still contains some peaks up to 1.4 cm during the acceleration peaks of the Koyna earthquake. The unreinforced model has almost no relative deformation in y-direction.

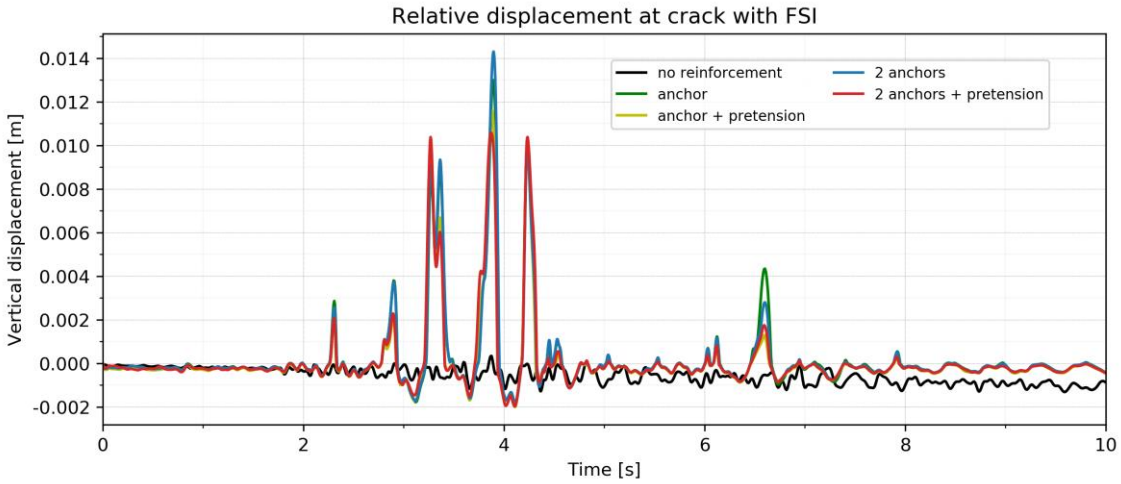

Figure 78: Relative displacement in y-direction in crack node with full reservoir

Figure 79 and Figure 80 show the scaled deformation figures of the dam with two anchors respectively two prestressed anchors with FSI at the time 3.9 s, where a peak in the vertical displacement of Figure 78 occurs. Due to the rocking of the crest part the distance of the crack node at top and bottom part is large, which explains the higher relative displacement at this point.

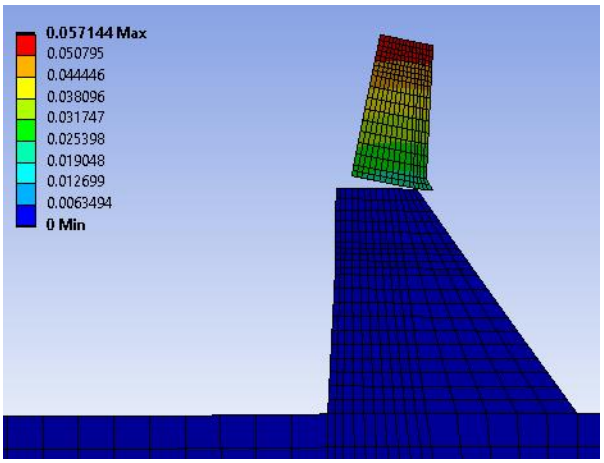

Figure 79: Deformation figure of dam with two anchors with FSI at time 3.9 s with a scaling of 2.4e2

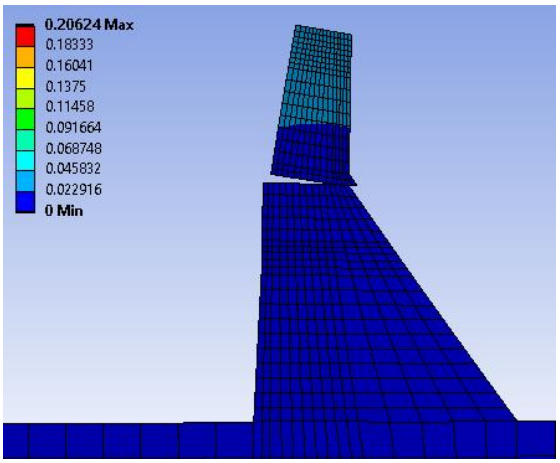

Figure 80: Deformation figure of dam with two prestressed anchors with FSI at time 3.9 s with a scaling of 2.4e2

It is important to mention that all models of Koyna Dam are idealized sections cut out of the whole dam with a given depth of 1 m. This means the obtained deformation figures are idealized as well and do not exactly correspond to the reality. Due to the fact that shear keys are installed in the concrete blocks and a lateral confinement is provided, the deformations would be smaller, especially at the unreinforced systems. But for first testing of stability of the crest block reinforced with anchors the relationship of the displacement values of different systems is an adequate approximation to reality. Since the absolute and relative displacements are analyzed and evaluated, it can be said that the total performance of the posttensioned anchors is noticeably better than that one of the passive anchors. The number and location of the anchors is also an important factor because in the results it is noticeable that the two anchor system works better than the one anchor system with the same sum of cross-section area. Both horizontal forces (e.g. hydrostatic pressure) and vertical forces can be resisted in a better way with the installation of anchors in different angles due to the response of the crest part.

7.3.2.1 Shear keys [37]

Concrete gravity dams as well as concrete arch dams are built of sections or monoliths, which are connected with contraction joints between the single monoliths. The so-called shear keys are situated in the contraction joints and help to withstand relative displacements between the monoliths. Relative displacements

can occur during seismic loadings and may cause cracking in the concrete. The maximum relative displacements in the horizontal direction of the Koyna models obtained in the numerical analysis are listed in Table 8:

Table 8: Maximum relative displacements in horizontal direction

Koyna Dam model		Maximum relative displacement in x-direction
Empty reservoir	No reinforcement	7.5 cm
	One passive anchor	2.2 cm
	One prestressed anchor	1.4 cm
	Two passive anchors	1.0 cm
	Two prestressed anchors	0.3 cm
Full reservoir	No reinforcement	9.10 m
	One passive anchor	4.1 cm
	One prestressed anchor	2.4 cm
	Two passive anchors	3.7 cm
	Two prestressed anchors	2.3 cm

The strength of shear keys can be determined with laboratory tests or FEM analysis. So a maximum relative displacement is possible to be identified. In order to avoid cracking or destruction of the contraction joints and the concrete itself, the

shear keys have to endure a maximum relative displacement of 5 cm for the selected types of reinforcement in the Koyna models.

7.3.3 Contact pressure in the crack

The contact pressure is determined in the crack area, where the frictional contact occurs and the pretension force is applied in the anchors. In the initial test model without dead load the contact pressure is used for a plausibility check to make sure the bolt pretension tool in ANSYS is working and the contact pressure corresponds to the applied pretension force. The following results are extracted from the final models with dead load of the crest block and show the contact pressures in 5 selected points, point 1 is located at the upstream side of the crack area and point 5 is located at the downstream side which is shown in Figure 81.

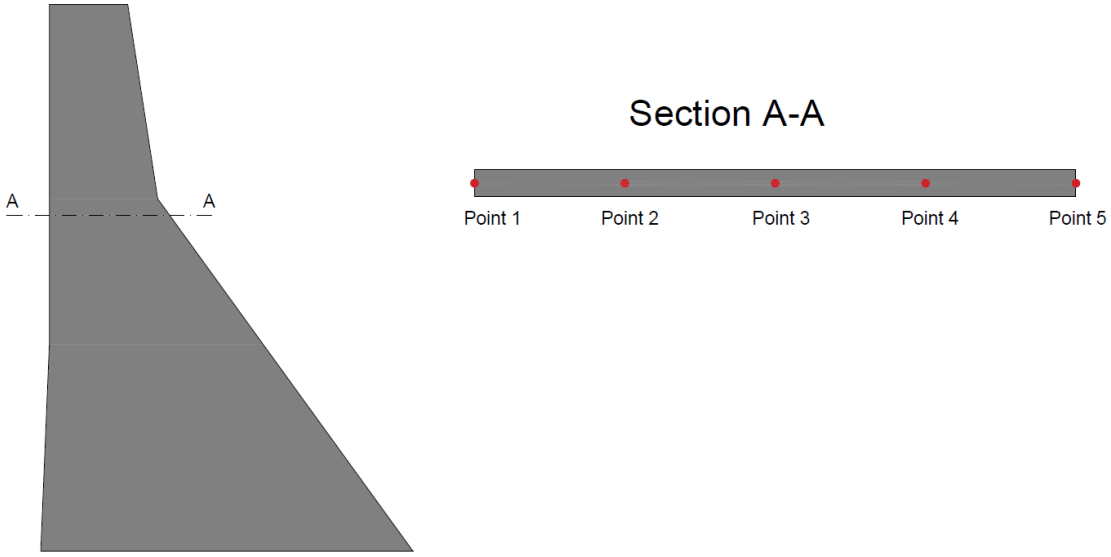

Figure 81: Contact pressure points

Figure 82 shows the contact pressure in 5 points of the one anchor model with pretension and with an empty reservoir. The highest pressure is about 8.2 MPa in point 1.

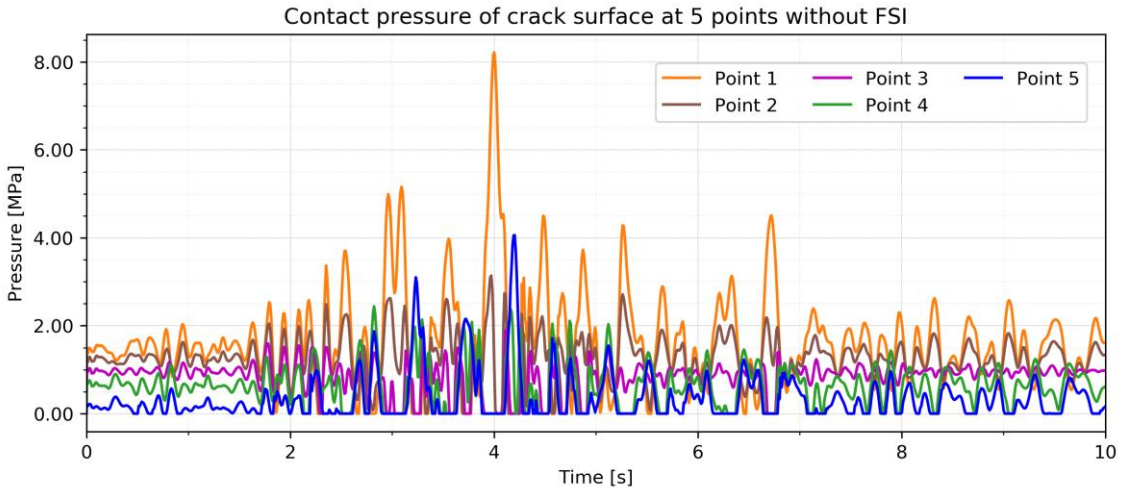

Figure 82: Contact pressure in the crack area with one anchor with empty reservoir

Figure 83 shows the contact pressure of the Koyna model with one prestressed anchor with empty reservoir at the crack area from upstream to downstream side. This is the stress distribution at time 4 s, where the peak of point 1 with about 8.2 MPa can be seen clearly.

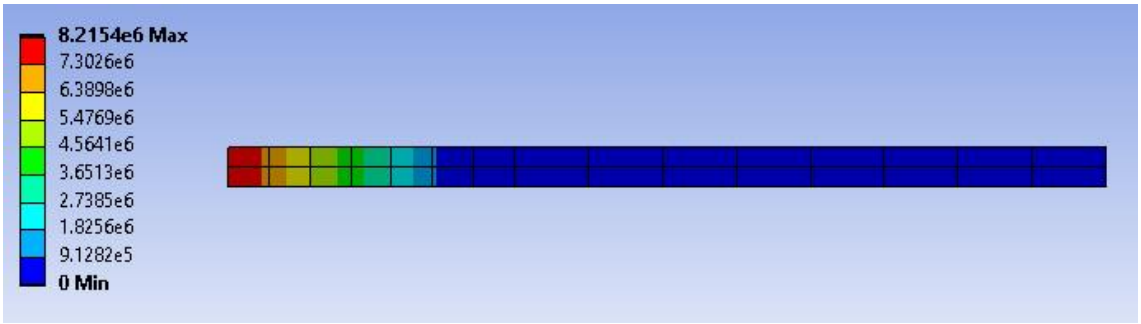

Figure 83: Contact pressure with one prestressed anchor without FSI at the crack area at time 4 s

Figure 84 shows the contact pressure in 5 points of the one anchor model with pretension and with a full reservoir. The highest pressure is about 7.8 MPa in point 1.

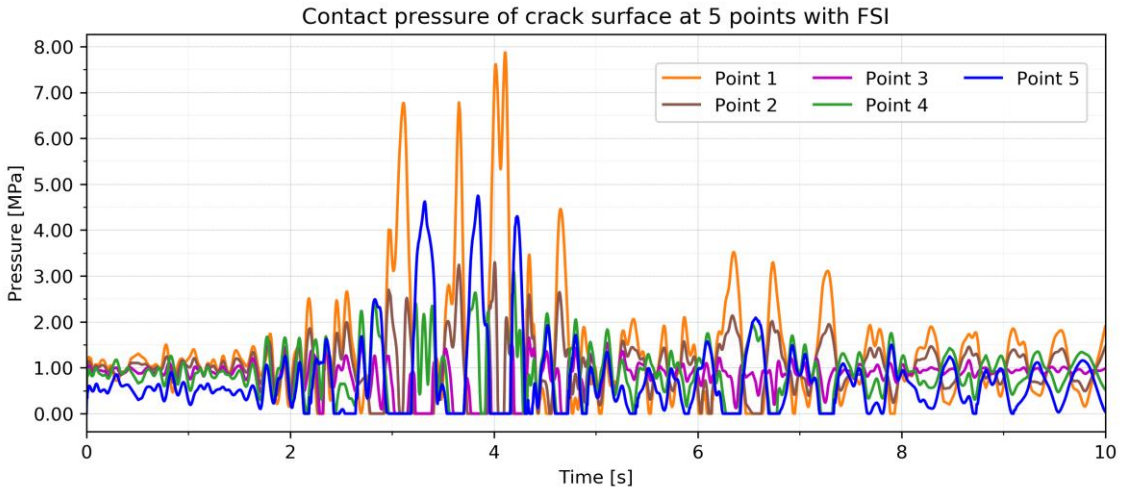

Figure 84: Contact pressure in the crack area with one anchor with full reservoir

Figure 85 shows the contact pressure of the Koyna model with one prestressed anchor with full reservoir at the crack area from upstream to downstream side. This is the stress distribution at time 4 s, where point 1 has a value of 6.85 MPa.

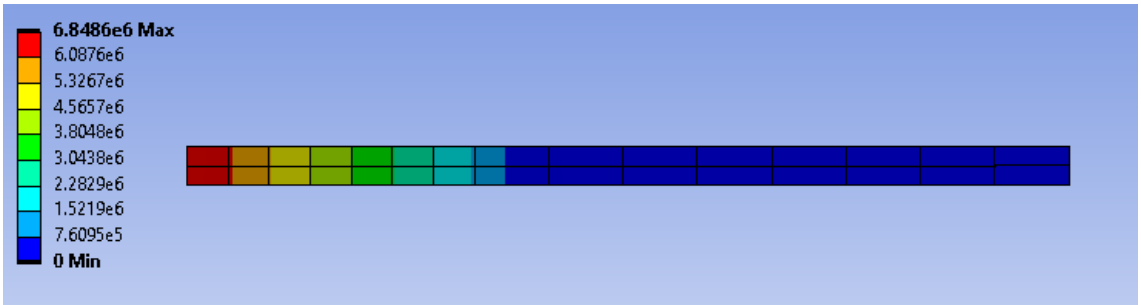

Figure 85: Contact pressure with one prestressed anchor with FSI at the crack area at time 4 s

Figure 86 shows the contact pressure in 5 points of the two anchors model with pretension and with an empty reservoir. The highest pressure is about 5.0 MPa in point 1.

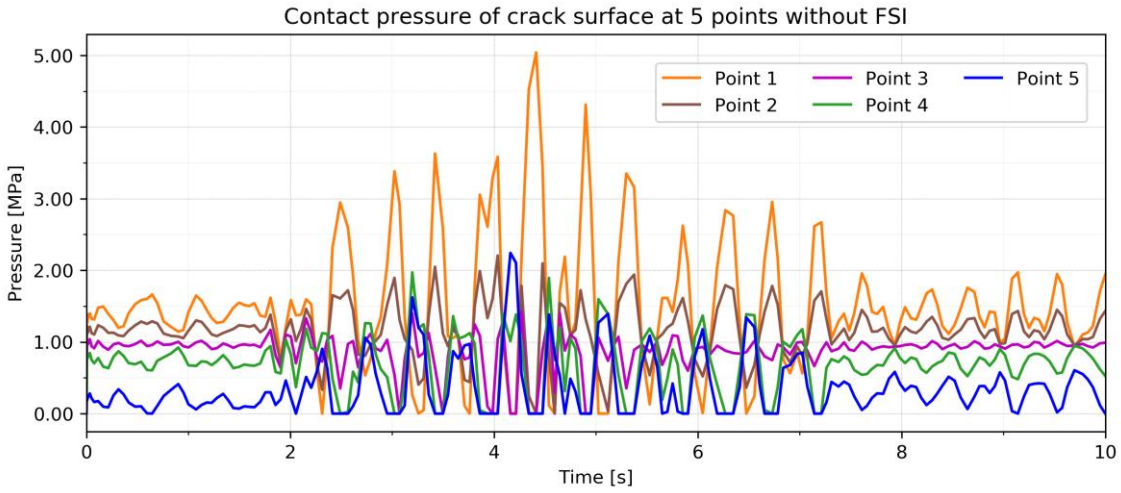

Figure 86: Contact pressure in the crack area with two anchors with empty reservoir

Figure 87 shows the contact pressure of the Koyna model with two prestressed anchors with empty reservoir at the crack area from upstream to downstream side. This is the stress distribution at time 4 s, where point 1 has a value of 3.3 MPa.

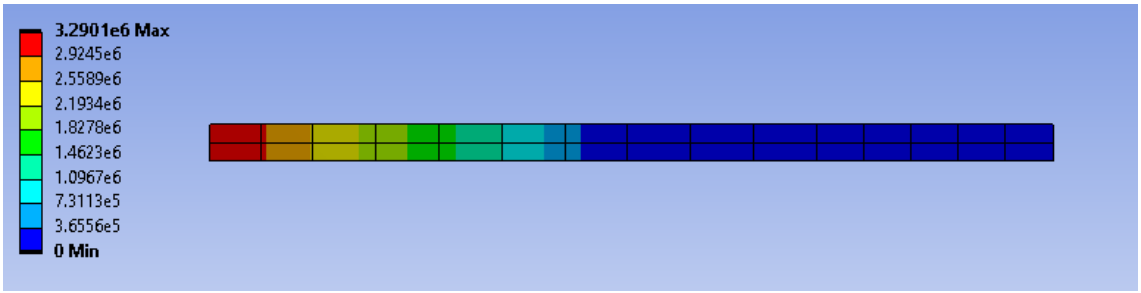

Figure 87: Contact pressure with two prestressed anchors without FSI at the crack area at time 4 s

Figure 88 shows the contact pressure in 5 points of the two anchors model with pretension and with a full reservoir. The highest pressure is about 7.7 MPa in point 1.

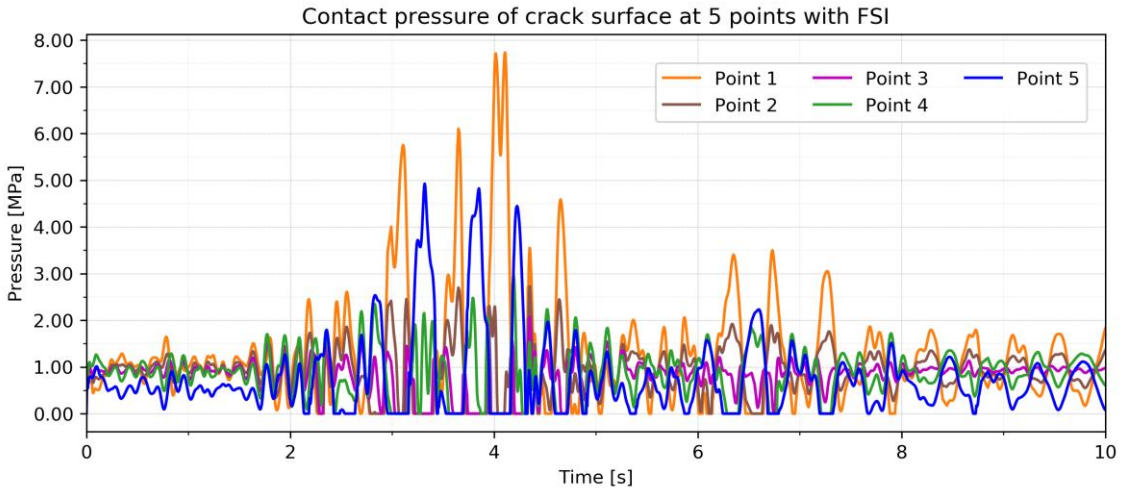

Figure 88: Contact pressure in the crack area with two anchors with full reservoir

Figure 89 shows the contact pressure of the Koyna model with two prestressed anchors with full reservoir at the crack area from upstream to downstream side. This is the stress distribution at time 4 s, where point 1 has a value of 6.86 MPa and is therefore similar to the model with one prestressed anchor and full reservoir.

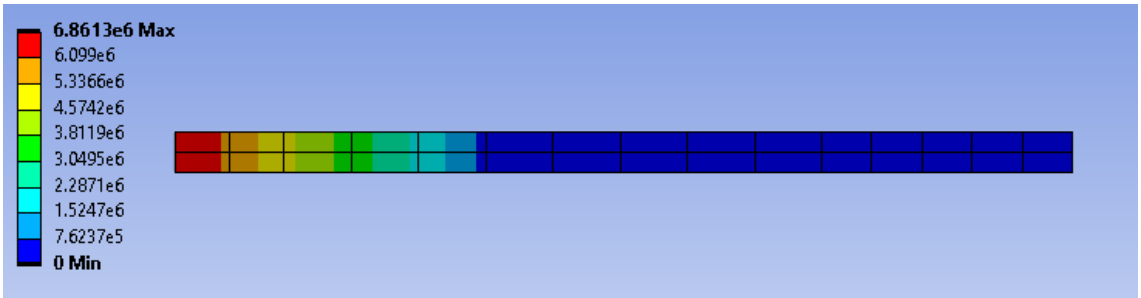

Figure 89: Contact pressure with two prestressed anchors with FSI at the crack area at time 4 s

In summary the contact pressure is quite similar of all models, the model with two prestressed anchors with an empty reservoir has lower peaks, but the average curves of the 5 points is almost equal to the model with one anchors with an empty reservoir. The FSI models (full reservoir) are quite similar as well and the curves are more balanced, which means the contact pressures in the different points are closer to each other.

7.3.4 Anchor forces

The axial forces in the anchors, especially the passive ones, are obtained from the different Koyna Dam models. Positive axial force is tension, the negative one compression. As explained before, the bolt pretension tool in ANSYS is used to apply the pretension force on the originally passive anchor.

Figure 90 shows the maximum axial force in the passive anchor of the one anchor system with a full reservoir and an empty reservoir. With FSI the force is slightly higher up to 0.06 MN than without FSI. Both are subjected to tensile force.

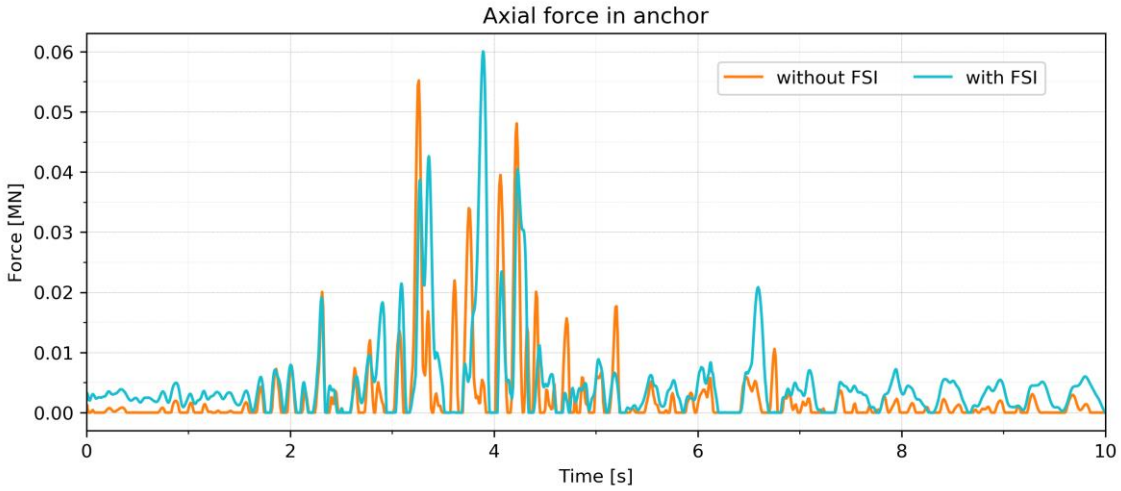

Figure 90: Axial force in the one anchor model

Figure 91 shows the maximum axial force in the anchor with pretension of the one anchor system with a full reservoir and an empty reservoir. With the bolt pretension tool the applied pretension is usually the force output of the system. This means the applied pretension force does not change over time due to this application, which is a simplification in the numerical modelling as in reality the anchor force would change with external static or dynamic loads. Still it is sufficient to get an overview of the performance of seismic retrofit. For completeness this diagram is shown, the two anchor system has the same curve with 1.225 MN for each anchor.

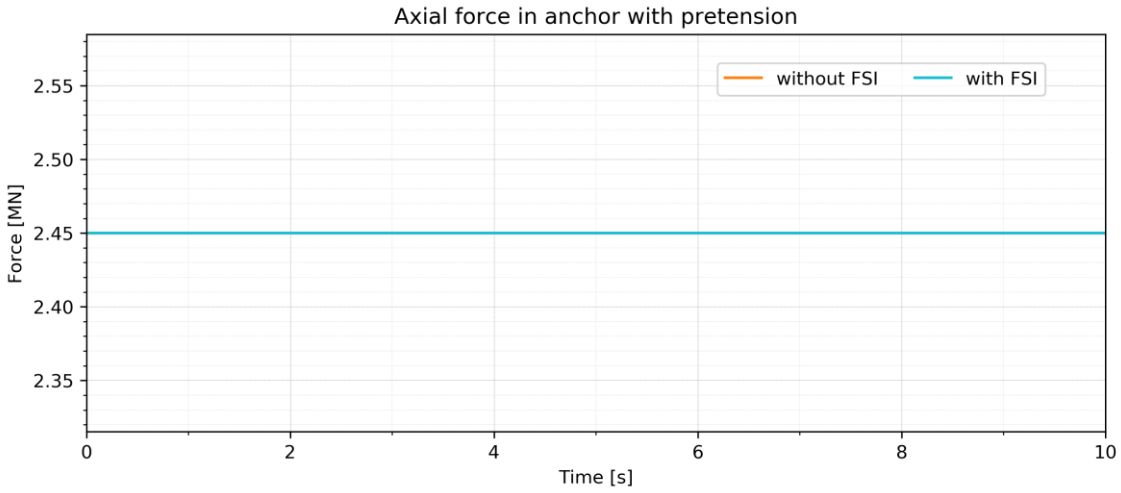

Figure 91: Axial force in the one anchor model with pretension

Figure 92 shows the maximum axial force in the passive anchors of the two anchor system with a full reservoir and an empty reservoir. The inclined anchor 2 situated at downstream side is subjected to compressive force due to the hydrostatic pressure. Without FSI anchor 2 is more active in the first seconds which may result from the location of the center of gravity near the upstream side. The highest axial force is about 0.154 MN.

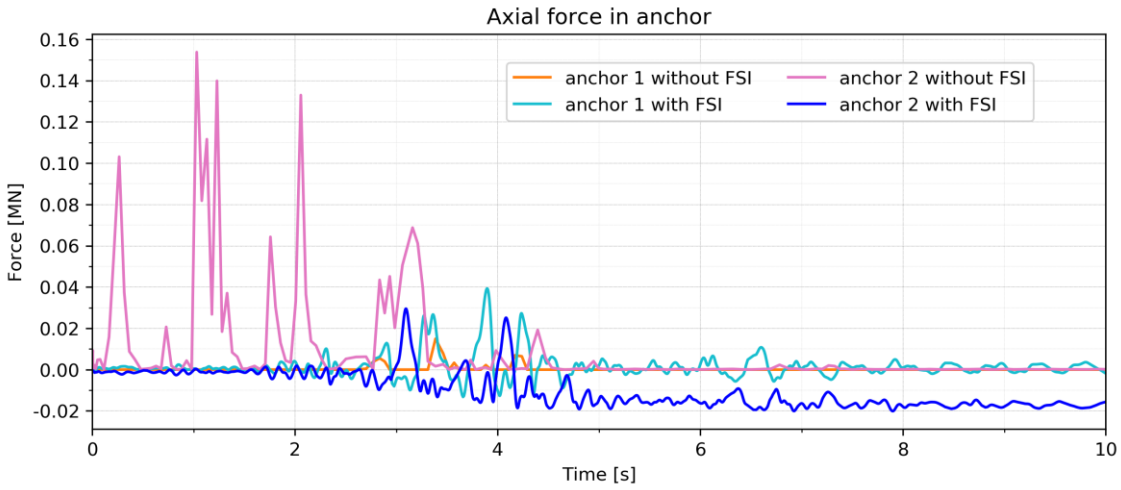

Figure 92: Axial force in the two anchor model

8. Newmark Sliding Block Analysis

The basics of the sliding block analysis of Newmark are described and furthermore a comparative calculation is done with the time histories data taken from ANSYS.

8.1 General description [3]

With the Newmark sliding block analysis introduced in 1965 it is possible to calculate slope displacements by taking acceleration data of an earthquake, for example. The yield acceleration has to be determined initially and when the slope accelerations is above this specified yield acceleration, displacements can be generated by the acting motion. First an earthquake accelerogram or a part out of it is needed of the required location of the slope, then the parts of higher acceleration than the yield acceleration are integrated to obtain the velocity and integrated once more to obtain the sum of permanent displacements. Newmark's method is originally called the rigid-block analysis as its manner is to define a slope as a rigid block. In comparison to the pseudostatic method it does not determine a factor of safety (<1.0 displacement occurs).

The blocks sliding on a plane that should represent the slope are shown in Figure 93.

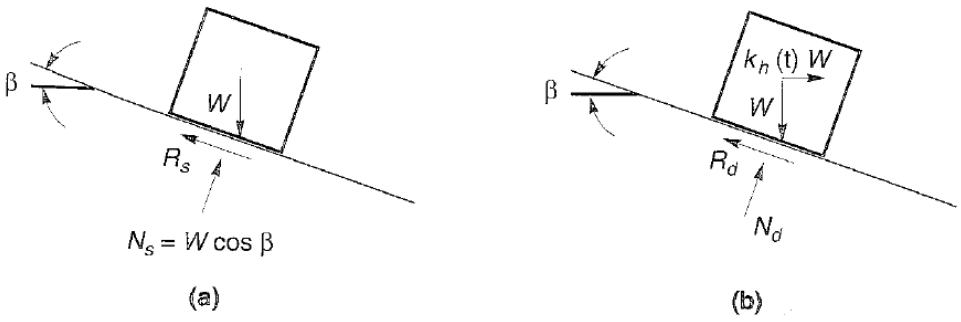

Figure 93: Slope assumed as a rigid block with forces for the (a) static and (b) dynamic case [3]

In the static equilibrium there are a resisting force R_S and a driving force D_S which is given in following formula:

$$FS = \frac{available\ resisting\ force}{static\ driving\ force} = \frac{R_s}{D_s} = \frac{W \cos\beta \tan\phi}{W \sin\beta} = \frac{\tan\phi}{\tan\beta} \quad (78)$$

There is also ϕ given as the friction angle. When the driving force is higher than the resisting force, the factor of safety FS is lower than 1. Additionally the horizontal acceleration is introduced which leads to $a_h(t) = k_h(t) * g$ in the dynamic conditions, which produces the inertial force $k_h(t) * W$. The vertical acceleration is not considered in this case. There is only frictional sliding resistance, so no cohesion exists. Hence, the FS for dynamic conditions is given as following:

$$FS_d(t) = \frac{available\ resisting\ force}{pseudostatic\ driving\ force} = \frac{R_d(t)}{D_d(t)} = \frac{[\cos\beta - k_h(t)\sin\beta]\tan\phi}{\sin\beta + k_h(t)\cos\beta} \quad (79)$$

As a result the factor of safety will reduce the larger the k_h becomes. Next is the determination of the yield acceleration which is the minimum acceleration to induce sliding of the block or slope, given as $a_y = k_y * g$. The yield coefficient in horizontal direction for the block in Figure 93 is given by:

$$k_y = \tan(\phi - \beta) \quad in\ downhill\ direction \quad (80)$$

$$k_y = \frac{\tan\phi + \tan\beta}{1 + \tan\phi \tan\beta} \quad in\ uphill\ direction \quad (81)$$

When FS ≤ 1, the k_h is the yield coefficient and furthermore the yield acceleration, at which the block starts sliding. In the next step the selected part of the earthquake accelerogram is taken a look at to determine the peaks higher than a_y and then these parts are integrated twice to get the approximated displacements (Figure 94).

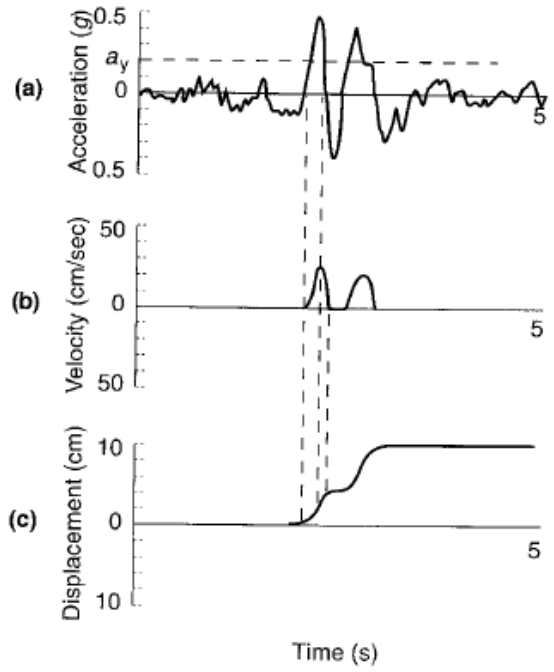

Figure 94: Integrated displacements from an accelerogram [38]

8.2 Results

The accelerogram is taken from the middle base point of the crack line of the bottom part in ANSYS and the whole calculation of the needed parameters and thus the permanent displacements is performed in Excel and Python. The accelerogram is exported with a full and with an empty reservoir.

The yield acceleration a_y for each system has to be determined. Therefore, the factor of safety has to be ≤ 1, so the block starts sliding. Following data is given to obtain the yield acceleration for each system:

- Specific weight of concrete of dam $\gamma_c = 25.93\ kN/m^3$
- Volume of crest part $V_{Crest} = 711.05\ m^3$
- Weight force G of crest part is given by:

$$G = V_{Crest} * \frac{\gamma_C}{1000} = 711.05\ [m^3] * \frac{25.93\left[\frac{kN}{m^3}\right]}{1000} = 18.44\ [MN] \tag{82}$$

- Specific weight of water $\gamma_w = 9.81\ kN/m^3$
- Height of water at crest part $h_w = 28.4\ m$
- Water pressure force of crest part W is given by:

$$W = \frac{1}{2} * g * \frac{h_W^2}{1000} = \frac{1}{2} * 9.81\ \left[\frac{m}{s^2}\right] * \frac{28.4^2[m^2]}{1000} = 3.96\ [MN] \tag{83}$$

- The added mass due to earthquake excitation and the additional water load is calculated with Westergaard's formula:

$$M_W = \frac{7}{12} * \rho_W * h_W^2 = \frac{7}{12} * 1000\ \left[\frac{kg}{m^3}\right] * 28.4^2[m^2] = 470493.33\ [kg/m] \tag{84}$$

$$W_E = M_W * \frac{a_y}{10^6}\ [MN] \tag{85}$$

- Pretension force of the one anchor model $F_{A1} = 2.45\ MN$
- Pretension force of the two anchor model $F_{A2} = 1.225\ MN$
- Friction angle $\phi = 45°$
- Inclination angle of the downstream located anchor $\alpha = 81.30°$
- Inclination angle of the crack surface $\beta = 0°$
- Yield coefficient where the block starts sliding k_y and yield acceleration a_y:

$$a_y = k_y * 9.81\ [\frac{m}{s^2}] \tag{86}$$

The calculations are performed for the unreinforced Koyna Dam with full and empty reservoir, for Koyna Dam with one anchor with full and empty reservoir and Koyna Dam with two anchors with full and empty reservoir. The area under the curve of the 10 second long accelerogram used is approximated by interpolation in order to avoid unrealistic acceleration peaks and to obtain the sum of

permanent displacements. When the yield acceleration is larger than the acceleration given in this accelerogram, each block respectively each acceleration value is double integrated with following formulas [3]:

$$v_{rel}(t) = \int_{t_0}^{t} a_{rel}(t)dt = \left(a - a_y\right) * (t - t_0) \tag{87}$$

$$d_{rel}(t) = \int_{t_0}^{t} v_{rel}(t)dt = \frac{1}{2}\left(a - a_y\right) * (t - t_0)^2 \tag{88}$$

The distribution of forces acting on the crest block is shown in Figure 95. First the Newmark analysis is done without the vertical base acceleration, so the G_y is neglected. In the results with an empty reservoir the static and dynamic water pressure forces W and W_E is not used, in the unreinforced models the anchor forces F_{A1} for the one anchor model and F_{A2} for each anchor of the two anchor model are not part of the calculation. The horizontal inertial force is given by $G_H = G * k_y$, which is given as a constant without the vertical base acceleration. When this part is included, the total yield acceleration is at some points smaller which causes higher displacements.

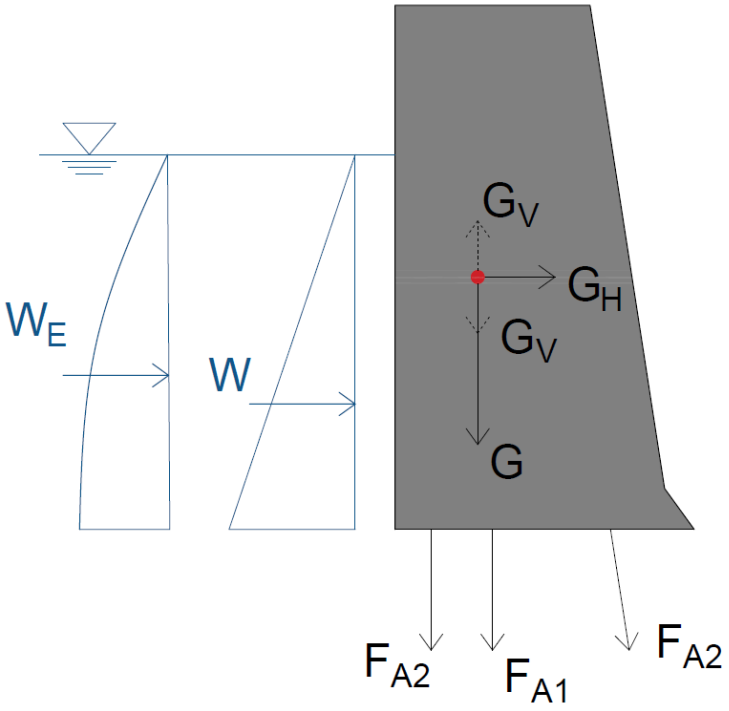

Figure 95: Horizontal and vertical forces acting on the crest block

Calculation without reinforcement and empty reservoir:

$$FS = 1 = \frac{G * \cos\beta \tan\phi - G * k_y * \sin\beta * \tan\phi}{G * \sin\beta + G * k_y * \cos\beta} = \frac{G * \tan\phi}{G * k_y}$$

$$\rightarrow \quad k_y = \tan\phi \tag{89}$$

- $k_y = 1$
- Yield acceleration $a_y = 9.81\ m/s^2$

Calculation without reinforcement and full reservoir:

$$FS = 1 = \frac{G * \tan\phi}{W + \frac{M_W}{10^6} * g * k_y + G * k_y} \quad \rightarrow \quad k_y = \frac{G * \tan\phi - W}{G + \frac{M_W}{10^6} * g} \tag{90}$$

- $k_y = 0.628$
- Yield acceleration $a_y = 6.162\ m/s^2$

Calculation with one prestressed anchor and empty reservoir:

$$FS = 1 = \frac{(G + F_{A1}) * \tan\phi}{G * k_y} \quad \rightarrow \quad k_y = \frac{(G + F_{A1}) * \tan\phi}{G} \tag{91}$$

- $k_y = 1.133$
- Yield acceleration $a_y = 11.114\ m/s^2$

Calculation with one prestressed anchor and full reservoir:

$$FS = 1 = \frac{(G + F_{A1}) * \tan\phi}{W + \frac{M_W}{10^6} * g * k_y + G * k_y} \quad \rightarrow \quad k_y = \frac{(G + F_{A1}) * \tan\phi - W}{G + \frac{M_W}{10^6} * g} \tag{92}$$

- $k_y = 0.7345$
- Yield acceleration $a_y = 7.205\ m/s^2$

Calculation with two prestressed anchors and empty reservoir:

$$FS = 1 = \frac{(G + F_{A2} + F_{A2} * \sin\gamma) * \tan\phi}{G * k_y + F_{A2} * \cos\gamma}$$

$$\rightarrow \quad k_y = \frac{(G + F_{A2} + F_{A2}\sin\gamma) * \tan\phi - F_{A2}\cos\gamma}{G} \tag{93}$$

- $k_y = 1.122$
- Yield acceleration $a_y = 11.007\ m/s^2$

Calculation with two prestressed anchors and full reservoir:

$$FS = 1 = \frac{(G + F_{A2} + F_{A2} * \sin\gamma) * \tan\phi}{W + \frac{M_W}{10^6} * g * k_y + G * k_y + F_{A2} * \cos\gamma} \tag{94}$$

$$\rightarrow \quad k_y = \frac{(G + F_{A2} + F_{A2}\sin\gamma) * \tan\phi - W - F_{A2}\cos\gamma}{G + \frac{M_W}{10^6} * g}$$

- $k_y = 0.7258$
- Yield acceleration $a_y = 7.120\ m/s^2$

8.2.1 Neglecting vertical base acceleration

The following figures show the accelerogram for the corresponding Koyna model and the yield acceleration calculated for each load case. After this diagram there are two more figures with the corresponding integrated relative velocities and the relative displacements.

Figure 96 shows the accelerogram with the yield acceleration for an unreinforced crest block with an empty reservoir, Figure 97 and Figure 98 show the integrated relative velocities and displacements. The final displacement of the crest block is 0.0007 m in downstream direction.

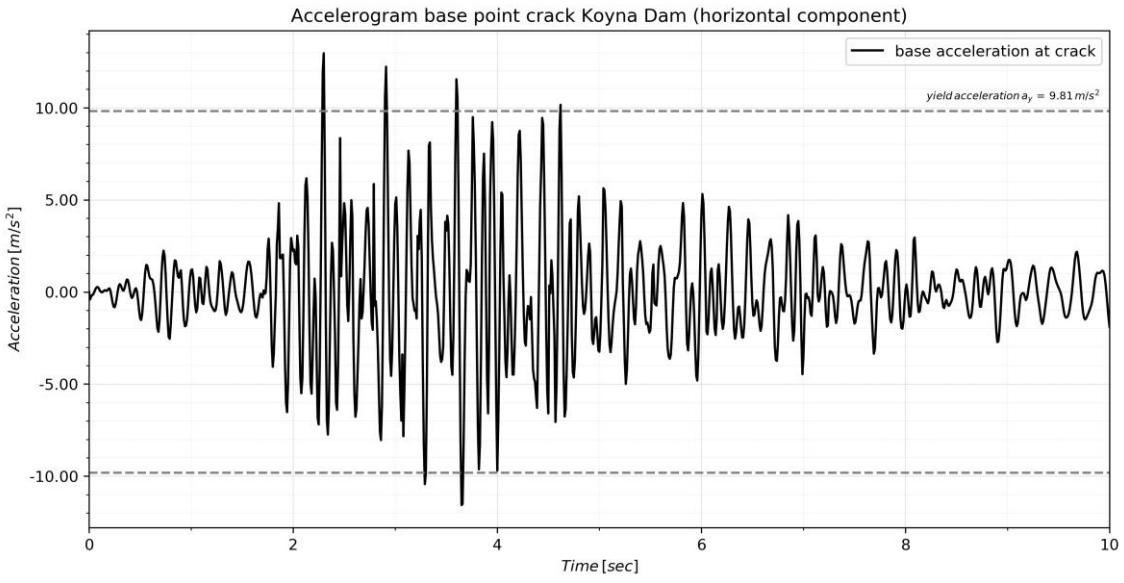

Figure 96: Accelerogram with empty reservoir and yield acceleration of unreinforced crest block

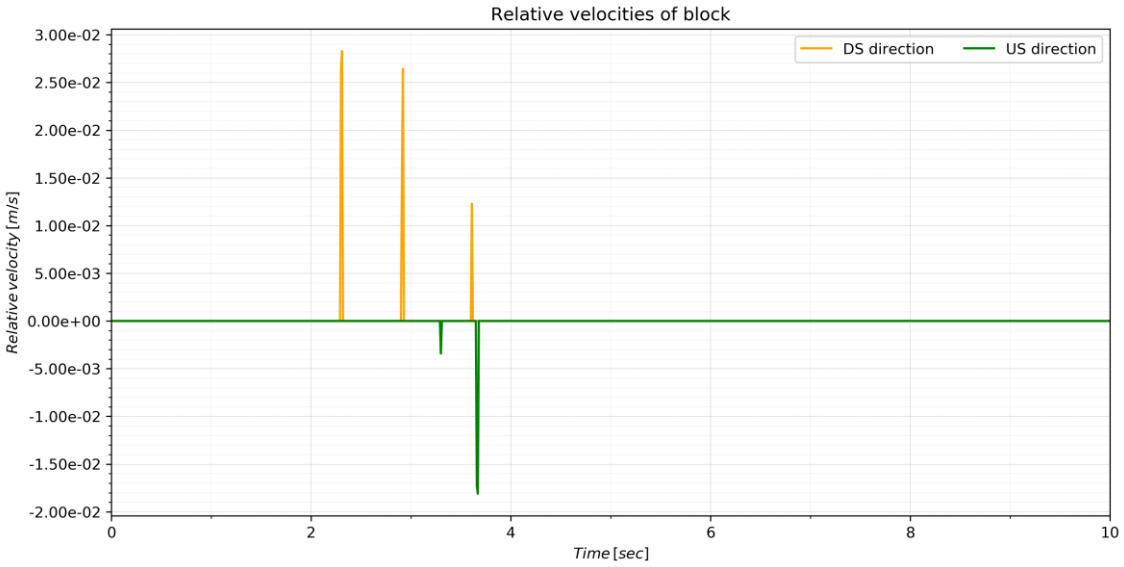

Figure 97: Relative velocities of unreinforced crest block

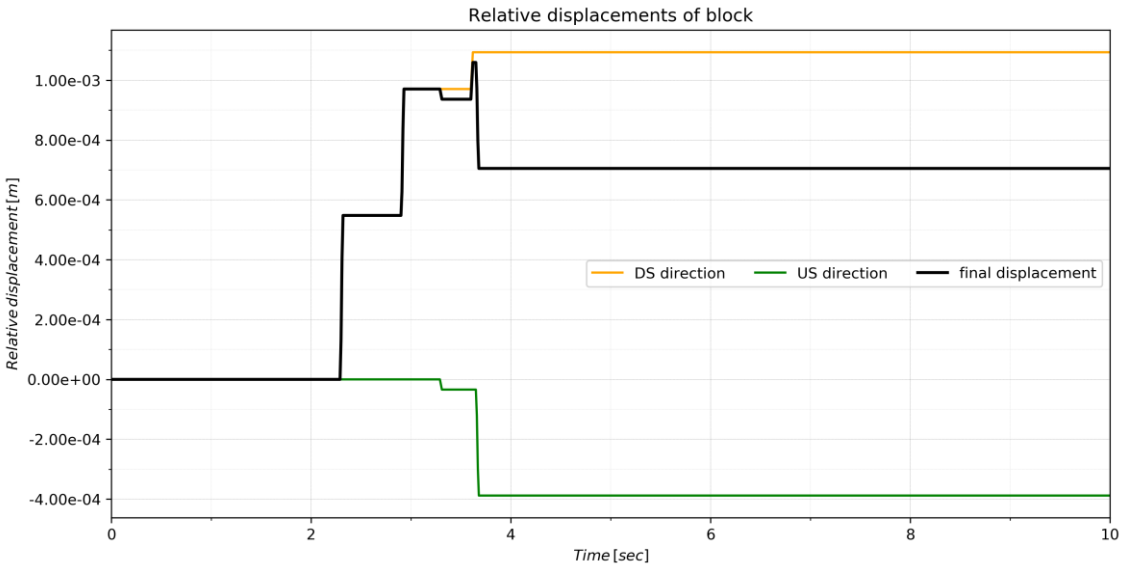

Figure 98: Relative displacements of unreinforced crest block

Figure 99 shows the accelerogram with the yield acceleration for crest block with one prestressed anchor and an empty reservoir, Figure 100 and Figure 101 show the integrated relative velocities and displacements. The final displacement of the crest block is 0.000146 m in downstream direction.

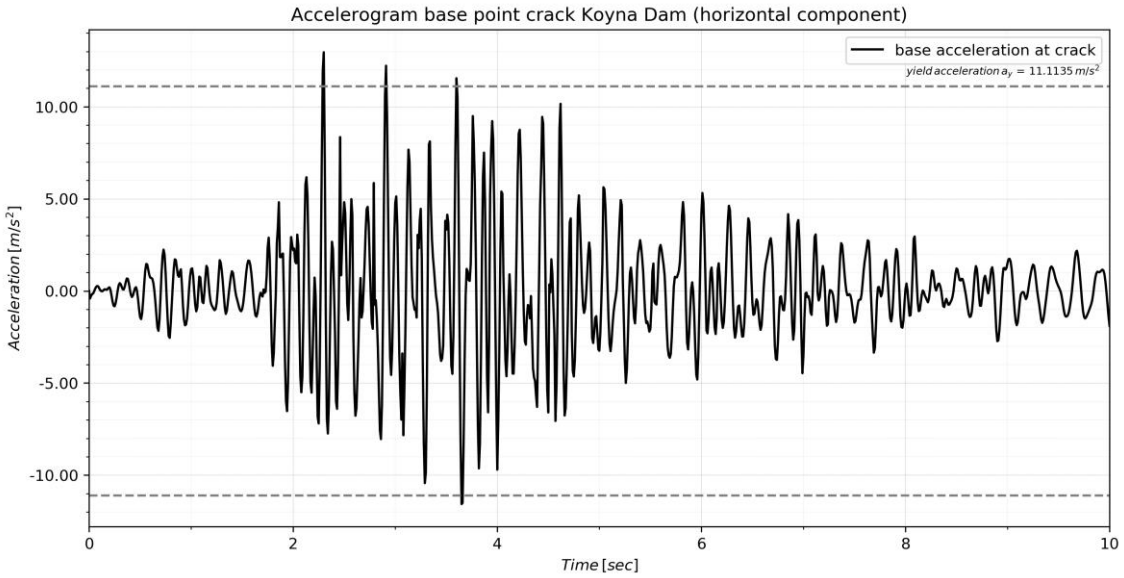

Figure 99: Accelerogram with empty reservoir and yield acceleration of crest block with one pre-stressed anchor

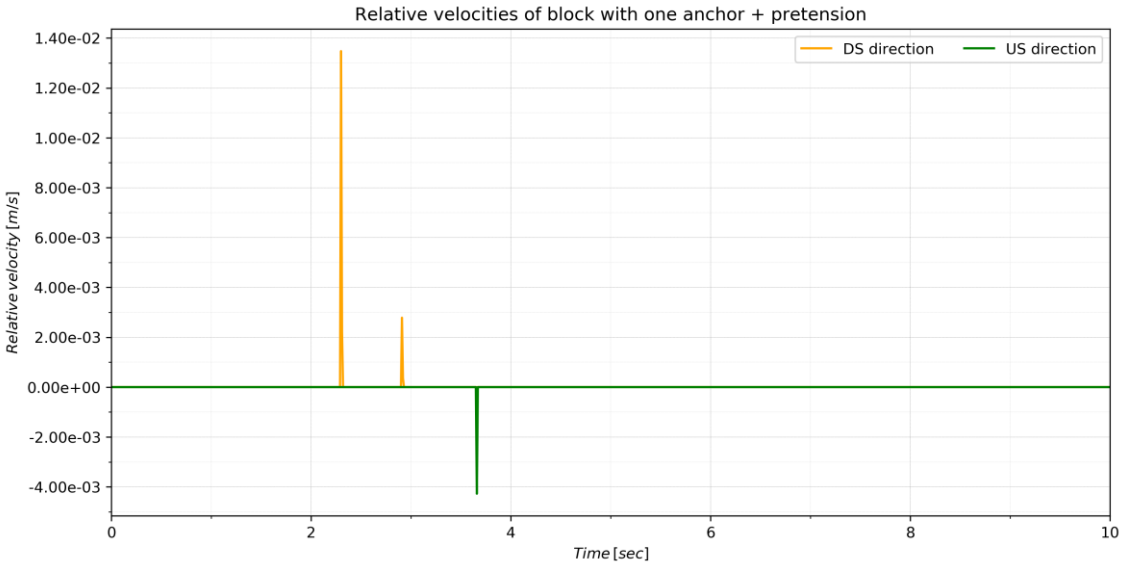

Figure 100: Relative velocities of crest block with one prestressed anchor

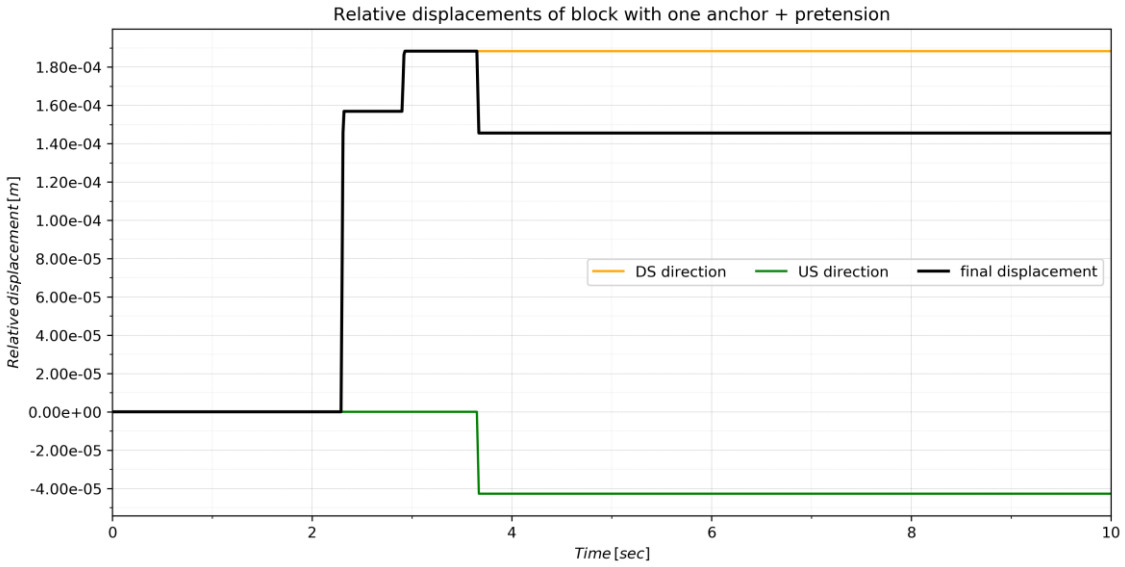

Figure 101: Relative displacements of crest block with one prestressed anchor

Figure 102 shows the accelerogram with the yield acceleration for crest block with two prestressed anchors and an empty reservoir, Figure 103 and Figure 104 show the integrated relative velocities and displacements. The final displacement of the crest block is 0.0002 m in downstream direction.

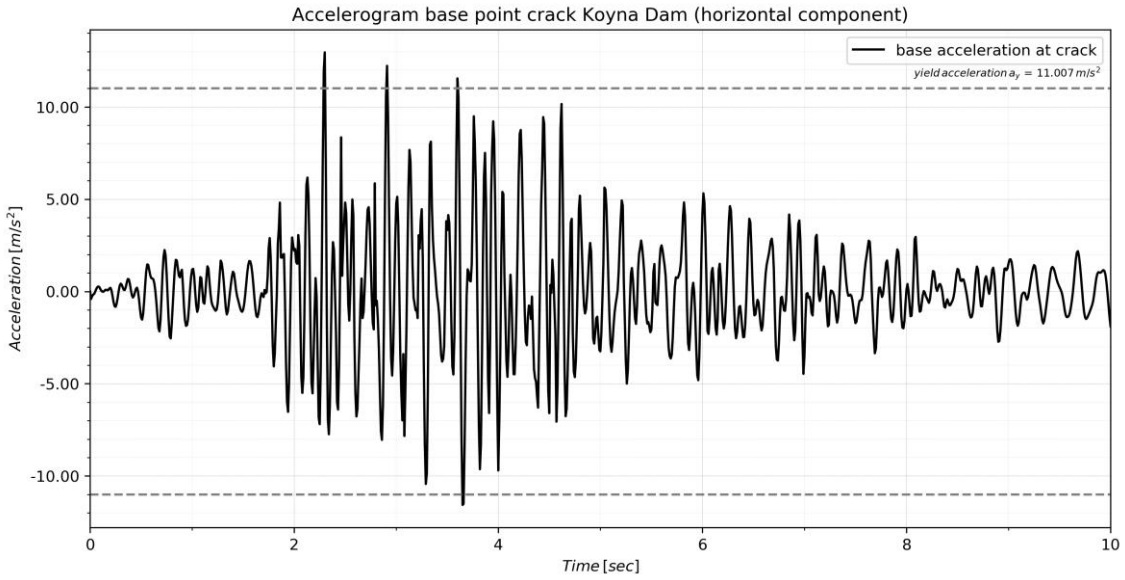

Figure 102: Accelerogram with empty reservoir and yield acceleration of crest block with two prestressed anchors

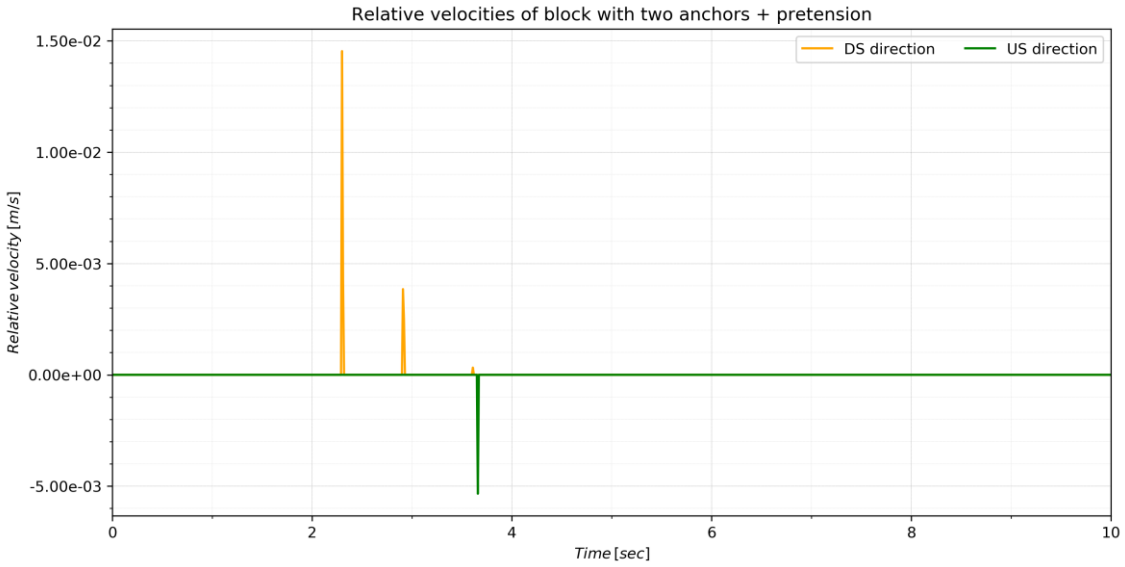

Figure 103: Relative velocities of crest block with two prestressed anchors

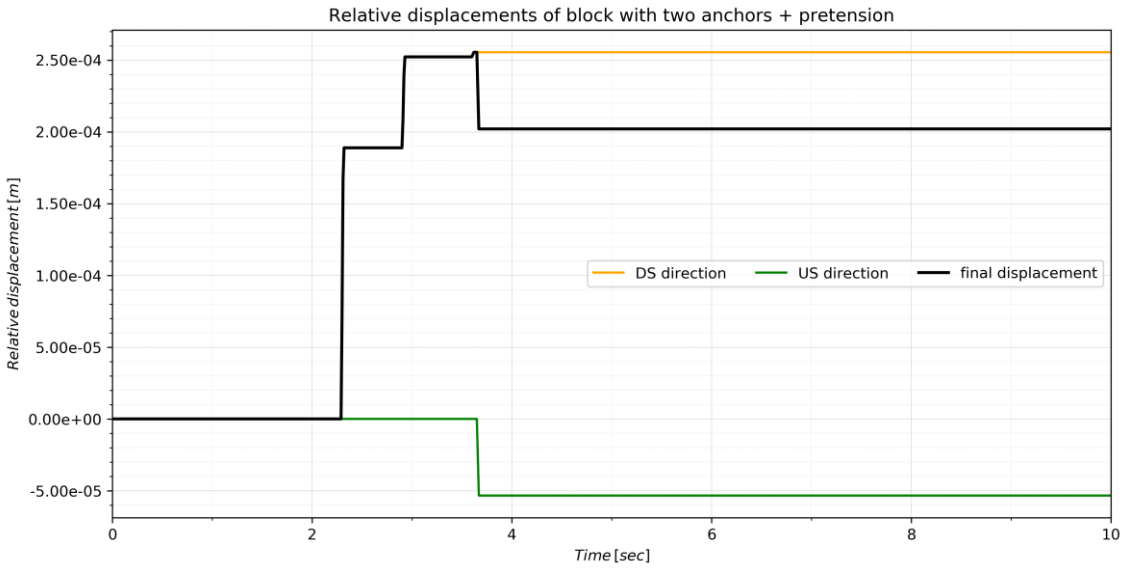

Figure 104: Relative displacements of crest block with two prestressed anchors

Figure 105 shows the accelerogram with the yield acceleration for an unreinforced crest block and a full reservoir, Figure 106 and Figure 107 show the integrated relative velocities and displacements. The final displacement of the crest block is 0.0025 m in upstream direction.

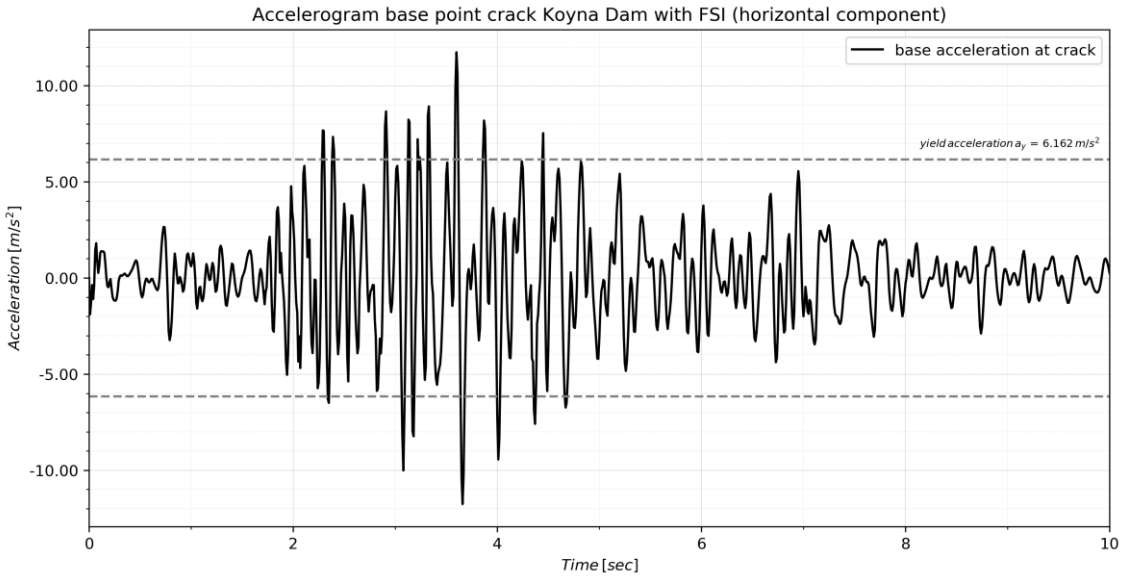

Figure 105: Accelerogram with full reservoir and yield acceleration of the unreinforced crest block

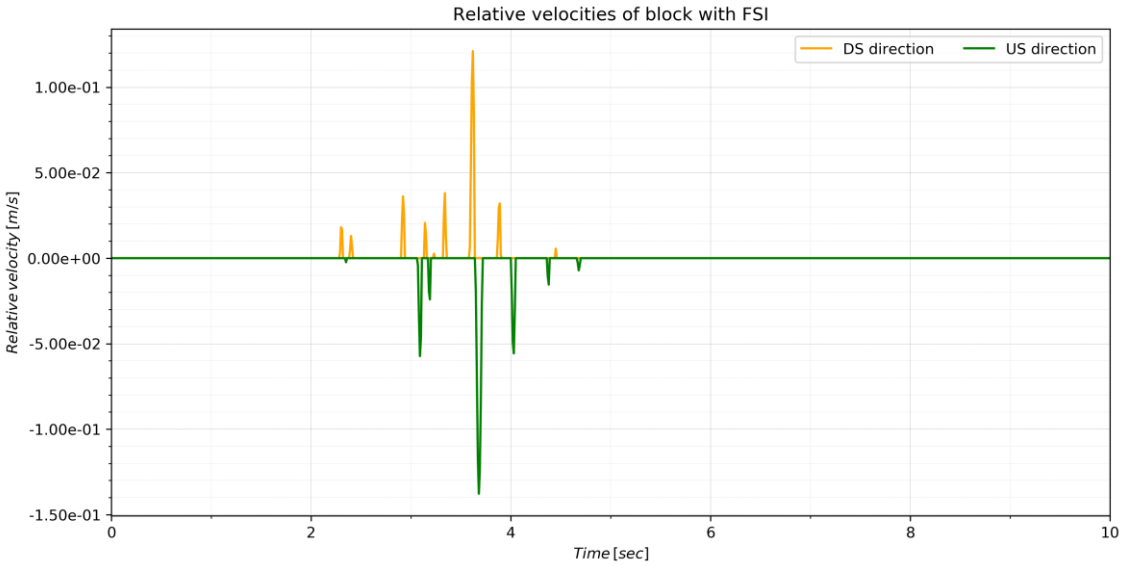

Figure 106: Relative velocities of unreinforced crest block with FSI

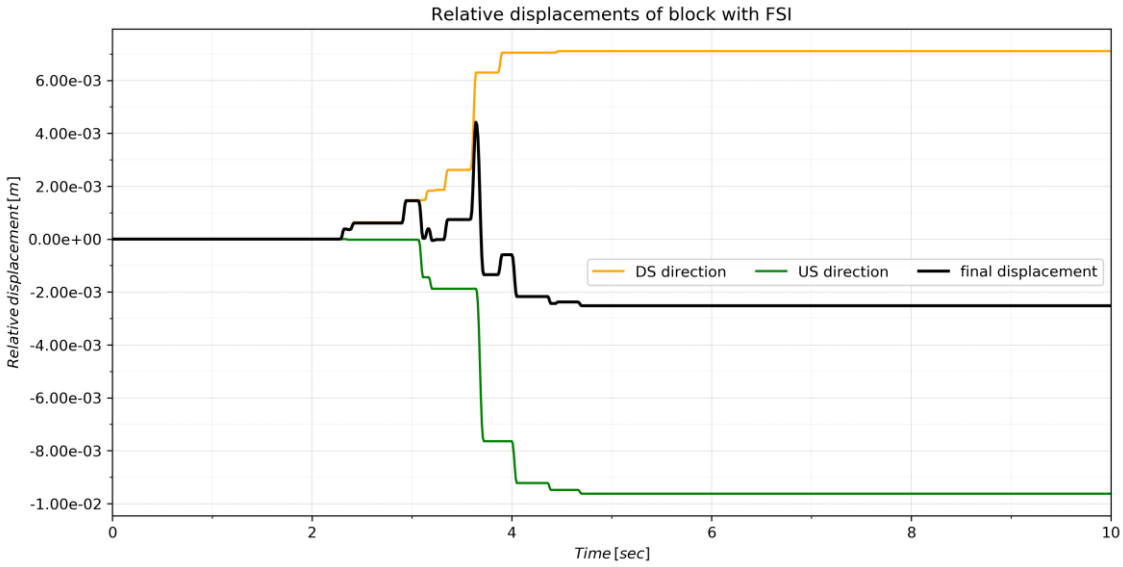

Figure 107: Relative displacements of unreinforced crest block with FSI

Figure 108 shows the accelerogram with the yield acceleration for a crest block with one prestressed anchor and a full reservoir, Figure 109 and Figure 110 show the integrated relative velocities and displacements. The final displacement of the crest block is 0.0015 m in upstream direction.

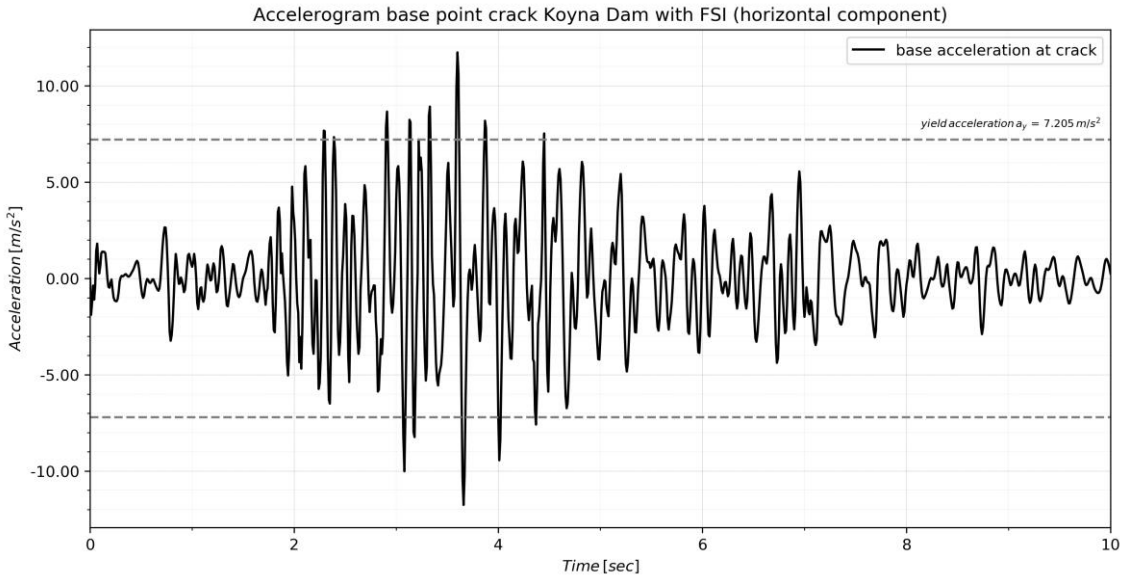

Figure 108: Accelerogram with full reservoir and yield acceleration of crest block with one pre-stressed anchor

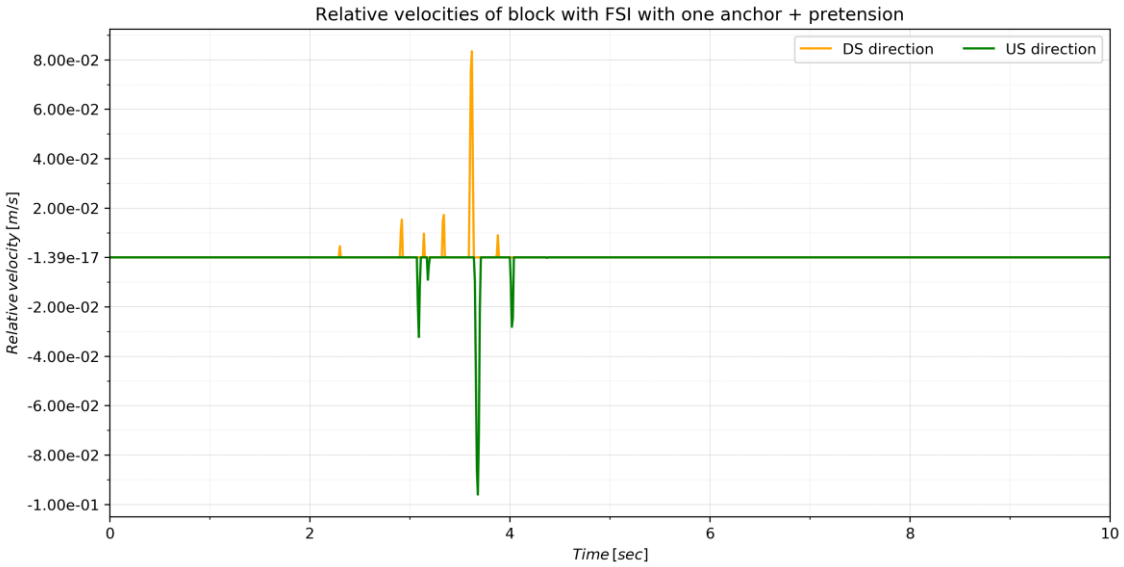

Figure 109: Relative velocities of crest block with one prestressed anchor with FSI

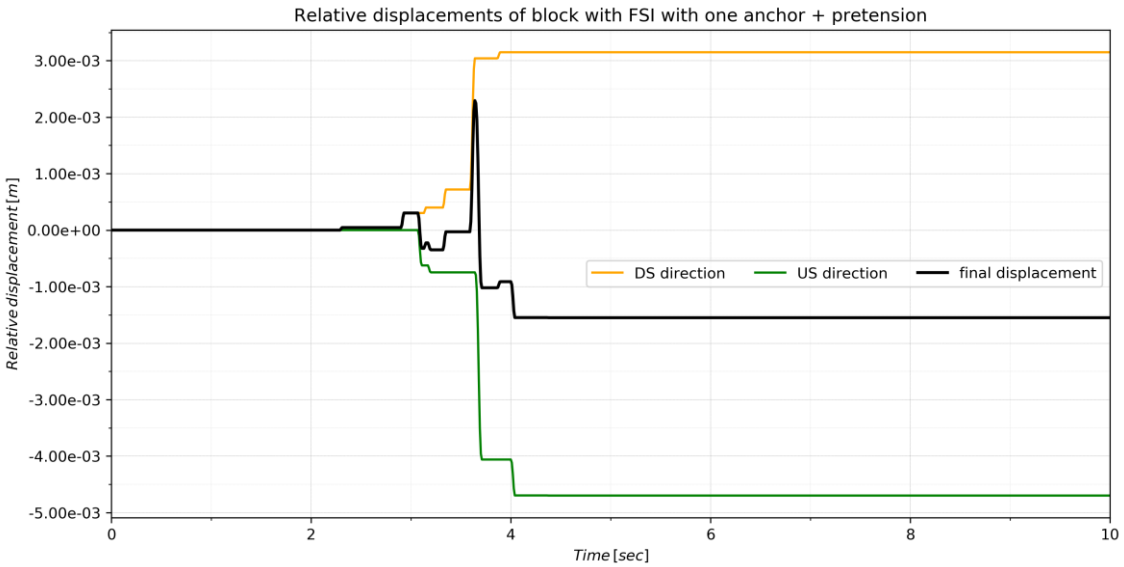

Figure 110: Relative displacements of crest block with one prestressed anchor with FSI

Figure 111 shows the accelerogram with the yield acceleration for a crest block with two prestressed anchors and a full reservoir, Figure 112 and Figure 113 show the integrated relative velocities and displacements. The final displacement of the crest block is 0.0017 m in upstream direction.

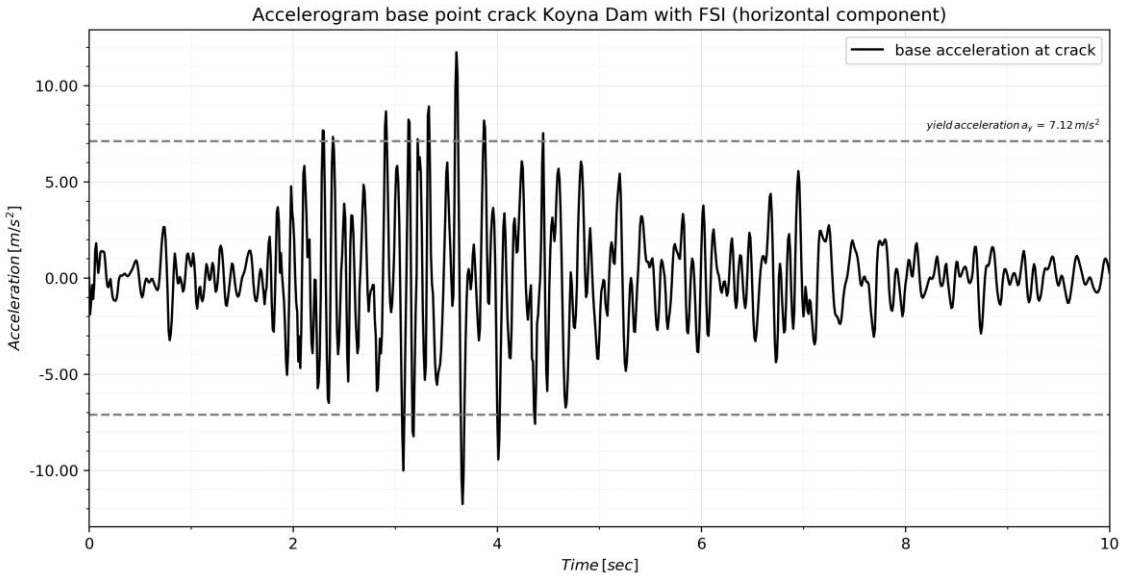

Figure 111: Accelerogram with full reservoir and yield acceleration of crest block with two pre-stressed anchors

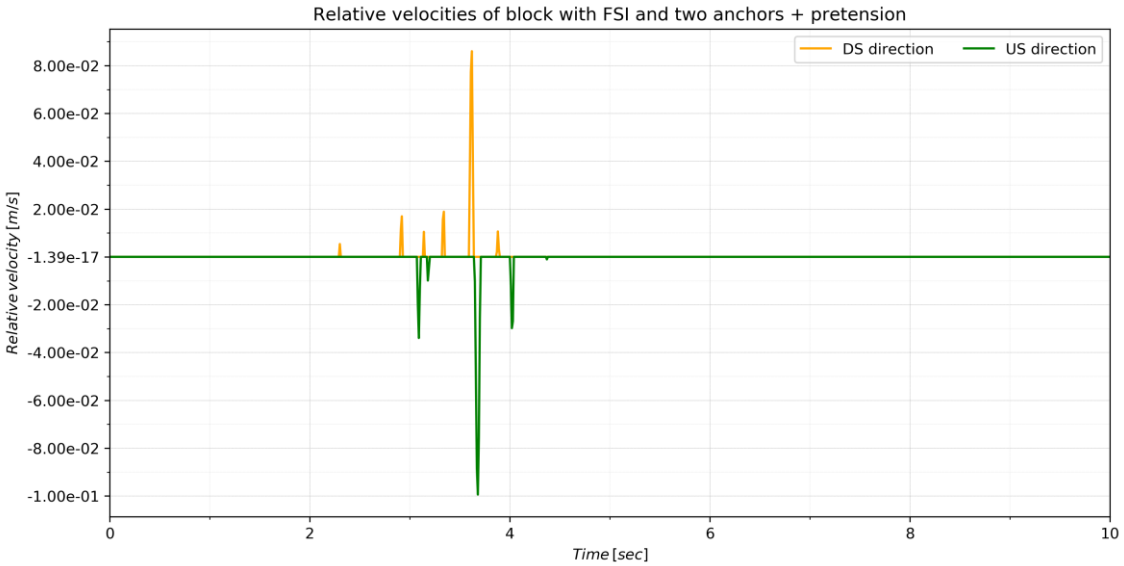

Figure 112: Relative velocities of crest block with two prestressed anchors with FSI

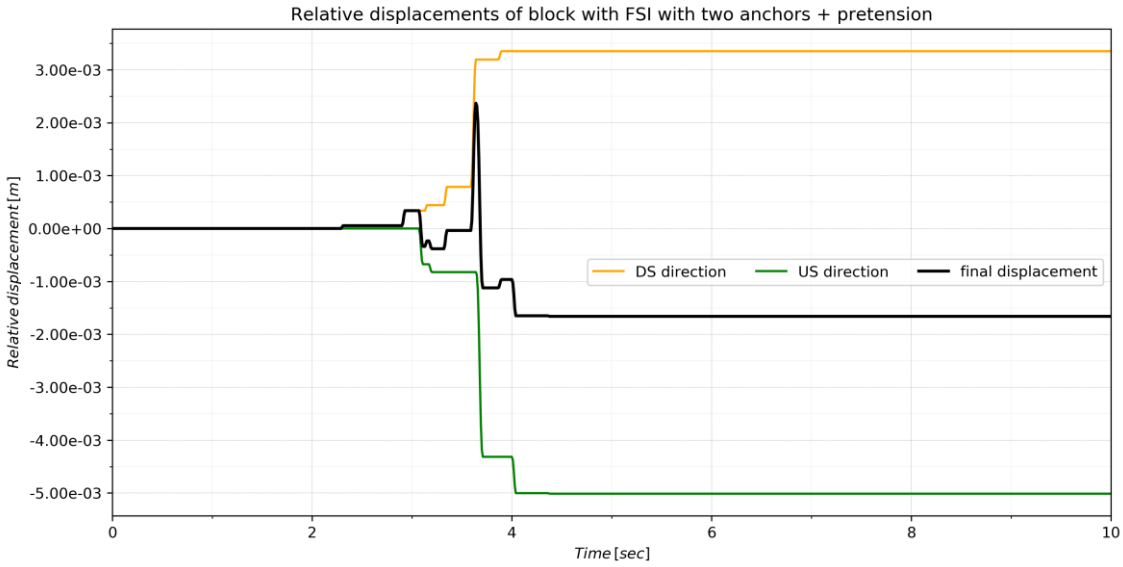

Figure 113: Relative displacements of crest block with two prestressed anchors with FSI

8.2.2 Including vertical base acceleration

In the following results the vertical base acceleration taken from ANSYS is included, therefore, the yield acceleration is not a constant anymore, as the vertical yield acceleration changes the factor of safety every time step. The following figures show the accelerogram for the corresponding Koyna model and the yield acceleration calculated for each load case. After this diagram there are two more figures with the corresponding integrated relative velocities and the relative displacements.

Figure 114 shows the accelerogram with the yield acceleration including the vertical base acceleration, which is implemented in the Python script with an accelerogram from ANSYS, for an unreinforced crest block with an empty reservoir. Figure 115 and Figure 116 show the integrated relative velocities and displacements. The final displacement of the crest block is 0.0062 m in downstream direction.

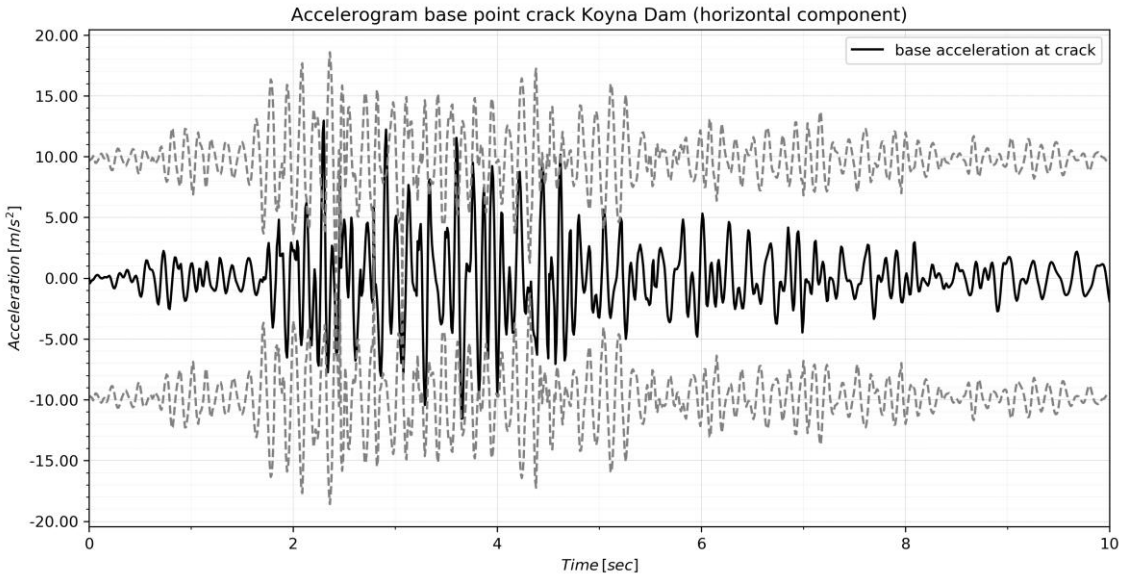

Figure 114: Accelerogram with empty reservoir and yield acceleration including vertical base acceleration of the unreinforced crest block

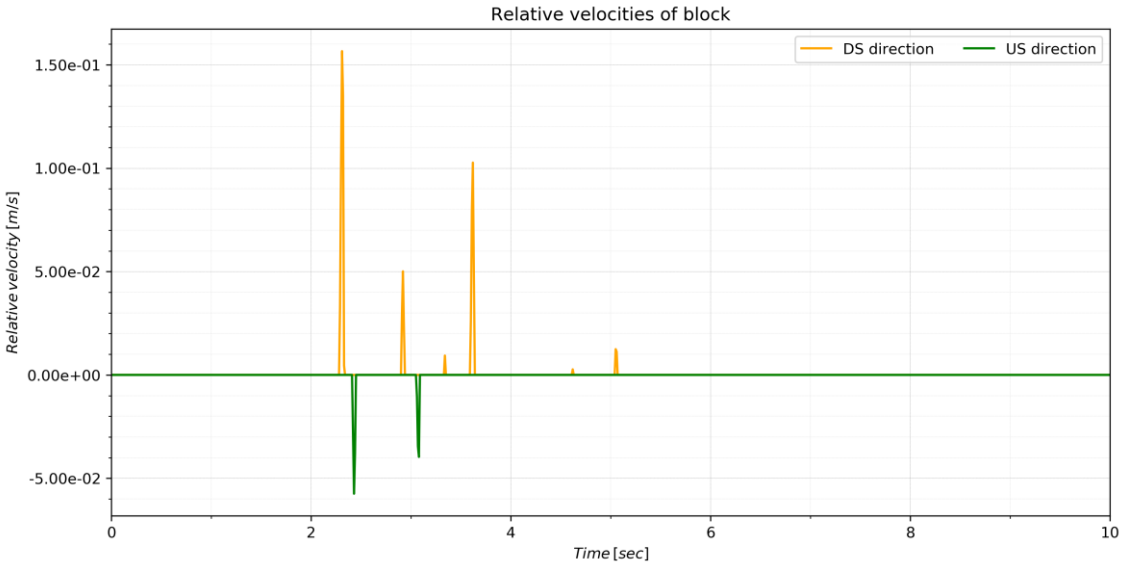

Figure 115: Relative velocities of the unreinforced crest block calculated with vertical base acceleration

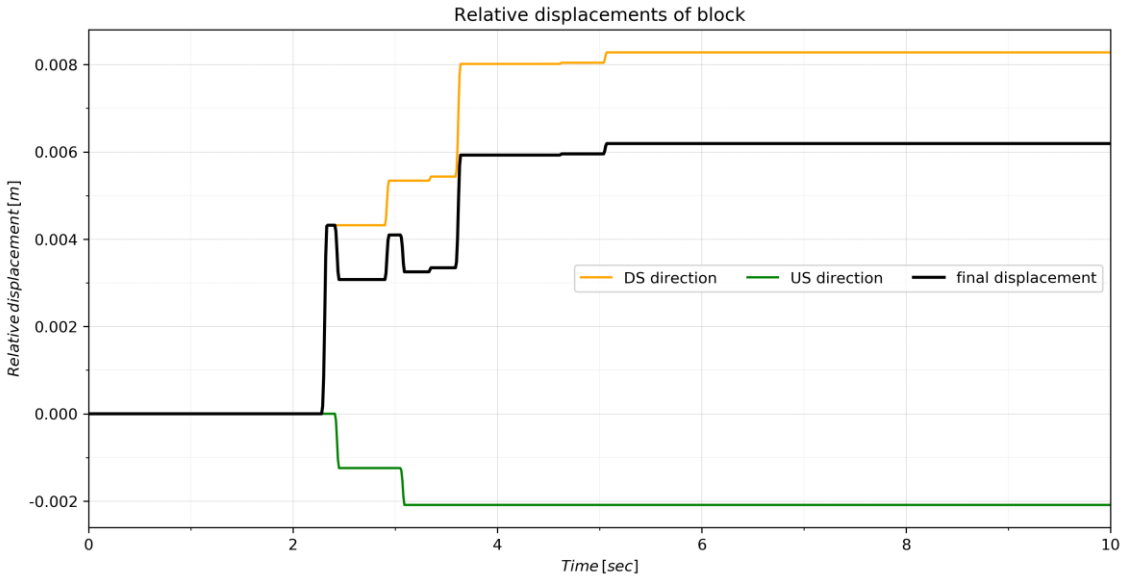

Figure 116: Relative displacements of the unreinforced crest block calculated with vertical base acceleration

Figure 117 shows the accelerogram with the yield acceleration including the vertical base acceleration for a crest block with one prestressed anchor with an empty reservoir, Figure 118 and Figure 119 show the integrated relative velocities and displacements. The final displacement of the crest block is 0.0041 m in downstream direction.

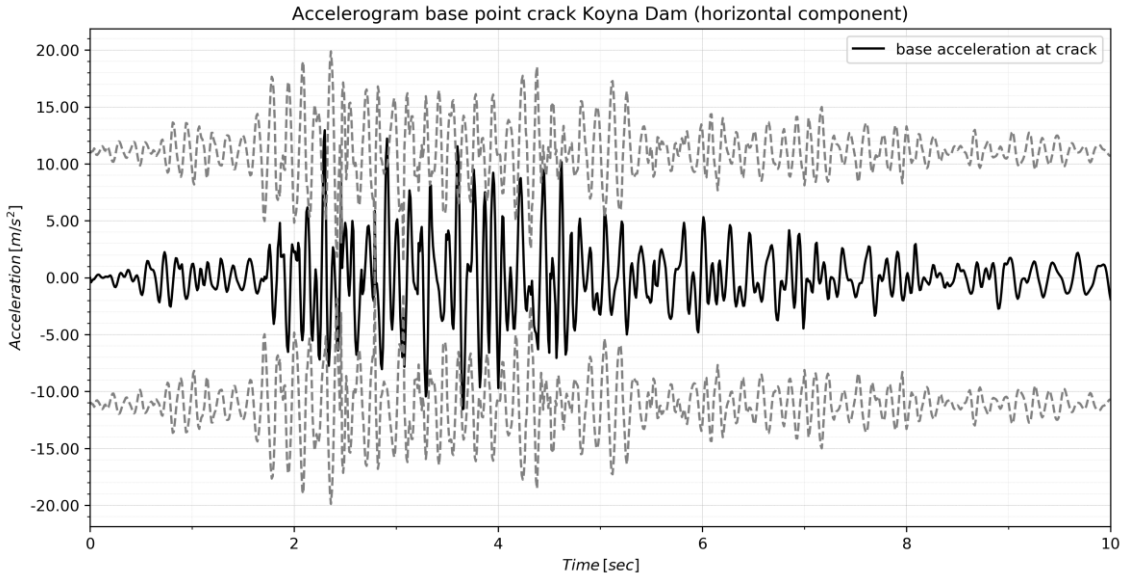

Figure 117: Accelerogram with empty reservoir and yield acceleration including vertical base acceleration of crest block with one prestressed anchor

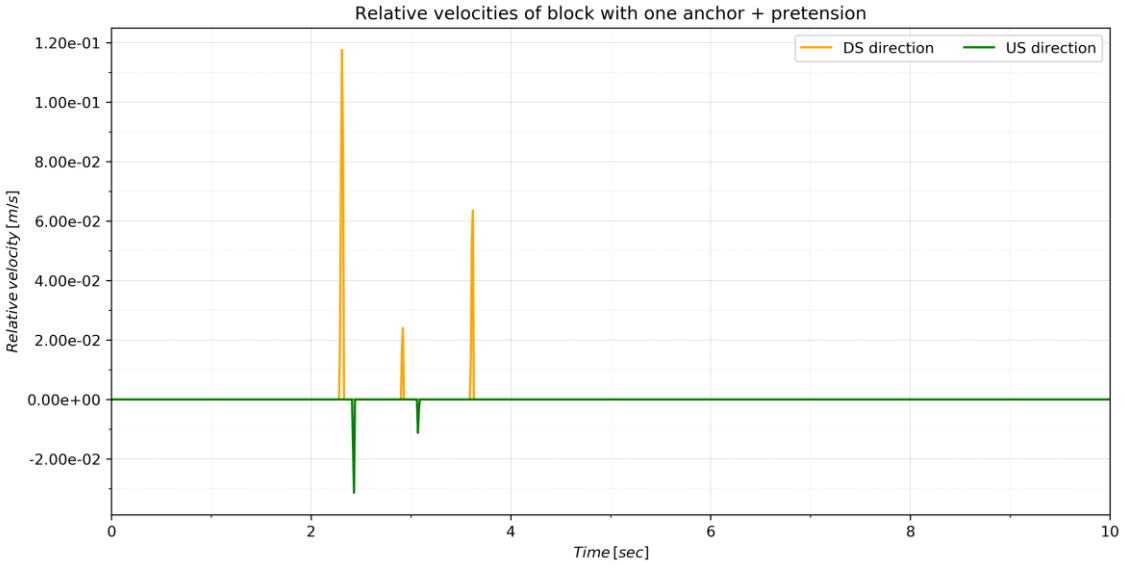

Figure 118: Relative velocities of crest block with one prestressed anchor calculated with vertical base acceleration

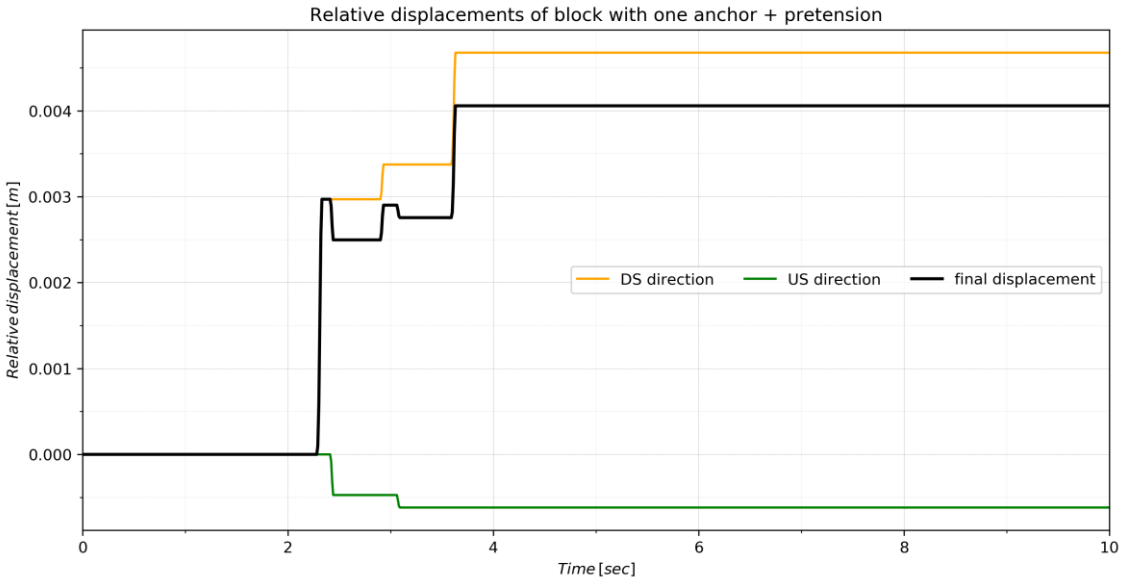

Figure 119: Relative displacements of crest block with one prestressed anchor calculated with vertical base acceleration

Figure 120 shows the accelerogram with the yield acceleration including the vertical base acceleration for a crest block with two prestressed anchors with an empty reservoir, Figure 121 and Figure 122 show the integrated relative velocities

and displacements. The final displacement of the crest block is 0.0042 m in downstream direction.

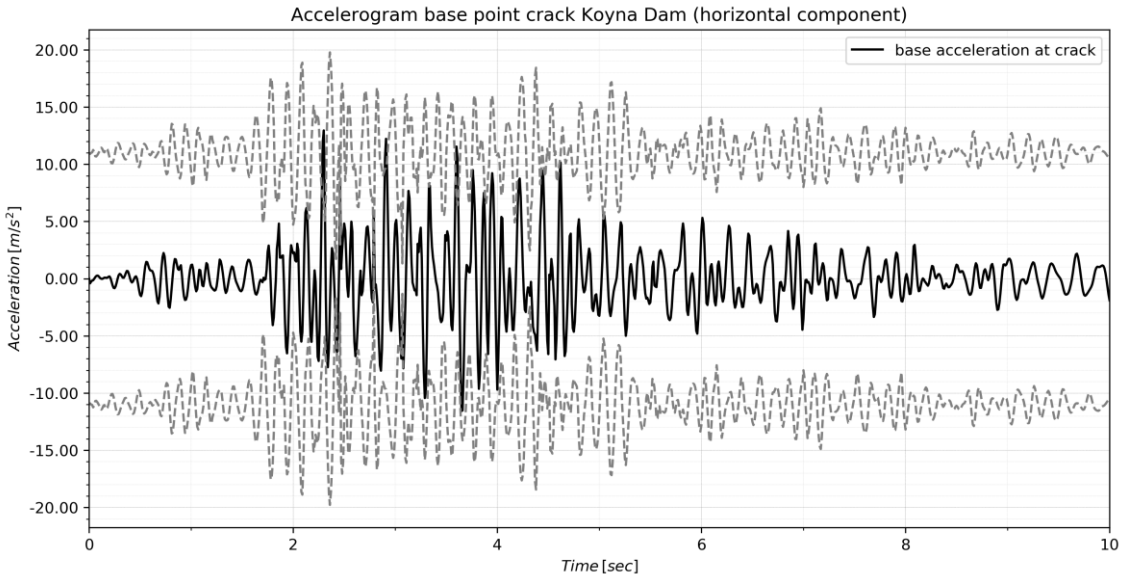

Figure 120: Accelerogram with empty reservoir and yield acceleration including vertical base acceleration of crest block with two prestressed anchors

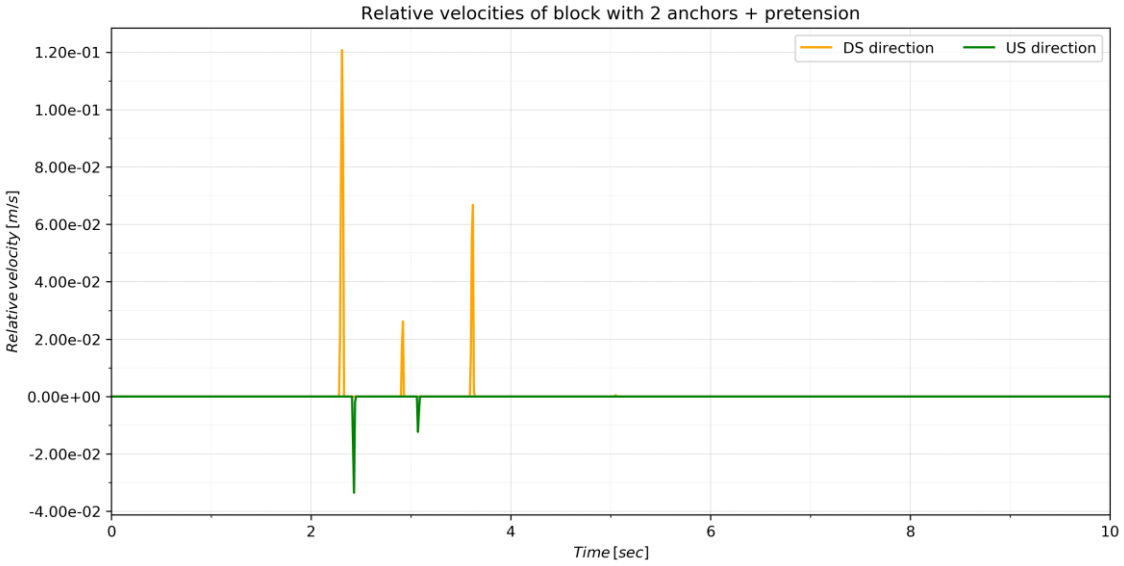

Figure 121: Relative velocities of crest block with two prestressed anchors calculated with vertical base acceleration

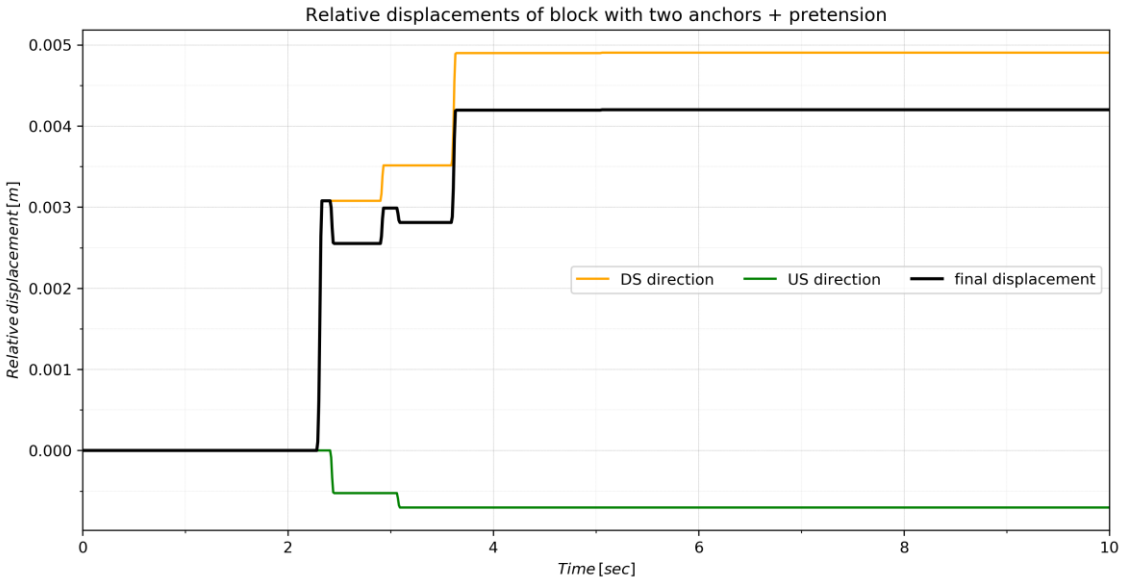

Figure 122: Relative displacements of crest block with two prestressed anchors calculated with vertical base acceleration

Figure 123 shows the accelerogram with the yield acceleration including the vertical base acceleration for an unreinforced crest block with a full reservoir, Figure 124 and Figure 125 show the integrated relative velocities and displacements. The final displacement of the crest block is 0.025 m in downstream direction.

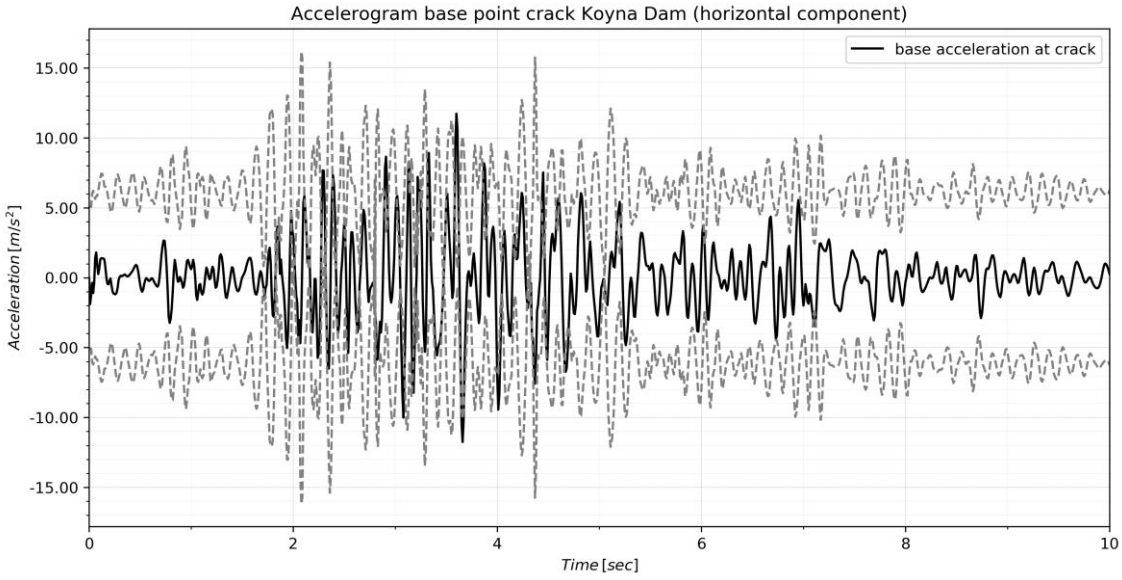

Figure 123: Accelerogram with full reservoir and yield acceleration including vertical base acceleration of the unreinforced crest block

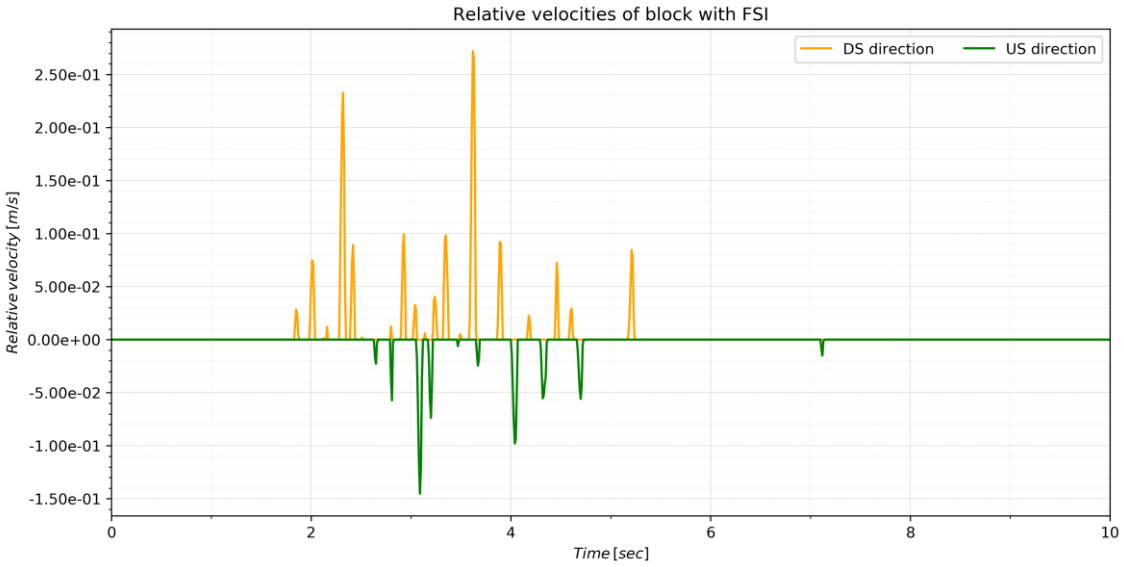

Figure 124: Relative velocities of the unreinforced crest block with FSI calculated with vertical base acceleration

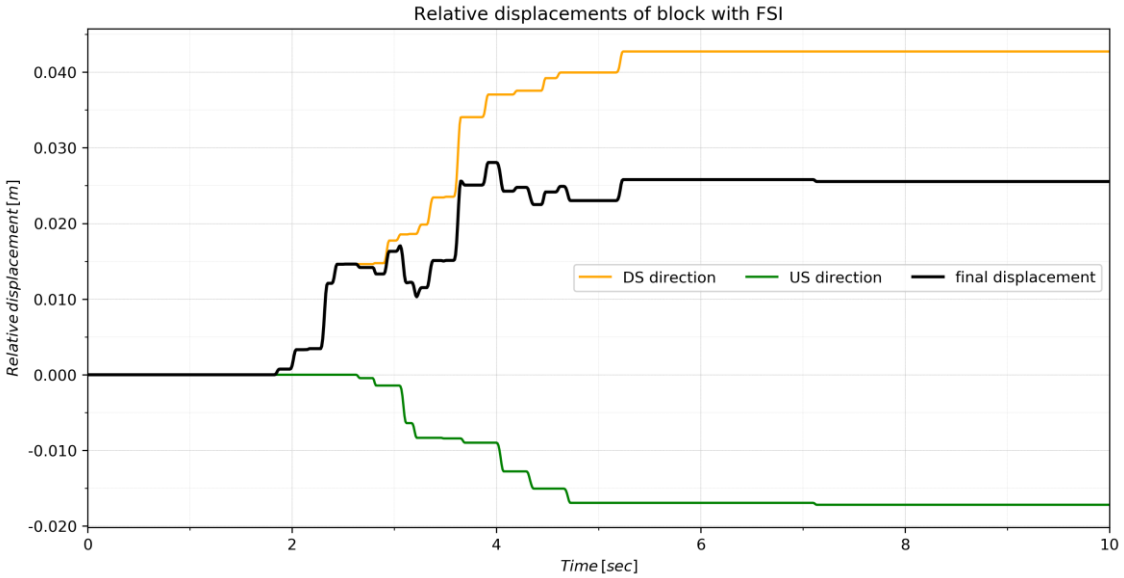

Figure 125: Relative displacements of the unreinforced crest block with FSI calculated with vertical base acceleration

Figure 126 shows the accelerogram with the yield acceleration including the vertical base acceleration for a crest block with one prestressed anchor with a full reservoir, Figure 127 and Figure 128 show the integrated relative velocities and displacements. The final displacement of the crest block is 0.0185 m in downstream direction.

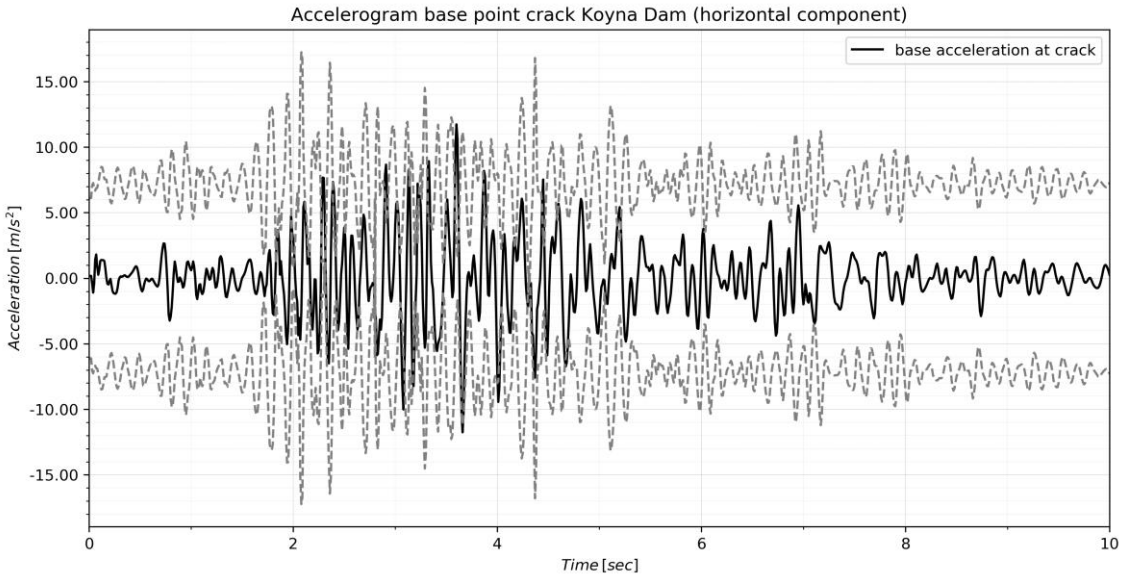

Figure 126: Accelerogram with full reservoir and yield acceleration including vertical base acceleration of crest block with one prestressed anchor

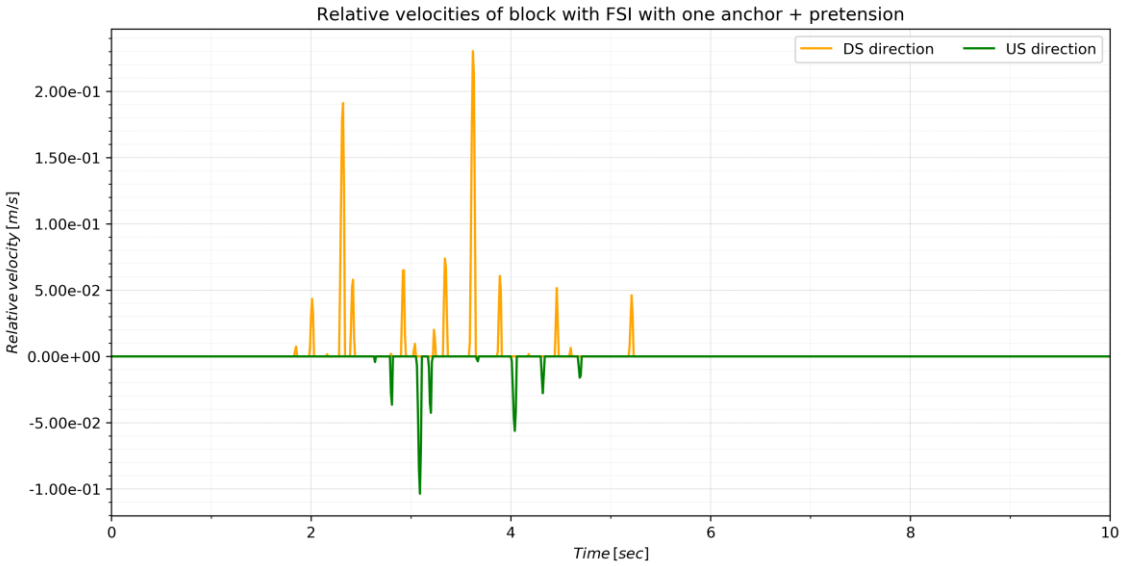

Figure 127: Relative velocities of crest block with one prestressed anchor with FSI calculated with vertical base acceleration

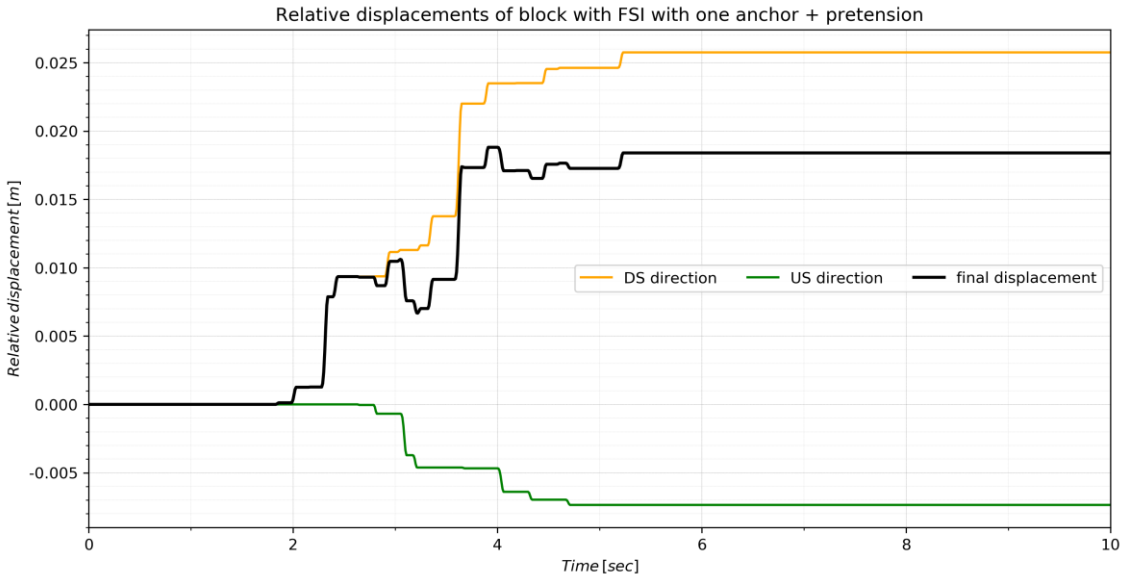

Figure 128: Relative displacements of crest block with one prestressed anchor with FSI calculated with vertical base acceleration

Figure 129 shows the accelerogram with the yield acceleration including the vertical base acceleration for a crest block with two prestressed anchors with a full reservoir, Figure 130 and Figure 131 show the integrated relative velocities and displacements. The final displacement of the crest block is 0.019 m in downstream direction.

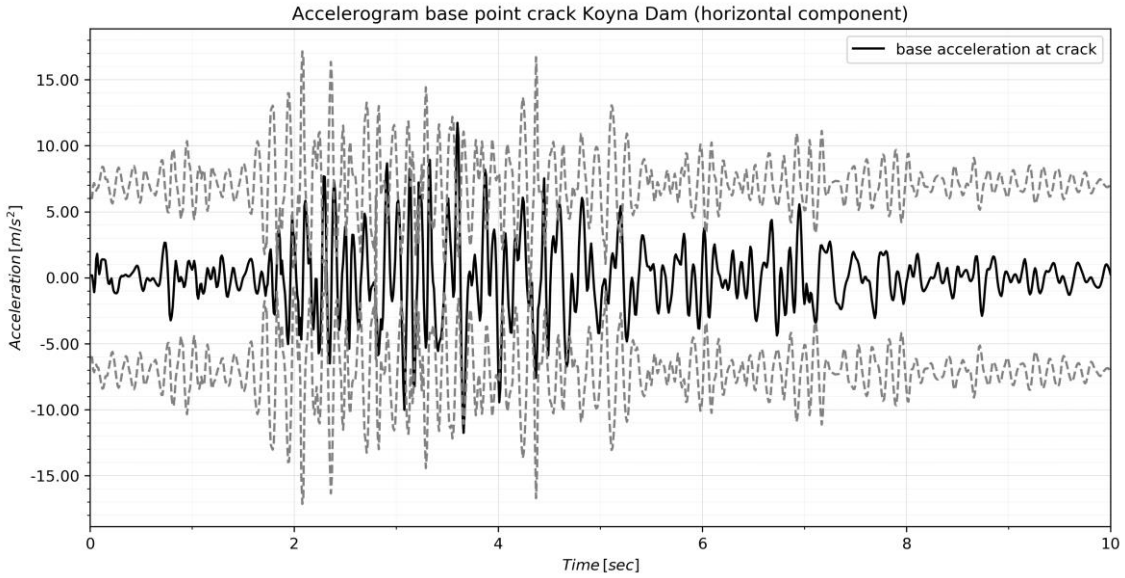

Figure 129: Accelerogram with full reservoir and yield acceleration including vertical base acceleration of crest block with two prestressed anchors

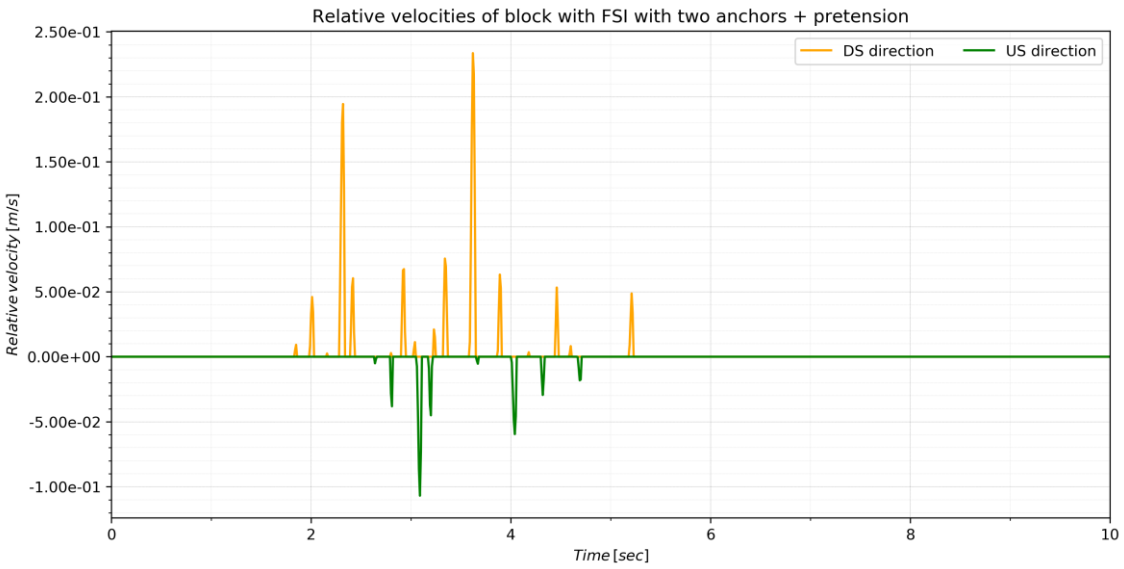

Figure 130: Relative velocities of crest block with two prestressed anchors with FSI calculated with vertical base acceleration

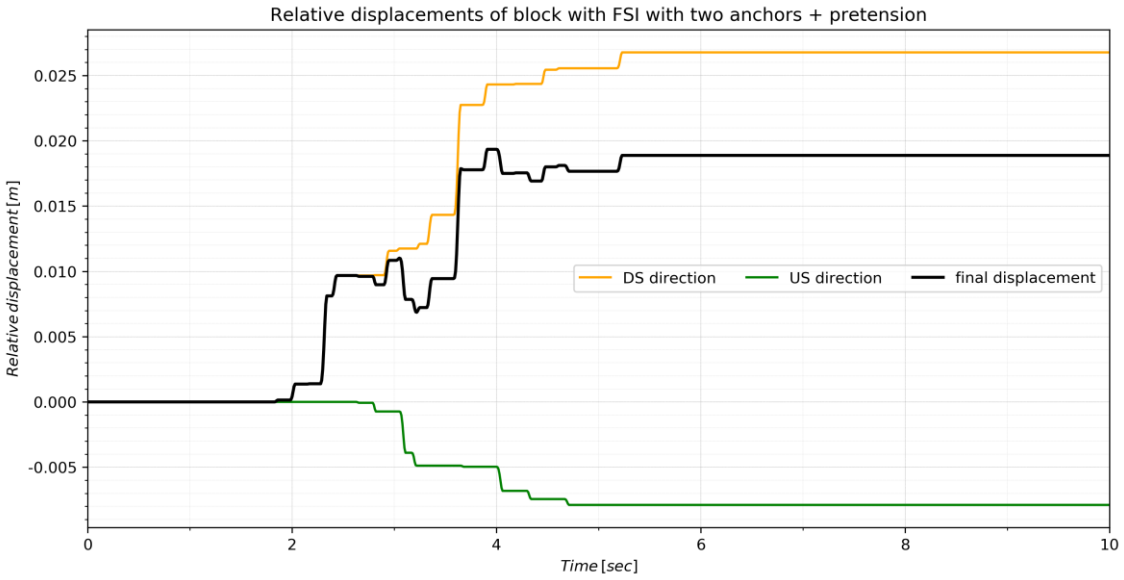

Figure 131: Relative displacements of crest block with two prestressed anchors with FSI calculated with vertical base acceleration

The Newmark rigid-block analysis is a good approach to get a first overview of the possible occurring displacements caused by seismic loading. In Table 9 the values of the final displacements of the crest part are listed:

Table 9: Comparison of displacements with Newmark method and FEM

Koyna Dam model		Final displacements		
		FEM	Newmark	
			Neglecting vertical base acceleration	Including vertical base acceleration
Empty reservoir	No reinforcement	-0.97 cm	0.07 cm	0.62 cm
	One prestressed anchor	-1.40 cm	0.0146 cm	0.41 cm
	Two prestressed anchors	-0.40 cm	0.02 cm	0.42 cm
Full reservoir	No reinforcement	9.10 m	-0.25 cm	2.50 cm
	One prestressed anchor	2.40 cm	-0.15 cm	1.85 cm
	Two prestressed anchors	2.30 cm	-0.17 cm	1.90 cm

The calculated cumulative final displacements of the crest block of Koyna Dam with an empty reservoir are in the range between 0.02 cm and 0.62 cm, whereas with full reservoir the final displacements reach values between 0.15 cm and 2.50 cm, depending on the type of reinforcement as well as on the additional vertical base acceleration which is taken into account or not. With the additional vertical base acceleration the values are higher and more similar to those of the numerical models. A negative sign means that the block is sliding in upstream direction. In comparison the obtained results taken from the relative displacements of the crack node of the model given by the FEM software, the values are between 0.40 cm and 1.40 cm for the dam with an empty reservoir, which is more

than in the Newmark calculation at the first appearance. In the unreinforced system the crest block is sliding about 9.10 m downstream when there is a full reservoir. It can be stated that the values of the reinforced systems coincide better than those ones of the non-reinforced systems. For example, the system with full reservoir and two prestressed anchors has a displacement about 2.30 cm in downstream direction in the numerical model and in the Newmark calculation the final displacement reaches about 1.90 cm, when the vertical base acceleration is included, which is also an important point to obtain more realistic results. So the displacements calculated with the Newmark method result into smaller values with partly sliding of the crest block in the opposite direction than in the numerical models, which can be explained with additional rocking and tilting of the crest parts, which is neglected in this analysis. Still the Newmark rigid-block method is invented to assume a slope as a rigid block and determine its displacements, so some other particular parameters of the numerical modelling are not included in this calculation and in the factor of safety. Hence, some difference in the results can be explained, why at some of the systems the results do not coincide well. Only the accelerogram of an earthquake is used to obtain the displacements and the response of the system itself and its certain properties are not taken into account. But this shows that is necessary not to rely only on numerical models, also the plausibility checks by manual calculations, whether the model is working in a proper way or not, or such kinds of approaches like the Newmark method are still important.

9. Summary and conclusion

In this master thesis the basics of the FEM and structural dynamics were described to get the knowledge carrying out the earthquake analysis in the following chapters. Also some theory about passive and prestressed anchors used as seismic retrofit was explained for concrete dams. The history and special case of Koyna Dam and the occurring earthquake in 1967 were described as well in order to use the available data for the numerical analysis. Different loading cases in numerical models of Koyna Dam with reservoir and foundation were set up. Initially the original cross-section was modelled as a linear 2D system and afterwards a crack, based on the reports of Koyna Dam, was implemented. In this analysis the response of the unreinforced, cracked system with a full and an empty reservoir was determined. Next step consisted of the mapping of the entire system from 2D to 3D to obtain the plain strain behavior as it is needed for concrete gravity dams, to implement the special elements for integrating anchors in the cracked dam section. First one anchor was implemented in the middle of the crest part, afterwards two anchors were arranged in the same way as the original Koyna Dam had been reinforced. Therefore, the performance of different reinforced systems could be compared reasonably and then with an alternative calculation method, the Newmark rigid-block method, as well.

First it can be stated that the values obtained in the numerical calculations are closer to reality as they would be without the dead load of the crest part as the first analysis was performed without dead load of Koyna Dam. Without the dead load the friction resistance would not be given with a selected friction coefficient of 1, which is usual for concrete.

The mapping of the whole Koyna system from 2D to 3D is verified in several test models to obtain the correct stress-strain conditions for a plane strain model, which means stresses can occur in longitudinal direction, but no strains. In the end the designed Koyna models are simplified in sections of 1 m thickness cut out of the real dam where the plane model is approximated with a 3D behavior, but the results can be seen as sufficient approach to reality.

The size respectively the diameter of the anchors is chosen based on the data given about the seismic retrofit of Koyna Dam. Thereby the cross-section area of

the one anchor model has double the value of one anchor in the two anchor model, it ensures a reasonable comparability of the obtained deformations. Just like the behavior of the anchors in a passive condition and in a pretensioned condition the difference is significant. So it is clearly visible that an adjusted pretension force is essential in order to achieve the smallest possible deformations in this Koyna Dam system. Also the number, the location as well as the inclination of the anchors is one of the main issues. Hence, the following key facts can be concluded and summarized from the numerical analysis:

- Without anchors – the unreinforced cracked systems - the largest deformation is present with both full and empty reservoir.
- The deformations are larger under conditions with hydrostatic water pressure and a full reservoir, which means the fluid-structure-interaction is included.
- Due to the neglecting of modelling the shear keys in the numerical analysis, the deformations of the unreinforced system are higher than they would be in reality.
- Two anchors demonstrated a better performance than one anchor with the same cross-section area, especially with an applied pretension force.
- Due to rocking of the reinforced crest part of the dam, the displacements in vertical direction are slightly larger than those of the non-reinforced dam, which has noticeably larger deformations in horizontal direction, as it is sliding along the crack surface.
- With the bolt pretension tool in the software the prestressed anchor force remains the same over time, which means there is no varying in force with external static or dynamic loads. This is also a simplification in the numerical analysis, but with the constant anchor force the deformations of the prestressed systems can be better compared with the Newmark calculation, since the anchor force is assumed constant as well.
- The absolute values of the anchored systems in the Newmark rigid-block calculation are similar or slightly smaller to those of the numerical analysis, provided the vertical base acceleration is included.

Based on the results of deformations, it can be concluded that the two anchor model are more appropriate against failure in an earthquake case with full and empty reservoir due to the response of the crest block. However, there are limitations of the numerical analysis including the linear-elastic material behavior of dam and anchors which represent an idealized system as well as the neglecting of the uplift pressure in the crack. Further detailed analysis on this topic can be performed, how concrete gravity dams can be reinforced with anchors to prevent against overturning, sliding or cracking caused by earthquake forces or water pressure. The shearing between separate monoliths of a concrete dam has to be avoided or reduced to a minimum as well, for this aim the shear keys are installed in the construction. In the case of reinforcement of a dam with prestressed anchors, the strands and the applied forces need to be verified and developed throughout the years.

The displacements calculated with the Newmark rigid-block analysis are basically an approximation. The reason why the cumulative displacements especially without the vertical base acceleration calculated with this method are smaller than these obtained with the FEM models can be explained by the additional rocking of the crest part in the Koyna models. This movement is not included in the Newmark method, it still works with the sum of displacements originally obtained by the accelerogram of a base point. All in all both of the rigid-block analysis and the FEM their existence is fully justified for calculating the response of a dam for a preliminary analysis.

List of figures

List of tables

Bibliography

[1] *Rao, S.S.:* The Finite Element Method in Engineering. Butterworth-Heinemann, Oxford: Camebridge, 2018.

[2] *Zienkiewicz, O.C.; Taylor, R.L.; Zhu, J.Z.:* The Finite Element Method – Its Basis and Fundamentals. Butterworth-Heinemann, 2013.

[3] *Kramer, S.L.:* Geotechnical Earthquake Engineering. Prentice Hall, Upper Saddle River, New Jersey, 1996.

[4] *Chopra, A.K.:* Dynamics of structures – Theory and Applications to Earthquake Engineering. Prentice Hall, 2012.

[5] *Wieland, M.:* State-of-the-Art Report über das dynamische Verhalten von Staumauern und von Staumauerbeton während Erdbeben. Nr. 24, Mitteilungen der Versuchsanstalt für Wasserbau, Hydrologie und Glaziologie. Vischer, D., ETH Zürich, Zürich, 1977.

[6] *Stefan, L.; Léger, P.:* Cracked Section Analysis of Gravity Dams including Passive Reinforcement and Uplift Pressures, Niagara Falls, ON, Canada Ausgabe 2010.

[7] *Brown, E.T.:* Rock engineering design of post-tensioned anchors for dams - A review, Queensland, Vol. 7 Ausgabe Februar 2015.

[8] *Cavill, B.A.:* Very high capacity ground anchors used in strengthening concrete gravity dams. *In:* Littlejohn GS, editor (1997), S. 262-271.

[9] ANCOLD: Guidelines on strengthening and raising concrete gravity dams Ausgabe 1992.

[10] USACE: Gravity dam design – Engineer Manual EM1110-2-2200 Ausgabe 1995.

[11] *Pease, K.A.; Kulhawy, F.H.:* Load transfer mechanisms in rock sockets and anchors. Electric Power Research Institute, Palo Alto, Report EL-3777 Ausgabe 1984.

[12] DYWIDAG SYSTEMS INTERNATIONAL: DYWIDAG Geotechnische Systeme, 2019, https://www.dywidag-systems.de/fileadmin/downloads/dywidag-systems.de/dywidag-geotechnische-systeme-de.pdf [Zugriff am: 20.04.2020].

[13] *Tortajada, C.; Altinbilek, D.; Biswas, A.K.:* Impact of large Dams: A global Assessment. Springer Verlag, Berlin Heidelberg, 2012.

[14] *Chopra, A.K.; Chakrabarti, P.:* The Koyna Earthquake of December 11, 1967 and the Performance of the Koyna Dam. Report No. EERC 71-1. Earthquake Engineering Research Center, University of California, Berkeley, California Ausgabe April 1971.

[15] *Auden, J.B.:* Geological Report on the Seismicity of Parts of Western India, including Maharashtra. Serial No. 1519/BMS.RD/SCE. UNESCO, Paris Ausgabe September 1969.

[16] *Gubin, I.E.:* Seismic Zoning of the Western Margin of the Indian Peninsula in Maharashtra State. Serial No. 1519/BMS.RD/SCE, Paris Ausgabe September 1969.

[17] *Mane, P.M.; Gupte, V.S.:* Koyna Dam, Koyna Project Special Number. *In:* Indian Journal of Power and River Valley Development 1962, **1962**, 19-28.

[18] U.S. Bureau of Reclamation: Laboratory Tests of Rock Cores from the Foundation of the Koyna Dam – Concrete Laboratory Report C-859. U.S. Bureau of Reclamation, Denver Ausgabe März 1958.

[19] *Gutenberg, B.; Richter, C.F.:* Seismicity of the Earth. Princeton University Press, Princeton, N. J., 1954.

[20] Indian Standard 1893-1966: Criteria for Earthquake Resistant Design of Structures, New Delhi Ausgabe November 1967.

[21] *Guha, S.K.; Gosavi, P.D.; Padale, J.G. et al.:* Crustal Disturbances in the Shivajisagar Lake Area of the Koyna Hydroelectric Project, Maharashtra,

India. Proceedings, Third Symbosium on Earthquake Engineering, Roorkee, India Ausgabe November 1966.

[22] *Guha, S.K.; Gosavi, P.D.; Varma, M.M. et al.:* Recent Seismic Disturbances in the Shivajisagar Lake Area of the Koyna Hydroelectric Project, Maharashtra, India – Research Report. Central Water and Power Research Station, Poona, India Ausgabe März 1968.

[23] *Murti, N.G.K.:* Write up on Koyna. Irritigation and Power Ausgabe April 1968.

[24] *Gupta, H.K.;* Rastogi B.K.: Dams and earthquakes. Elsevier Scentific Publishing Company, Developments in Geotechnical Engineering, Vol. 11 Ausgabe 1976.

[25] Patrick McCully: Dam–Induced Seismicity – Excerpt from Silenced Rivers: The Ecology and Politics of Large Dams. Zed Books, 1996, https://www.internationalrivers.org/dam%E2%80%93induced-seismicity [Zugriff am: 20.02.2020].

[26] UNESCO: Intergovernemental Conference on the Assessment and Mitigation of Earthquake Risk, Paris Ausgabe Februar 1976.

[27] *Murti, N.G.K.:* The Koyna Project. *In:* Indian Journal of Power and River Valley Development (1962), S. 1-2.

[28] Indian Standard 1893 - 1966. Ausgabe November 1967.

[29] *Murti, N.G.K.; Mane, P.M.; Vinayaka, M.R.:* Evaluation of Rubble Concrete for the Koyna Dam and its performance in the Structure. Transactions, Eigth International Congress on Large Dams, Edinburgh Ausgabe 1964.

[30] Koyna Earthquake of December 11, 1967 – Report of the UNESCO Committee of Experts, New Delhi Ausgabe April 1968.

[31] Hari Narain and Harsh Gupta: The Koyna Earthquake. Nature, Vol. 217 Ausgabe 1968.

[32] *Krishna, J.; Chandrasekaran, A.R.; Saini, S.S.:* Analysis of the Koyna Accelerogram of December 11, 1967. *In:* Bulletin of the Seismological Society of America (1969), Vol. 59, No. 4, S. 1719-1731.

[33] *Berg, G.V.; Das, Y.C.;* Gokhale, K. V. G. K. *et al.:* The Koyna, India Earthquakes. Proceedings, Fourth World Conference on Earthquake Engineering, Santiago, Chile Ausgabe 1969.

[34] ANSYS: ANSYS Help, https://ansyshelp.ansys.com/.

[35] ANSYS: Lecture 3 Introduction to Contact – ANSYS Mechanical Structural Nonlinearities. ANSYS, Inc., 2010.

[36] ABAQUS: Example Problems Guide, version 6.14. SIMULIA, The Dassault Systems, Providence, RI, 2014.

[37] *Guerra, A.:* Shear Keys Research Project - Literature Review and Finite Element Analysis – Dam Safety Technology Development Program. U.S. Department of Interior, Denver, Colorado, Report DSO-07-05 Ausgabe Dezember 2007.

[38] *Wilson, R.C.; Keefer, D.K.:* "Predicting areal limits of earthquake-induced landsliding," in Evalutation Earthquake Hazards in the Los Angeles Region. Professional Paper 1360, 317-345, Reston, Virginia Ausgabe 1985.